

Aus der Medizinischen Universitätsklinik Tübingen

Abteilung Innere Medizin I

Schwerpunkt Gastroenterologie, Hepatologie und Infektionskrankheiten

**Evaluation of a novel, suicide gene-armed
measles vaccine virus for the treatment of
cholangiocarcinoma**

Inaugural-Dissertation
zur Erlangung des Doktorgrades
der Medizin

der Medizinischen Fakultät
der Eberhard Karls Universität
zu Tübingen

vorgelegt von
Lange, Sebastian

2016

Aus der Medizinischen Universitätsklinik Tübingen

Abteilung Innere Medizin I

Schwerpunkt Gastroenterologie, Hepatologie und Infektionskrankheiten

**Evaluation of a novel, suicide gene-armed
measles vaccine virus for the treatment of
cholangiocarcinoma**

Inaugural-Dissertation
zur Erlangung des Doktorgrades
der Medizin

der Medizinischen Fakultät
der Eberhard Karls Universität
zu Tübingen

vorgelegt von
Lange, Sebastian

2016

Dekan: Professor Dr. I. B. Autenrieth

1. Berichterstatter: Professor Dr. U. M. Lauer

2. Berichterstatter: Professor Dr. T. Iftner

3. Berichterstatter: Professor Dr. O. Ebert

Tag der Disputation: 16.12.2016

FÜR MEINE FAMILIE

CONTENTS

| | |
|--|-----------|
| FRONT MATTER | vi |
| Table of Contents | vi |
| List of Figures | viii |
| List of Tables | x |
| List of Abbreviations | xi |
| 1 INTRODUCTION | 2 |
| 1.1 Clinical significance of cholangiocarcinoma | 4 |
| 1.2 Wild-type measles infection and vaccination | 5 |
| 1.3 Molecular biology of measles virus | 7 |
| 1.4 Oncolytic virotherapy | 10 |
| 1.5 Measles vaccine virus as a potent vector for virotherapy | 12 |
| 1.6 Arming of oncolytic viruses | 13 |
| 1.7 Generation and rescue of recombinant MeV | 15 |
| 1.8 Aim of this thesis | 17 |
| 2 METHODS | 18 |
| 2.1 Methodical remarks | 18 |
| 2.2 General techniques of cell culture | 18 |
| 2.3 Cell lines | 19 |
| 2.4 Flow cytometry | 20 |
| 2.5 Modified measles viruses | 21 |
| 2.6 Production and titration of MeV | 22 |
| 2.7 Growth curves | 24 |
| 2.8 SDS-PAGE and western blotting | 25 |
| 2.9 SRB and LDH assays | 27 |
| 2.10 Animal experiments | 29 |
| 3 RESULTS | 32 |
| 3.1 CD46 is expressed on human cholangiocarcinoma cells | 32 |

| | | |
|------|---|-------|
| 3.2 | Cholangiocarcinoma cells are susceptible to MeV infection | 34 |
| 3.3 | Measles vaccine virus infection leads to transgene expression | 36 |
| 3.4 | Differences of MeV replication in cholangiocarcinoma cells | 37 |
| 3.5 | Measles vaccine virus spreads rapidly in cell culture | 37 |
| 3.6 | Toxification of the 5-FC prodrug impairs tumour cell growth | 40 |
| 3.7 | Therapy with suicide gene-armed MeV vectors and prodrug application efficiently reduces cell survival | 40 |
| 3.8 | TFK-1 and HuCCT1 cells successfully engraft in nude mice | 46 |
| 3.9 | Suicide-gene armed MeV virotherapeutic vectors reduce tumour growth in TFK-1 xenografts | 47 |
| 3.10 | Treatment with MeV prolongs survival in HuCCT1 xenografts | 49 |
| 4 | DISCUSSION | 52 |
| 4.1 | CD46 expression varies between cholangiocarcinoma cell lines | 52 |
| 4.2 | Susceptible cell lines exhibit different growth characteristics | 53 |
| 4.3 | Resistance to MeV oncolysis can be overcome by prodrug-mediated activation of the MeV-encoded SuperCD suicide gene function | 54 |
| 4.4 | Armed MeV reduces tumour growth and prolongs survival in mice | 56 |
| 5 | SUMMARY | 60 |
| 6 | MATERIALS | 62 |
| 6.1 | Consumables | 62 |
| 6.2 | Reagents | 63 |
| 6.3 | Animals | 63 |
| 6.4 | Manufacturers | 63 |
| 7 | REFERENCES | 66 |
| | BACK MATTER | xii |
| | Zusammenfassung | xii |
| | Veröffentlichungen | xiv |
| | Erklärung zum Eigenanteil | xv |
| | Danksagung | xviii |
| | Curriculum Vitae | xx |

LIST OF FIGURES

| | | |
|----|--|----|
| 1 | Characteristic rash caused by the measles virus. | 6 |
| 2 | Yearly measles cases reported in the United States, 1944 - 2011. . . . | 7 |
| 3 | Ultrastructural appearance of a measles virus particle by transmission electron micrograph. | 7 |
| 4 | Morphology of a polyploid measles virus particle containing three genomes. | 8 |
| 5 | Fluorescence microscopy of Vero cells producing green fluorescent protein after infection with a modified measles vaccine virus. | 8 |
| 6 | Transcription gradient of mRNA after measles virus infection (schematic). | 10 |
| 7 | Regression of Burkitt's lymphoma after infection with wild-type measles. | 12 |
| 8 | Mechanisms of toxification of 5-fluorouracil. | 14 |
| 9 | Representative phase contrast images of human cholangiocarcinoma cell lines 24 hours after seeding. | 20 |
| 10 | Schematic representation of the MeV P-SCD, MeV P-DsRed, and MeV Id-SCD genomes. | 22 |
| 11 | CD46 expression on human cholangiocarcinoma cell lines. | 33 |
| 12 | Phase contrast and fluorescence microscopy of syncytia formation in RBE cells 72 hours after infection with MeV P-DsRed. | 34 |
| 13 | Phase contrast and fluorescence microscopy of human cholangiocarcinoma cells 48 hours after infection with MeV P-DsRed. | 35 |
| 14 | Phase contrast and fluorescence microscopy of human cholangiocarcinoma cells 96 hours after infection with MeV P-DsRed. | 35 |
| 15 | Detection of MeV nucleoprotein and SuperCD in MeV-infected cells. | 36 |
| 16 | Replication of MeV P-DsRed in human cholangiocarcinoma cell lines. | 38 |
| 17 | Rate of infection of human cholangiocarcinoma cell lines by MeV P-DsRed. | 39 |
| 18 | Cytotoxic effect of 5-fluorouracil on RBE, TFK-1, and HuCCT1. | 41 |
| 19 | Cytotoxic effects of MeV P-SCD + 5-fluorocytosine. | 43 |

| | | |
|----|--|----|
| 20 | Effects of MeV P-SCD + 5-fluorocytosine. | 44 |
| 21 | Cytotoxic effects of MeV Id-SCD + 5-fluorocytosine in human cholangiocarcinoma cell lines. | 45 |
| 22 | Tumour volumes of nude mice after implantation with TFK-1 or HuCCT1 human cholangiocarcinoma cells. | 47 |
| 23 | Antitumour effect of MeV P-SCD + 5-fluorocytosine in a TFK-1 human cholangiocarcinoma xenograft mouse model. | 48 |
| 24 | Individual tumour volumes of mice with TFK-1 xenograft tumours treated with MeV P-SCD + 5-fluorocytosine and corresponding controls at start of treatment and on day 46. | 49 |
| 25 | Antitumour effect of MeV Id-SCD + 5-fluorocytosine in a HuCCT1 human cholangiocarcinoma xenograft mouse model. | 50 |
| 26 | Individual tumour volumes of mice with HuCCT1 xenograft tumours treated with MeV Id-SCD + 5-fluorocytosine and corresponding controls at start of treatment and on day 48. | 50 |
| 27 | Kaplan-Meier survival curves of mice treated with MeV Id-SCD in combination with 5-fluorocytosine and corresponding controls. . . | 51 |

LIST OF TABLES

| | | |
|---|---|----|
| 1 | Characterisation of the structural and non-structural proteins of measles virus. | 9 |
| 2 | Recipes for resolving and stacking gels used in SDS-PAGE. | 26 |
| 3 | Primary and secondary antibodies used for western blotting. | 27 |
| 4 | Oncolytic capacity of MeV P-SCD and MeV Id-SCD in comparison. | 46 |
| 5 | Comparison of successful tumour engraftments of different human cholangiocarcinoma cell lines in nude mice. | 46 |

LIST OF ABBREVIATIONS

| | |
|-----------------------|---|
| 5-FC | 5-Fluorocytosine |
| 5-FU | 5-Fluorouracil |
| CD46 | Cluster of Differentiation 46 |
| FBS | Fetal Bovine Serum (heat-inactivated) |
| GM-CSF | Granulocyte Macrophage Colony Stimulating Factor |
| hpi | hours post infection |
| LDH | Lactate Dehydrogenase |
| MeV | Measles Vaccine Virus |
| MOI | Multiplicity of Infection |
| MV | wild-type Measles Virus |
| PBS | Phosphate-Buffered Saline |
| pfu | plaque forming units |
| SDS-PAGE | Sodium Dodecyl Sulfate Polyacrylamide Gel Electrophoresis |
| SRB | Sulforhodamine B |
| SuperCD/SCD | Super Cytosine Deaminase |
| TBS | Tris(hydroxymethyl)aminomethane-Buffered Saline |
| TCA | Trichloroacetic Acid |

CHAPTER 1

INTRODUCTION

Cholangiocarcinoma is a devastating tumour usually associated with late diagnosis, poor quality of life, and low survival rates. Therapeutic options are limited, and no definitive treatment other than early surgery has been identified to date. At this point, therapeutics employing new mechanisms of action are desperately needed.

Increasing evidence suggests that oncolytic viruses might be a viable treatment option in many different cancer types. Over the past 50 years, the field of oncolytic viruses has evolved from very early case reports of single patients to phase III trials including hundreds of patients, and finally to the first approval of an oncolytic virus by the United States Food and Drug Administration (FDA) and the European Medical Agency (EMA) in 2015. These viruses spread preferentially in cancer cells, exploiting certain aspects of the tumour cell biology and its pathways. Lately, they have been targeted, shielded, and armed to allow for more efficient tumour reduction.

Although engineered viruses have been portrayed as dangerous and uncontrollable in popular culture (e.g. 'I Am Legend' by Warner Bros. Pictures, 2007), patient safety has been paramount in the development of these new drugs so far. Both the measles vaccine virus and the vaccinia virus, two oncolytic viruses used in the majority of the first clinical trials, were developed to protect the population from life-threatening diseases (i.e. measles and smallpox). Hundreds of millions of vaccinations have been carried out in the last century, eliminating the

smallpox virus and bringing the wild-type measles virus to the verge of extinction. From what we know today, the adverse effects resulting from this use remain well-controlled.

In this study, we tested the feasibility of using an engineered, suicide gene-armed measles vaccine virus in the treatment of cholangiocarcinoma. We evaluated growth kinetics and tumour death, and then translated these findings into two *in vivo* trials.

The main results of this thesis were published in 2013 by our group [1]. Direct citations from this study are marked accordingly.

In the following chapter, the epidemiology and therapy of cholangiocarcinoma are summarised briefly (Section 1.1). Then, the biology and epidemiology of the measles virus are recapitulated (Sections 1.2 and 1.3). Later, the concept of oncolytic viruses is introduced in detail (Section 1.4), with special emphasis on the measles vaccine virus (Sections 1.5 to 1.7).

1.1 Clinical significance of cholangiocarcinoma

Malignant tumours of the biliary tract comprise cholangiocellular and gallbladder adenocarcinomas as well as a minor (<10%) fraction of papillary tumours [2]. "Cholangiocarcinoma is the second most common form of primary hepatic tumour (after hepatocellular carcinoma), accounting for approximately 20% of the deaths from hepatobiliary malignancies, which cause 13% of the total cancer mortality worldwide [3, 4]. Epidemiologic studies suggest an increasing incidence in Western countries during the last decades [5, 6]." [1] The highest incidences of cholangiocarcinoma are found in Thailand, China, and other parts of Southeast Asia, in part due to a very high incidence of liver fluke [7].

Risk factors with a strong association to cholangiocarcinoma include primary sclerosing cholangitis, *Opisthorcosis viverrini* infection, choledochal cysts, hepatolethiasis, and liver cirrhosis [8]. Possible associations have been made to *Clonorchis sinensis* infection, viral hepatitis B and C infection, and alcohol consumption, as well [7, 9].

Five-year survival from hepatobiliary malignancies has improved over the last 35 years, yet still remains staggeringly low (3% in the 1980s, 5% in the 1990s, and 15% between 2001 and 2007) [10]. "The only curative option for patients with gallbladder or bile duct cancer is surgical resection. Unfortunately, most cholangiocarcinomas remain clinically silent until having reached an advanced and then unresectable stage." [1] The rate of resectability has been reported as approximately 70% in distal cancer and 15 to 20% in cases of central bile duct tumours [11]. Although progressively more aggressive surgical approaches have been developed in the last years, curative or margin-free resection rates remain less than 70% [12]. Accordingly, the overall five-year survival rate after resection is between 16 to 52% [13].

Currently, there is no clearly defined standard of care for adjuvant therapy of cholangiocarcinoma following surgery. Potential benefits of radiotherapy have been reported; however, these findings are limited to single-centre trials [14, 15]. To

date, no studies have shown a clear benefit of adjuvant chemotherapy after resection [11, 16].

In patients with advanced stage cholangiocarcinoma, palliative (chemo-)therapy is often complicated by cholestasis and recurring cholangitis (a bacterial infection of the bile ducts) leading to severely reduced quality of life. The ABC-02 trial established the combination of cisplatin plus gemcitabine as an appropriate standard of care for unresectable advanced biliary tract cancer [17]. Following the advent of targeted therapies in other cancer entities, different phase II/III trials are currently evaluating the potential benefits of these agents [18].

1.2 Wild-type measles infection and vaccination

Measles is a highly contagious viral disease transmitted by droplet infection causing fever, malaise, and conjunctivitis, followed by the development of a characteristic exanthema (Figure 1). 90% of exposed individuals develop the clinical disease after six to twenty-one days [19]. The case fatality rate is highest in infants and young children, mostly caused by pneumonia [20].

Severe neurologic complications are rare but usually fatal. These include acute disseminated encephalomyelitis and subacute sclerosing panencephalitis. The latter is a degenerative disease of the central nervous system occurring seven to ten years after measles virus infection (infection at an earlier age increases the risk). It has been shown that this is caused by persistent infection of the central nervous system by measles viruses with genetic defects in the M, F, or H proteins [21].

There is no causal treatment for infection by the wild-type measles virus. Therapy is usually only supportive in nature and includes antipyretics, fluids, and treatment of bacterial superinfections with antibiotics. For individuals at high risk for complications (infants, pregnant women without evidence of immunity, and severely immunocompromised patients regardless of immunologic status), guidelines recommend therapy with pooled, polyvalent human immunoglobulin G antibodies within six days of exposure [22].

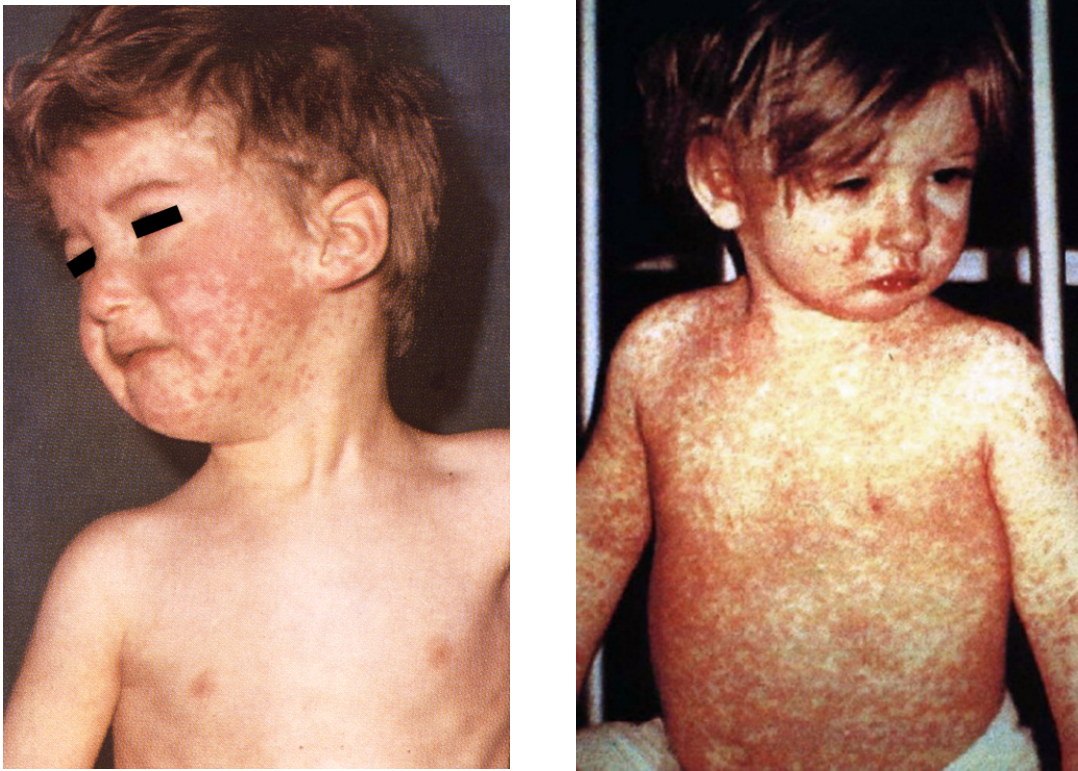


Figure 1. Two children exhibiting the characteristic rash caused by infection with the measles virus. Left panel reproduced from [23], right from [24].

Measles virus was first isolated from the blood of a child with measles (David Edmonston) by Enders and Peeble in 1954 [25]. This virus (Edmonston-Enders strain) was propagated in human and monkey cells. Later, attenuation in chick embryo fibroblasts produced the Edmonston B strain (the first attenuated live measles vaccine) [26]. Further passaging in chick embryo fibroblasts produced the Schwarz strain [27, 28], which served as the standard measles vaccine worldwide and is also used in this study for virotherapeutic purposes [29].

Vaccination has greatly reduced the worldwide burden of measles virus infection (as illustrated exemplarily in Figure 2 for the United States), reducing the number of measles-associated deaths by 80% between 2000 and 2014 [30]. The Robert Koch Institute (Berlin, Germany) recommends vaccinating children with a quadrivalent vaccine containing attenuated measles, mumps, rubella, and varicella viruses twice (at 11-14 months and 15-23 months) [31].

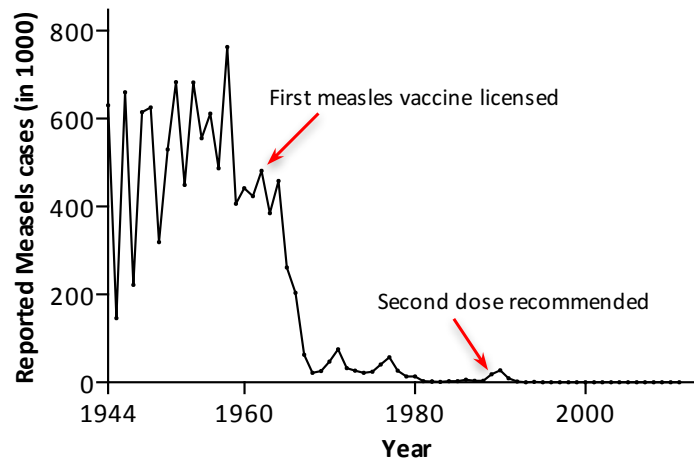


Figure 2. Yearly measles cases reported in the United States, 1944 - 2011. The first measles vaccines were licensed in 1963. In 1989, after an increase of measles incidence in children vaccinated before, a second dose was recommended by the Centers for Disease Control and Prevention. Adapted from [32, 33]

1.3 Molecular biology of measles virus

The measles virus belongs to the genus *Morbillivirus* within the *Paramyxoviridae* family. These are enveloped negative-strand RNA viruses characterised by two surface proteins F and either H, HN or G. Inside the envelope, the RNA genome and the N, P, and L proteins needed for viral replication can be found (Figures 3 and 4). The M protein is situated between the envelope and the nucleocapsid core (as reviewed in [34]).

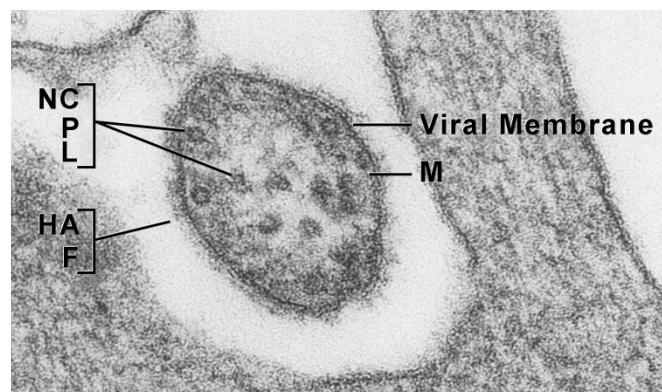


Figure 3. Ultrastructural appearance of a measles virus particle by transmission electron micrograph. Nucleocapsid protein (*NC*), Phosphoprotein (*P*), Matrix protein (*M*), Fusion protein (*F*), Hemagglutinin (*HA*) and Large protein (*L*). Please refer to Table 1 for an extensive characterisation of these structural proteins and to Figure 4 for a schematic depiction of an MV particle. Reproduced from [35].

The measles genome is coated by nucleocapsid proteins. It contains six genes coding for the six structural proteins as well as leader and trailer regions (3'-ld-N-P-

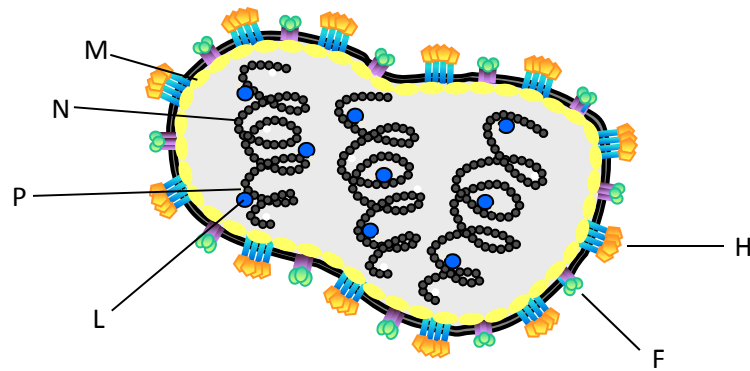


Figure 4. Morphology of a polyploid measles virus particle containing three genomes. MV expresses 6 structural proteins: Nucleocapsid protein (*N*), Phosphoprotein (*P*), Matrix protein (*M*), Fusion protein (*F*), Hemagglutinin (*H*) and Large protein (*L*). *C* and *V* (not depicted) are non-structural proteins. Adapted from [36].

M-F-H-L-tr-5'). Additionally, the *P* gene contains open reading frames for the non-structural *C* and *V* proteins. Between these six genes, untranslated regions contain conserved sequences serving as transcription initiation and termination signals (as reviewed in [34]). An overview of the viral proteins and their functions can be found in Table 1.

The measles virus nucleocapsid is released into the cytoplasm of the infected cell after binding of the *H* protein to the cellular receptor (SLAM/CD150, Nectin 4, or CD46) and fusion of both membranes by the activated *F* protein. This protein mediates not only fusion between the virus and cell membranes, but can additionally initiate fusion between infected and uninfected cells (compare Figure 5).

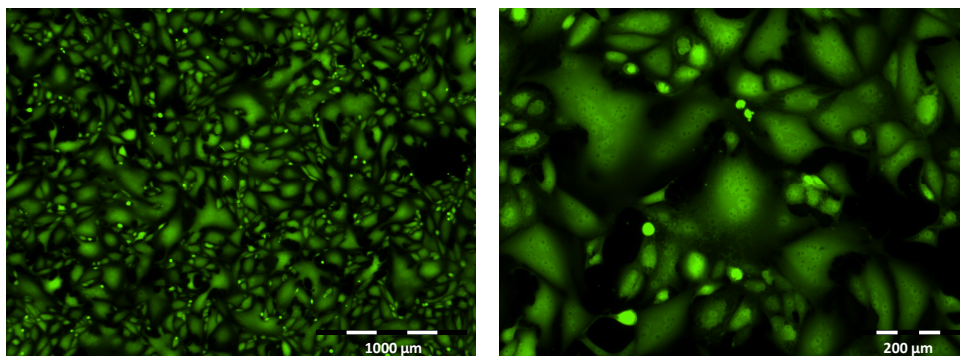


Figure 5. Fluorescence microscopy of Vero cells producing green fluorescent protein after infection with a modified measles vaccine virus. Syncytia with multiple condensed nuclei (up to 20) surrounded by cell membranes are visible in the enlarged picture on the right. Own work.

Table 1. Characterisation of the structural and non-structural proteins of measles virus. Adapted from [34, 37]

| | Protein | Function |
|--------------------------------|---------------------------------|---|
| Structural proteins | Nucleocapsid protein (N) | RNA-binding protein, coats full-length viral (-) sense genomic and (+) sense antigenomic RNAs to form the helical nucleocapsid template |
| | Phosphoprotein (P) | binds to N and L proteins during viral transcription and genome replication |
| | Matrix protein (M) | interacts with nucleocapsid and plasma membranes, directs intracellular trafficking |
| | Fusion protein (F) | mediates virus-cell and cell-cell fusion |
| | Hemagglutinin (H) | binds cellular receptors CD46 ¹ , Nectin 4 ² and SLAM/CD150 ³ , hemagglutinates erythrocytes |
| | Large protein (L) | RNA-dependent RNA polymerase |
| Non-structural proteins | C | inhibits interferon signaling and prevents cell death |
| | V | interferes in interferon signaling |

¹ expressed on nucleated human cells, wild-type MV cannot bind to CD46 [38, 39]² expressed on lymphoid cells [40, 41]³ expressed on epithelial cells [42, 43]

After release of the nucleocapsid, primary transcription by the viral RNA-dependent RNA polymerase, a complex formed by P and L proteins, produces mRNA encoding for the viral proteins. The transcription, starting at the 3' end of the genome, is repeatedly terminated and reinitiated in the non-coding regions between the different genes [44, 45]. If the polymerase fails to recognise the gene start signal, it detaches from the template and does not reinitiate the transcription. This leads to a transcription gradient as illustrated in [Figure 6](#). Importantly, this gradient affects transgenes introduced into the genome likewise.

After accumulation of sufficient amounts of free N protein in the cell, the RNA-dependent RNA polymerase starts replication of the antigenome (a full-length copy of the genome in 5'-3' orientation) [46, 47]. This antigenomic RNA is then used as a template for the replication of the genome in 3'-5' orientation. The assembled nucleocapsid is attached to the M protein, which is located at the cyto-

plasmatic side of the cellular plasma membrane. The M proteins, in return, interact with the F and H transmembrane glycoproteins [48]. The viral particles are released by budding from the host cell [34].

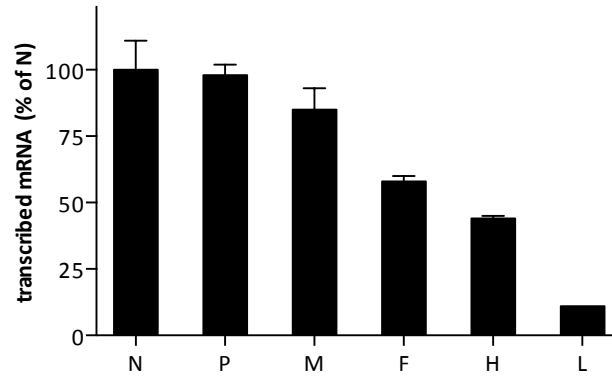


Figure 6. Transcription gradient of mRNA after MV infection (schematic). Adapted from [44]

Wild-type measles virus (MV) as well as measles vaccine virus (MeV) cannot infect rodent animals due to lack of a cellular receptor. Therefore, the oncolytic effect of measles virus can only be determined in human xenograft models in immunodeficient mice (as performed in this study) or transgenic mice that express the human CD46 receptor [49, 50].

1.4 Oncolytic virotherapy

Virotherapy is the use of viruses in the treatment of medical conditions. One aspect of this is using viruses as vectors for the delivery of gene therapy. The latest breakthrough in this field has been the approval of alipogene tiparvovec (developed by Uniqure) for the treatment of lipoprotein lipase deficiency by the European Medicines Agency in 2012 [51]. Here, an intact copy of the lipoprotein lipase is delivered to muscle cells by a non-replicating adeno-associated virus serotype 1 vector [52].

The second aspect of virotherapy is the treatment of cancer by replicating oncolytic viruses that preferentially infect and kill cancer cells. Beyond the destruction of these cells by lysis, oncolytic viruses often lead to stimulation of a host antitumour immune response which is instrumental for the systemic antitumoural effect of oncolytic viruses [53].

Publications reporting the use of oncolytic viruses as cancer therapeutics date back to as early as 1948 [54–56], although tumour regression after rabies vaccination was reported as early as 1912 [57, 58]. The first clinical trials using oncolytic viruses were published in the following years, employing viral hepatitis [59], rabies [60], West Nile virus/Egypt 101 virus [61, 62], or Adenoidal-Pharyngeal-Conjunctival viruses [63].

"In the last years, a variety of viruses from different families have been tested pre-clinically and clinically, including adenovirus, herpes simplex virus, vaccinia virus, reovirus, vesicular stomatitis virus, Newcastle disease virus, and measles vaccine virus [53, 57, 58, 64]." [1]

After the death of Jesse Gelsinger in 1999 following an adenovirus-based gene therapy trial [65, 66], patient safety in clinical trials involving viral vectors came into the spotlight. Therefore, vectors that had previously been used as vaccines, often administered hundreds of millions of times with an evidentiary safety record (e.g. measles vaccine virus [29] and vaccinia virus [67, 68]) became the frontrunners in the first clinical trials of virotherapy.

A multitude of phase I, II, and III virotherapy trials have been initiated [69, 70]: Oncolytic viruses in stage IIb/III trials include Reolysin (a reovirus developed by Oncolytics Biotech) in combination with paclitaxel and carboplatin for patients with platinum-refractory head and neck cancers [71], JX-594 (a vaccinia virus encoding granulocyte macrophage colony-stimulating factor (GM-CSF) developed by Jennerex) for patients with sorafenib-resistant advanced hepatocellular carcinoma [72], and CG0070 (an adenovirus expressing GM-CSF, developed by Cold Genesys) for patients with non-muscle invasive bladder cancer who have failed bacillus Calmette-Guérin therapy [73].

In 2005, H101, an replication-selective adenovirus developed by Sunway Biotech, was approved for the treatment of head and neck cancer in China and thus became the first approved oncolytic virus worldwide [74, 75]. Later, in 2015, talimogene laherparepvec (developed by Amgen) became the first oncolytic virus to be approved in the United States and the European Union for the treatment of unresect-

able stage III/IV melanoma. This vector is an attenuated oncolytic herpes simplex 1 virus expressing GM-CSF [76, 77].

1.5 Measles vaccine virus as a potent vector for virotherapy

An early case report, dating back as far as 1949 [78], as well as a series of case reports published in the 1970s, suggested that infection with wild-type measles virus has anti-tumour effects in haematologic malignancies [79–83]. Figure 7 summarises one of these reports. However, only in the mid-1990s, when the first systems allowing rescue of measles vaccine virus from cloned DNA were developed [84, 85], research of MeV-based anti-cancer therapy started.

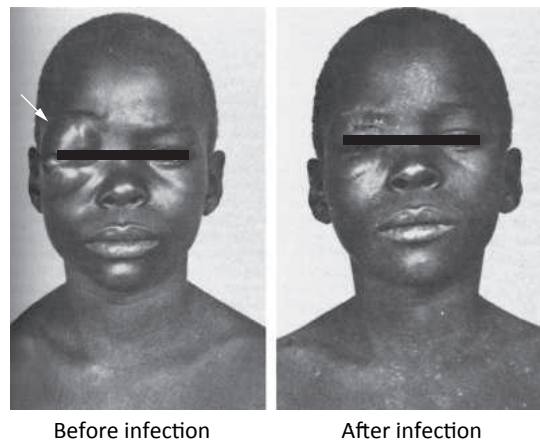


Figure 7. Regression of Burkitt's lymphoma after infection with wild-type measles. Two weeks after the diagnosis of Burkitt's lymphoma (left picture), an eight-year-old African boy developed a characteristic measles exanthema. Over the course of the next two weeks, the tumour regressed without additional therapy (right picture). The boy remained tumour-free for the next four months, when the case report was published. From [80].

Measles vaccine virus has been shown to be an oncolytic vector infecting a broad range of tumour entities and is currently under clinical investigation as a new treatment modality against ovarian cancer [86], multiple myeloma, and glioblastoma multiforme (reviewed in [87, 88]).

Regarding the safety profile of measles vaccine virus, no dose-limiting toxicity has been reached so far, suggesting a very safe vector system [89]. The safety of administering measles vaccine virus via different routes have been evaluated in recent studies: Intrahepatic injections of suicide gene-encoding oncolytic

MeV (MeV Id-SCD) in conjunction with a systemic 5-FC prodrug administration was found to be safe in both transgenic mice and rhesus macaques [90]. "Moreover, clinical studies have shown that intravenous, intraperitoneal and intracerebral injections of MeV-based virotherapeutics are well-tolerated [86]." [1]

The preferential spread in tumour cells has been attributed, at least in part, to an overexpression of regulatory membrane-bound proteins including CD46 [91]. CD46 is typically not expressed sufficiently on nontransformed cell to allow for direct infection by measles vaccine virus [92]. Additionally, some tumours are deficient in their innate antiviral response, which renders them more susceptible to viral infection than non-transformed cells [93, 94].

1.6 Arming of oncolytic viruses

"To enhance the antitumour effect of oncolytic viruses, these vectors have been armed with suicide genes that convert nontoxic prodrugs into toxic substances, leading to a localised/restricted chemotherapy at sites of viral gene expression and thus to minimised systemic side effects compared with conventional chemotherapies (overview in [95])." [1]

"For oncolytic measles vaccine virus, arming with *Escherichia coli* purine nucleoside phosphorylase, which toxifies fludarabine or 6-methylpurine-2'-deoxyriboside, has shown preclinical efficacy in lymphoma [96, 97], pancreatic cancer [98], and an immunocompetent model of murine colon carcinoma [99]. However, fludarabine can cause cytotoxicity when administered systemically [100]." [1]

In this study, a measles vaccine virus vector expressing SuperCD, a fusion of *yeast cytosine deaminase* and *yeast uracil phosphoribosyltransferase*, is used (first described by Erbs et al. [101]). These enzymes convert the clinically approved antimycotic 5-fluorocytosine (5-FC) into the chemotherapeutic 5-fluorouracil (5-FU) and further into 5-fluorouracil monophosphate. This leads to inhibition of DNA and protein synthesis [102], which is detailed extensively in [Figure 8](#).

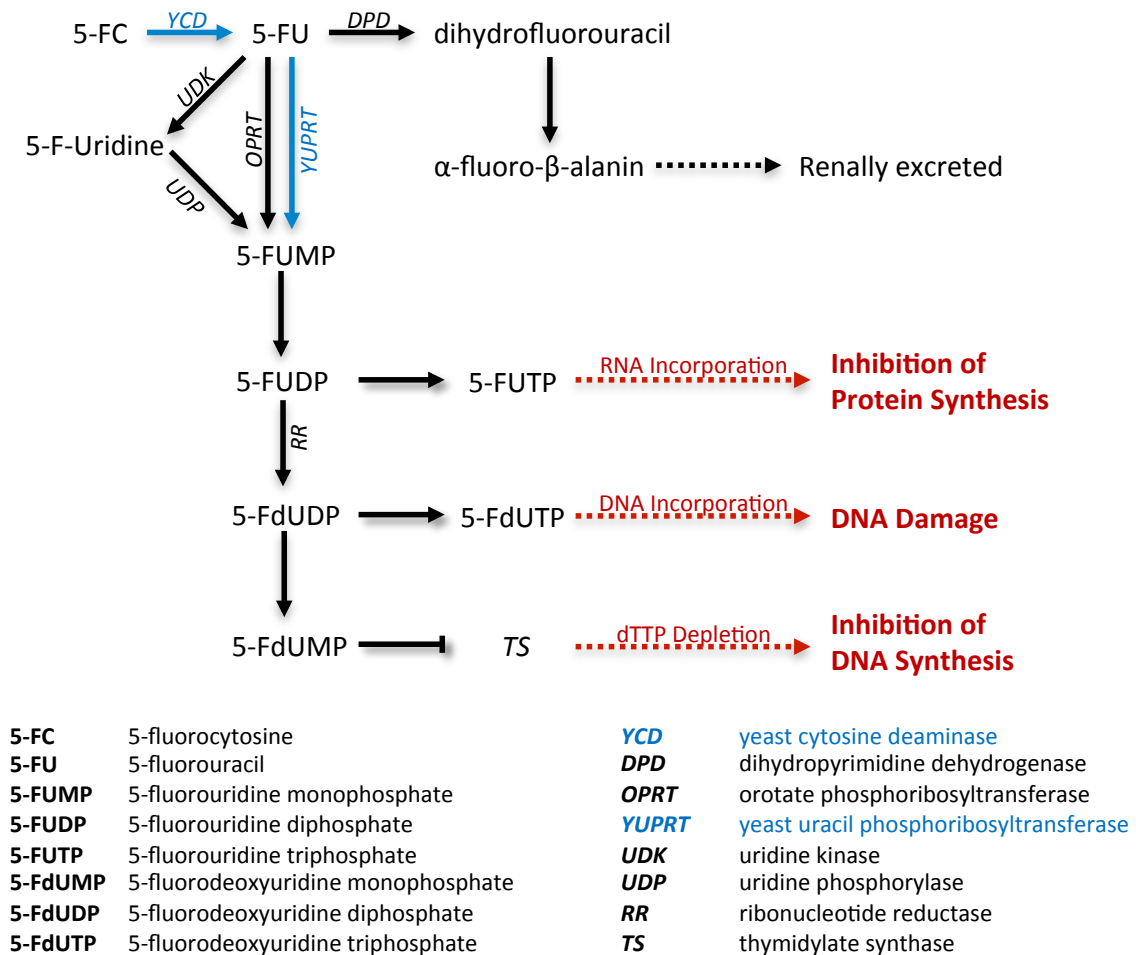


Figure 8. Mechanisms of toxicification of 5-fluorouracil. The major metabolites important in the process of 5-FU toxicification are (i) 5-fluorouridine triphosphate, which is incorporated into RNA; (ii) 5-fluorodeoxyuridine triphosphate, which is incorporated into DNA; and (iii) 5-fluorodeoxyuridine monophosphate, which inhibits deoxythymidine monophosphate synthesis. 5-FU is converted to 5-fluorouridine monophosphate either directly by *orotate phosphoribosyltransferase* or indirectly by *uridine phosphorylase* and *uridine kinase*. Subsequently, 5-FUMP is phosphorylated to its diphosphate and either hydrolysed to 5-fluorodeoxyuridine diphosphate by *ribonucleotide reductase* or further phosphorylated to 5-fluorouridine triphosphate. Phosphorylation or dephosphorylation of 5-FdUDP leads to either 5-FdUMP or 5-FdUTP. SuperCD is a fusion protein of *yeast cytosine deaminase* and *yeast uracil phosphoribosyltransferase*. CD enables the deamination of 5-FC, which enters the cell through diffusion, to 5-FU, thereby allowing toxicification in mammalian cells. UPRT catalyses the conversion of 5-FU to 5-FUMP. Adapted from [102].

A potent effect of *cytosine deaminase* in suicide gene therapy was first shown in 1992 [103]. Later, this enzyme was used in combination with *uracil phosphoribosyltransferase* [104], which is thought to bypass the rate-limiting step of 5-FU metabolism: *dihydropyrimidine dehydrogenase*, which rapidly converts 5-FU to dihydrofluorouracil (an inactive metabolite) and is expressed in all tissues [105].

The fusion protein SuperCD was later reconstructed in the laboratory of Professor Ulrich Lauer in 2005 [101, 106]. Recently, an armed measles vaccine virus expressing these enzymes was used for chemovirotherapy of head and neck squamous cell carcinoma [107].

5-fluorouracil is used as a component of standard chemotherapy in a variety of tumours, most notably including esophagogastric, colorectal and pancreatic carcinoma (compare the German S3-guidelines [108–110]). Because of its rapid intrahepatic degradation by *dihydropyrimidine dehydrogenase*, 5-fluorouracil is mainly administered intravenously [105]. Methods to allow oral administration primarily include capecitabine, which is an oral prodrug converted to 5-fluorouracil in the liver and in the tumour. Capecitabine has been shown to be equivalent to 5-FU-based chemotherapy for both gastric [111] and colorectal cancer [112].

1.7 Generation and rescue of recombinant MeV

To produce genetically modified measles viruses, different components are needed: Modified measles virus cDNA (for example, encoding a suicide gene or a reporter protein) can be constructed by restriction cloning. In addition to this engineered genome, the N, P, and L proteins are needed in the producer cells to allow for assembly and replication (termed *rescue*).

In one of these systems, baby hamster kidney cells are stably transfected with a plasmid expressing phage T7 RNA polymerase under the control of a cytomegalovirus promoter [113]. For rescue of the virus, these cells are transfected with a plasmid containing the genomic cDNA and plasmids encoding the viral proteins N, P, and L under the control of the T7-Promotor. This system is a refinement of

the first T7 polymerase-based system first described by Radecke et al. in 1995 [84].

Another system allows rescue of MeV in different cell lines. "For this, the viral cDNA is inserted into a plasmid containing regulatory sequences (promoter and terminator) derived from cytomegalovirus which are recognised by the cellular RNA polymerase II." [1] Vero cells are then transfected with the viral plasmid, and plasmids encoding for N, P, and L. This system was developed by Professor Wolfgang Neubert and his laboratory and is described by Lampe et al. in [114] and [115].

1.8 Aim of this thesis

"To date, there have been only a very limited number of publications testing virotherapy against cholangiocarcinoma. These investigations employed either adenovirus [116–119], herpes simplex virus [120], or vaccinia virus [121] enhanced by *cytosine deaminase*/5-fluorocytosine [116, 117], *uracil phosphoribosyltransferase*/5-fluorouracil [118], and/or radiotherapy [116–118]. No studies have involved the measles vaccine virus so far." [1]

Thus, we sought to evaluate a new measles vaccine virus based suicide gene therapy for the treatment of cholangiocarcinoma. Different vectors with 100% genetic identity to the Schwarz vaccine strain [27] armed with a prodrug convertase with enhanced efficacy, SuperCD [106], had previously been constructed by our collaborators.

First, we tested whether these vectors are able to infect and replicate in cholangiocarcinoma cell lines. Then, we quantified the efficacy of tumour cell killing by the viruses alone as well as in combination with the prodrug. Later, we translated these findings into two xenograft mouse trials in which tumour growth in an *in vivo* model could be evaluated.

CHAPTER 2

METHODS

2.1 Methodical remarks

All materials were stored and used according to the manufacturer's specifications. Sterilisation of materials was performed at 120 °C and a pressure of 2 bar for 20 minutes in a Systec Autoklav 3850 EL. Consumables and reagents are listed in [Chapter 6](#). Unless specified otherwise, all chemicals were obtained from Merck, Carl Roth, Sigma-Aldrich, and Becton-Dickinson.

2.2 General techniques of cell culture

All cell lines were grown in a humidified atmosphere at 37 °C, containing 5% CO₂. RBE, TFK-1 and HuCCT1 were cultured in Roswell Park Memorial Institute 1640 cell culture medium (RPMI-1640 [122]), supplemented with 10% heat-inactivated fetal bovine serum (FBS) and L-Glutamine. The Vero kidney cell line was cultured in FBS- and L-Glutamine-supplemented Dulbecco's Modified Eagle Medium (DMEM [123]). The addition of antibiotics or fungicides was not necessary. Cell lines were regularly tested for mycobacterial infection, via a polymerase chain reaction detection kit.

For routine passaging, cells were washed with Phosphate-Buffered Saline (PBS) once, treated with 0.05% Trypsin-EDTA at 37 °C for 10 to 15 minutes, and quenched with cell culture medium. Cell clumps were disrupted by repeated pipetting.

In order to seed appropriate cell numbers in the experiments, cells were counted with the help of an improved Neubauer haemocytometer as described by Strober et al. [124].

For cryopreservation of cells [125], an appropriate number of cells (approximately 1×10^6 cells/ml) was suspended in freezing buffer (70% RPMI-1640 or DMEM, 20% FBS and 10% dimethyl sulfoxide) and frozen at $1^\circ\text{C}/\text{min}$ in cryogenic vials. Vials were stored in an ultra-low temperature freezer (-145°C), or in liquid phase nitrogen, for long-term storage. When needed, vials were thawed at 37°C and pre-warmed cell culture medium was added (five times the freezing buffer volume). The suspension was centrifuged at $150 \times g$ for 5 minutes to remove supernatant, then resuspended in the appropriate cell culture medium and transferred to a cell culture flask.

Cells were visualized by phase contrast microscopy (Olympus CK40). For fluorescence microscopy, an Olympus IX50 (attached to a F-View camera system) was used with the corresponding filters (excitation/emission): eGFP: 489 nm/509 nm; DsRed: 556 nm/589 nm; Alexa Flour 546: 556 nm/573 nm. Pictures were acquired and handled with SIS Analysis 3.1 software.

2.3 Cell lines

Three different human cholangiocarcinoma cell lines were used in this study: RBE cells [126] were isolated from a 64-year-old Japanese woman with an intrahepatic cholangiocarcinoma. Another intrahepatic cholangiocarcinoma cell line (HuCCT1, [127]) was established from cells recovered from malignant ascites of a 53-year-old Japanese male. The TFK-1 cell line [128] was established from an extrahepatic cholangiocarcinoma, which had occurred in a 63-year-old Japanese man. According to the original publications, cell number doubling times are 45, 55 and 37 hours, respectively [126–128].

Under culture conditions, RBE and HuCCT1 cells form an adherend monolayer, when grown on tissue culture-treated polystyrene. TFK-1 cells tend to grow on top

of neighbouring cells, even after very few cell cycles and are, consequentially, easily detached during medium changes or in assays (Figure 9).

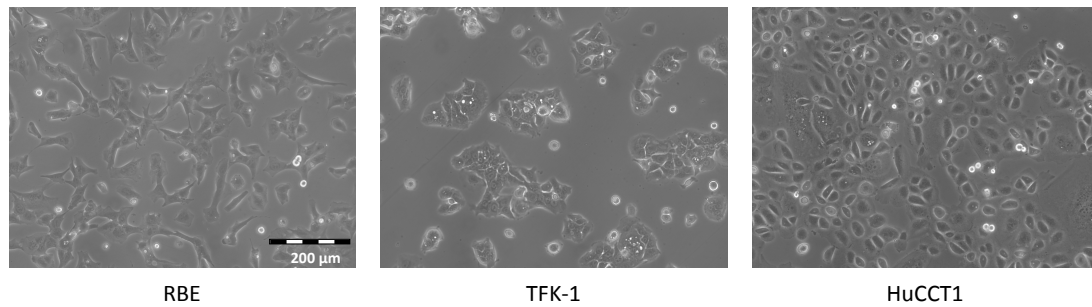


Figure 9. Representative phase contrast images of human cholangiocarcinoma cell lines 24 hours after seeding. RBE and HuCCT1 cell lines derive from intrahepatic cholangiocarcinomas, TFK-1 was established from an extrahepatic cholangiocarcinoma. The scale bar (200 μm) in the left panel applies to all panels.

Vero cells [129] were used for the production of measles vaccine virus in this study. Originally, these cells were isolated from kidney epithelial cells of an african green monkey. Vero cells are interferon-deficient [130] and can be used for the propagation of a variety of different viruses, including cell-based vaccine virus production [131].

RBE and HuCCT1 cells were purchased from Riken Cell Bank (RIKEN BioResource Center, Tsukuba, Japan). The TFK-1 cell line was a kind gift from Dr. Hans-Dieter Nischalke (Rheinische Friedrich-Wilhelms-Universität, Bonn, Germany). Vero cells were purchased from the German Collection of Microorganisms and Cell Cultures (Deutsche Sammlung von Mikroorganismen und Zellkulturen, Braunschweig, Germany).

2.4 Flow cytometry

In order to quantify CD46 expression, cells were plated and allowed to attach. After washing with PBS, cells were detached with Accutase and transferred into a flow cytometry tube. After washing (add 4 ml PBS, centrifuge at 1000 $\times g$ and 4 °C for 5 min), 5×10^5 cells were diluted in 50 μl FACS-Buffer (10% FBS in PBS) and blocked with 10 μl of pooled, polyvalent human IgG antibodies (at 4 °C for 5 min).

Cells were labelled with either a monoclonal mouse IgG1 anti-CD46 antibody or a

monoclonal mouse IgG1 isotype control, conjugated to phycoerythrin (both diluted 1:20 in FACS-Buffer and incubated at 4 °C for 30 min). After another washing step, cells were resuspended in 200 µl FACS-Buffer and fixed with 100 µl 4% paraformaldehyde (in PBS). Flow cytometry analysis was performed on a FACS Calibur flow cytometer, using Cell Quest, and analyzed with WinMDI. The mean fluorescence index (compare [92]) is the ratio of the mean FL-2 height of antiCD46-stained cells and the respective isotype control.

Additionally, the rate of MeV infection was determined by flow cytometry. Here, cholangiocarcinoma cells were plated in 6 well plates (2×10^5 cells/well) and infected at an MOI of 0.01, 0.1 or 1. The amount of virus used is expressed as multiplicity of infection (MOI), meaning number of plaque forming units (pfu) per cell (as determined by endpoint dilution assay, compare Section 2.6). After three hours and every 24 hours thereafter, cells were washed with PBS, detached with Accutase, and transferred into a flow cytometry tube. After washing (see above), cells were resuspended in 200 µl FACS-Buffer and fixed with 100 µl 4% paraformaldehyde (in PBS). The ratio of DsRed-positive cells was determined by flow cytometry analysis on a FACS Calibur flow cytometer, using Cell Quest and analyzed with WinMDI.

2.5 Modified measles viruses

Overall, three different viruses were used in this study (compare Figure 10). All were provided either by laboratory colleagues (Dr. rer. nat. Johanna Lampe) or by collaborators (Group of Professor Wolfgang Neubert). The author wishes to express his deep gratitude for this support.

Professor Wolfgang Neubert and his laboratory (Max Planck Institute of Biochemistry, Martinsried, Germany) kindly provided MeV P-SCD and MeV P-DsRed (rescued in a T7 polymerase-based system), as well as the cDNA used in the construction of MeV Id-SCD. The latter was then rescued in a CMV promoter/RNA polymerase II system by Dr. rer. nat. Johanna Lampe, as part of her doctoral thesis in the laboratory of Professor Ulrich Lauer. The backbone for these viruses is the Schwarz

vaccine strain.

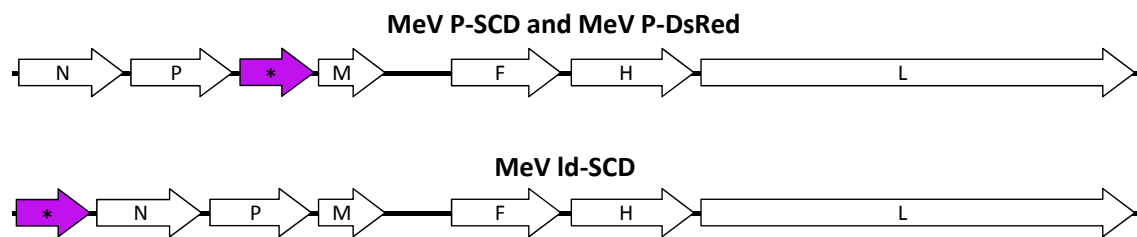


Figure 10. Schematic representation of the MeV P-SCD, MeV P-DsRed, and MeV Id-SCD genomes. "Open reading frames (purple arrows) encoding for SuperCD (*yeast cytosine deaminase* fused to *uracil phosphoribosyltransferase*), or DsRed, were inserted into an empty additional transcription unit (*) at genome position 3 of the Schwarz measles vaccine strain" [1], in order to generate MeV P-SCD and MeV P-DsRed, or at genome position 1, for MeV Id-SCD, respectively. The open reading frames encoding the measles vaccine virus proteins are depicted as white arrows: Nucleocapsid protein (N), Phosphoprotein (P), Matrix protein (M), Fusion protein (F), Hemagglutinin (H) and Large protein (L). Reproduced from [1].

2.6 Production and titration of MeV

Measles vaccine viruses (MeV P-DsRed, MeV P-SCD, MeV Id-SCD) were propagated in Vero cells. For this, 1×10^7 cells were seeded in 15 cm plates. The next day, cells were washed with DBPS once and inoculated at MOI 0.03 in Opti-MEM. For the infection, the virus was thawed on ice, vortexed and diluted in OPTI-MEM. Cells were exposed to 10 ml Opti-MEM containing viral particles at 37 °C for three hours, and gently moved every 20 minutes to ensure sufficient distribution of the virus.

After three hours, medium was replaced with 20 ml DMEM supplemented with 10% FBS. 54 hours later, when most cells were infected, the supernatant was discarded and cells were scraped into 1 ml Opti-MEM per plate. The cell solution was frozen in liquid nitrogen and rethawed in water at 37 °C once (we found no appreciable benefit (i.e. higher viral titers), using a higher number of freeze/thaw cycles compared to one cycle). After centrifugation (1.900 xg, 4 °C, 15 min), the supernatant was aliquoted into cryogenic vials, and stored at -86 °C.

Viral titers were determined for each produced batch, by endpoint dilution assay, expressed as TCID₅₀ (50% tissue culture infective dose, amount of virus needed to cause pathological change in 50% of the cell cultures inoculated). These assays

were performed in duplicates and repeated three times. 5×10^4 cells/well were plated in a 96 well plate. The following day, a 96 well plate with 270 μ l/well of DMEM supplemented with 5% FBS in the first twelve wells was prepared: 30 μ l of the viral stock was added to the first well and the content was mixed thoroughly. Then, by transferring and mixing 30 μ l of the virus solution to the adjacent well repeatedly, 12 dilution factors (spanning from 10^{-1} to 10^{-12}) were generated and 30 μ l of the diluted solutions were transferred to each well containing Vero cells in octuplicate.

After 96 hours, plates were inspected microscopically for cythopathic effect of the virus (syncytia formation) and for presence of red fluorescence (only for MeV P-DsRed).

For viruses not expressing a reporter gene (MeV P-SCD, MeV Id-SCD), readout was simplified by indirect immunofluorescence staining. After 96 hours of incubation, wells were washed with PBS, fixed with 4% formaldehyde (CH_2O , in PBS) for 10 minutes at room temperature, and again washed with PBS. Next, to prevent non-immunological binding of the primary antibody to other sites and permeabilize cell membranes, wells were incubated with Tris-buffered saline containing FBS and Triton (50 mM Tris(hydroxymethyl)aminomethane ($\text{NH}_2\text{C}(\text{CH}_2\text{OH})_3$) (adjusted to pH 7.5 with HCl), 150 mM NaCl, 0.02% Triton X-100 and 1% FBS). Cells were stained with a polyclonal mouse IgG antibody directed against the MeV nucleoprotein (diluted 1:1000 in TBS with 0.02% Tween) for 30 minutes, washed with TBS-Tween (three times) and incubated with the secondary antibody (polyclonal goat IgG antibody directed against both the heavy and light chain of mouse IgG conjugated to Alexa Fluor 546, diluted 1:1000 in TBS-Tween) for 30 minutes. After washing with TBS-Tween (three times), PBS was added to allow phase contrast and fluorescence microscopy.

After evaluating each well for virus-associated cytopathic effects and fluorescence, viral titers were calculated by the method of Spearman [132] and Kärber [133]: $\text{TCID}_{50}/\text{ml} = 10^{(f - d/2 + (d \times S) + g)}$, where f is the log of the first dilution, d is the log of the dilution factor, S is the sum of the fraction of positive cells per dilution factor and g is the log of the volume used.

In this study, the TCID₅₀ was converted into plaque forming units by multiplying the TCID₅₀ with 0.69. This number derives from applying the Poisson distribution [134]: $P(0) = e^{-m}$, where $P(0)$ is the proportion of negative wells (i.e. TCID₅₀ $\hat{=}$ 0.5) and m is the mean number of infectious units per volume.

However, recent studies found that the TCID₅₀ is proportional to $e^{-\gamma} \approx 0.56$, where γ is the Euler-Mascheroni constant (theoretical calculations in [135], validated in [136] by Monte Carlo simulations).

Because these two studies were published after completion of the experiments, the factor of 0.69 as determined by the Poisson distribution is used throughout this study.

2.7 Growth curves

2×10^5 cells/well human cholangiocarcinoma cells were plated in 6 well plates and allowed to attach. After washing with PBS, cells were infected with MeV P-DsRed in 1 ml Opti-MEM, at an MOI of 0.1 for three hours (see [Section 2.6](#)).

After infection, cells were washed with PBS (three times) and RPMI-1640, containing 5% FBS, was added into the wells. Directly after the first medium change (time point: three hours) and every 24 hours after infection, the supernatant of one well (1 ml) was collected and these cells were scraped into 1 ml Opti-MEM. Both samples were stored at -86°C . After collecting samples for all time points, the vials were thawed (2 min at 37°C), vortexed (10 to 15 seconds) and centrifuged (3000 rpm for 2 min).

Then, viral titers were determined by endpoint dilution assay (compare [Section 2.6](#)). In contrast to evaluating the titers after virus production, the protocol was altered to account for the expected smaller amount of virus in the samples: The first step of dilution was omitted, only eight serial 1:10 dilutions were prepared and 50 μl of each dilution were added to the Vero cells.

2.8 SDS-PAGE and western blotting

Cells were seeded in 10 cm plates (2×10^6 cells/plate) and later infected at an MOI of 0.1, with either MeV P-SCD, MeV P-DsRed, or mock-infected, as described in Section 2.6. Fifty-four hours after infection, cells were washed with PBS and scraped into lysis buffer (80 mM Tris (adjusted to pH 7.6 with HCl), 150 mM NaCl and 1% Nonidet-P40). The cells were lysed by three freeze/thaw-cycles (liquid nitrogen and water bath or heating block at 37 °C) and the remaining cell debris was spun down (7000 \times g, 4 °C, 10 min). The supernatants were stored at -86 °C.

The protein concentrations of the samples were determined by the Bradford protein assay [137]. This assay is based on a shift of the absorption maximum of Coomassie Brilliant Blue G-250 from 465 nm to 595 nm after binding to mostly arginyl and lysyl residues of proteins. Therefore, an increase in protein concentration leads to an increased measurable absorption. For this assay, the samples were diluted 1:20 in H₂O and 10 μ l of this dilution were pipetted into a clear bottom 96 well plate. The optical density was measured at 595 nm in a microplate reader after the addition of 200 μ l of dye reagent (diluted 1:5 in H₂O). Bovine serum albumin was diluted to at least four different concentrations, covering the expected range of protein concentrations in the samples and measured likewise. By linear regression, a standard curve was fitted using these standards and the protein concentrations of the samples were calculated.

Polyacrylamide gel electrophoresis (SDS-PAGE) was used for molecules according to their linearized size through a gel matrix. Adding sodium dodecyl sulfate (an anionic tenside) linearises proteins (by denaturing secondary structures and non-disulfide-bonds) and charges them negatively roughly proportional to size [138]. The stacking and resolving gels were prepared consecutively in a Biorad Mini Protean 3 electrophoresis system: First, the resolving gel (Table 2) was filled into the gel cassette, overlaid with isopropanol and allowed to solidify. After approximately 30 minutes, the isopropanol was removed, the surface was washed with H₂O and the

stacking gel (Table 2) was filled into the cassette. A 10-slot comb was inserted immediately afterwards.

Table 2. Recipes for resolving and stacking gels used in SDS-PAGE.

| | 10% Resolving Gel (15 ml) | 3% Stacking Gel (8 ml) |
|-------------------------------|---------------------------|------------------------|
| 30% acrylamide mix | 5 ml | 1.3 ml |
| 1 M Tris¹ | – | 1 ml |
| 1.5 M Tris² | 3.8 ml | – |
| 10% SDS³ | 0.15 ml | 0.08 ml |
| 10% APS⁴ | 0.15 ml | 0.08 ml |
| TEMED⁵ | 0.006 ml | 0.008 ml |
| H₂O | 5.9 ml | 5.5 ml |

¹ adjusted to pH 6.8 with HCl

² adjusted to pH 8.8 with HCl

³ Sodium dodecyl sulfate ($\text{CH}_3(\text{CH}_2)_{11}\text{SO}_4\text{Na}$)

⁴ Ammonium persulfate ($(\text{NH}_4)_2\text{S}_2\text{O}_8$)

⁵ Tetramethylethylenediamine ($(\text{CH}_3)_2\text{NCH}_2\text{CH}_2\text{N}(\text{CH}_3)_2$)

After solidifying, 20 μg of protein and 5 μl of Roti-Load (a modified Laemmli loading buffer) were diluted up to a total of 20 μl with PAGE running buffer (25 mM Tris (adjusted to pH 8.3 with HCl), 190 mM glycine and 0.1% SDS). The samples were denatured at 95 °C and loaded onto the gel, together with a molecular weight marker (Full-Range Rainbow Marker, M_r 12000 to 225000). The run was started at 90 V for 20 minutes, then the voltage was increased to 140 V for approximately 3 hours.

Following SDS-PAGE, proteins were transferred onto polyvinylidene difluoride membranes (Hybond-P) by electroblotting. Membranes were activated in methanol (15 seconds), then washed in H₂O, and transfer buffer (43 mM Tris, 39 mM glycine and 20% Methanol). Gel and membrane were enclosed with two Whatman papers and one sponge on each side, soaked in transfer buffer and blotted at 400 mA for 2 hours.

After blotting, the membrane was cut between the expected molecular weights of the proteins (visualized by the marker): 116 kDa (human vinculin), 58 kDa (measles vaccine virus nucleoprotein) and 42 kDa (SuperCD). The membrane was blocked with Roti-Block for human vinculin and SuperCD and with 5% cow milk in TBS-Tween for MeV nucleoprotein (at 4 °C for 12 hours). Next, the membranes were washed in TBS-Tween twice and incubated with the primary

antibodies at 4 °C for four hours. Surplus antibodies were washed off with TSB-Tween three times. Incubation with the secondary antibodies was performed at room temperature for one hour and surplus antibodies were removed likewise. The primary and secondary antibodies used for western blotting are listed in Table 3. Washing, blocking and incubating were performed on an orbital shaker.

Table 3. Primary and secondary antibodies used for western blotting.

| targeted against | type & clonality | species | diluted in |
|-----------------------|---|---------|-----------------------------|
| Human Vinculin | monoclonal IgG | mouse | 1:6000 in Roti-Block |
| MeV N-Protein | polyclonal IgG | rabbit | 1:6000 in 5% milk/TBS-Tween |
| SuperCD | polyclonal IgG | rat | 1:2000 in Roti-Block |
| Mouse IgG | polyclonal IgG, HRP-linked ¹ | goat | 1:30000 in Roti-Block |
| Rabbit IgG | polyclonal IgG, HRP-linked ¹ | goat | 1:30000 in Roti-Block |
| Rat IgG | polyclonal IgG, HRP-linked ¹ | goat | 1:30000 in Roti-Block |

¹ The secondary antibodies used are conjugated to horseradish peroxidase, which, utilizing hydrogen peroxide, oxidizes luminol (which then exhibits chemiluminescence)

Luminol was activated by the horseradish peroxidase after incubation with both luminol reagent and peroxide solution for 1 minute. An X-Ray film was used for capturing the luminescence (Hyperfilm ECL) and developed immediately afterwards.

2.9 SRB and LDH assays

The day before treatment, RBE, TFK-1, or HuCCT1 were plated in 24 well plates (7.5×10^4 cells/well in 0.5 ml culture medium). For the 5-fluorouracil treatment, the medium was changed to a medium containing the adequate amount of 5-FU after the cells were allowed to attach. For treatments involving viral infection, cells were washed with PBS and infected with measles vaccine virus at varying MOIs (the volume used for infection was 0.25 ml/well for 24 well plates) following the procedure described in Section 2.6. Three hours post-infection (hpi), the infection medium was replaced with RPMI-1640 + 10% FBS containing the appropriate amount of 5-FC.

After 96 hours, remaining cell mass was determined by Sulforhodamine B assay and cell membrane damage was measured by the lactate dehydrogenase release as-

say. For these assays, independent experiments were performed in quadruplicate and repeated three times.

The Sulforhodamine B assay is an assay to determine remaining cell mass, after different treatments in an adherent cell culture [139]. SRB is a water-soluble red fluorescent dye, which binds electrostatically and pH-dependent onto basic amino acid residues of cells fixed with trichloroacetic acid (TCA, $C_2HCl_3O_2$).

Cells were washed with cold PBS (4 °C) twice, fixed in 10% TCA at 4 °C for 30 minutes, washed with tap water (four times) and dried for at least 12 hours. Then, cells were covered with the SRB staining solution (0.04% Sulforhodamine B sodium salt and 1% TCA in H_2O) for 10 minutes, washed repeatedly with 1% TCA to remove unbound SRB dye and dried again. The dye was solubilized in 10 mM Tris (adjusted to pH 10.5 with HCl) on ice. 80 μ l of the solution was transferred into a clear bottom 96 well plate and the optical density was measured at 550 nm in a Tecan Genios plus microplate reader. Values were normalized to the untreated controls for each experiment.

The lactate dehydrogenase (LDH) release assay can be used to indirectly measure cell membrane damage after cytotoxic treatment [140, 141]. LDH is a stable cytoplasmic enzyme present in all cells. In this assay, LDH released from the treated cells reduces pyruvate to lactate, while oxidizing NADH to NAD^+ . Photometrically, NADH has an absorption maximum at 340 nm while the absorption of NAD^+ at this wave length is negligible. The amount of released LDH in the sample is, therefore, directly proportional to the the rate of decrease of NADH, which can be measured easily in a microplate reader. To correctly determine the total amount of LDH in each well (free and intracellularly) and allow calculation of the relative LDH release, cells were lysed after measuring LDH in the supernatant and LDH release was determined again.

In this study, 10 μ l of the supernatant were transferred into a clear bottom 96 well plate. Then, 200 μ l of the prepared working reagent were added to each well (consisting of 80 mM Tris (adjusted to pH 7.5 with HCl), 200 mM NaCl, 1.6 mM Pyruvate and 0.2 mM NADH + H^+ at room temperature). The optical density was measured

at 340 nm in a microplate reader five times, every two minutes. Afterwards, the supernatant of each well was discarded and cells were lysed with 0.1% Triton X-100 in PBS (at 37 °C for 10 min). Then, LDH activity was measured in the lysate likewise. Relative LDH release was calculated by dividing the measured LDH activity in the supernatant by the sum of the LDH activities in the supernatant and the lysate.

2.10 Animal experiments

All animal experiments were conducted according to the German Animal Protection Act (Tierschutzgesetz) and were approved by the local authorities (Regierungspräsidium Tübingen). The experiments were registered as 35/9185.81-2 M6/09 (preliminary engraftment tests and MeV P-SCD vs TFK-1 in CanN.Cg-Foxn1^{nu}/Crl mice) and 35/9185.81-2 M6/11 (MeV Id-SCD vs HuCCT1 in Hsd:Atymic Nude-Foxn1^{nu} mice).

Mice were kept in isolated ventilated cages in rooms set at 22 °C with a 12 hours/12 hours dark-light cycle. Mouse handling, recordings, and injections were performed in a laminar flow cabinet. Mice had free access to standard chow and water. Mice were monitored three times per week for general health, and their bodyweights were recorded. "Tumours were measured with a caliper and tumour volume was calculated from the ellipsoid volume formula (length \times (width)² \times π / 6) [142]. Animals were sacrificed when tumour volumes reached 2000 mm³, weight loss over 20% of body weight occurred, or a relevant change in behaviour or ulcerating tumours were observed." [1] Animals were sacrificed in carbon dioxide anaesthesia followed by cervical dislocation.

In these *in vivo* experiments, RBE, TFK-1 or HuCCT1 cells (1×10^7 cells in 100 μ l PBS) were injected subcutaneously into the right flank of four to six week old female CanN.Cg-Foxn1^{nu}/Crl or Hsd:Atymic Nude-Foxn1^{nu} mice on day 0 of the experiments. Beforehand, cells were detached in 0.05% Trypsin-EDTA, then washed with PBS and centrifuged (200 g for 15 min). Cells were injected with a 22 gauge needle without the need for anaesthesia.

When tumours reached a volume of about 100 mm³, mice were randomized (matched for tumour volume) into four treatment groups: vehicle control, vehicle control + 5-FC, MeV and MeV + 5-FC. Then, mice received daily injections of either MeV P-SCD (1×10^6 pfu) or MeV Id-SCD (1×10^7 pfu) in 100 µl Opti-MEM intratumourally with a 27 gauge needle (days 0-4, control groups received vehicle medium only). From days 5-11, mice received seven intraperitoneal injections of 500 mg/kg of 5-fluorocytosine (control groups were not treated intraperitoneally). 5-FC was dissolved in 50 °C-warm PBS and ultrasound-treated until the solution was clear. Until use, the solution was stored at 42 °C.

For comparison between two groups, the unpaired, two-tailed Student's t-test was used. The Log-rank test was used to calculate differences between survival curves. It was specified before beginning of the experiments that the group sizes of mice treated with vehicle control and 5-FC would be reduced compared to the other groups and excluded from statistical analysis. Analysis was done with GraphPad Prism 6.0f (GraphPad Software, San Diego, CA, USA). P-values less than 0.05 were considered as statistically significant.

CHAPTER 3

RESULTS

The aim of this thesis was to evaluate the feasibility of using a suicide gene-armed measles vaccine virus as a new form of treatment against cholangiocarcinoma. First, the growth characteristics of different measles vaccine virus vectors in well-defined cholangiocarcinoma cell lines were analysed through various methods (Sections 3.2 to 3.5). Subsequently, the potential benefits of this vector-based suicide gene therapy were explored in the same cholangiocarcinoma cell lines (Sections 3.6 and 3.7). Two mouse-based *in vivo* trials (Sections 3.8 to 3.10) concluded the experiments.

3.1 CD46 is expressed on human cholangiocarcinoma cells

Measles vaccine virus uses CD46, an inhibitory complement receptor found on all nucleated cells, to mediate cell entry. "Overexpression of CD46 has been shown to be a prerequisite for the typical cytopathic effect of measles vaccine virus and thus seems to play an important role in MeV-mediated oncolysis [92]." [1] Accordingly, CD46 expression on human cholangiocarcinoma cell lines was determined by flow cytometry analysis using a phycoerythrin-labelled antibody directed against CD46 (Section 2.4). "The minimum mean fluorescence index required for substantial MeV-mediated oncolysis has been shown to be between 25 and 50 (compare Section 1.5 and [92])." [1]

The mean fluorescence index of TFK-1 cells was detected at 139 ± 29 (mean \pm SD), which was highest among the three cell lines; the indices of RBE, and

HuCCT1 cells were 51 ± 14 and 36 ± 5 , respectively. Thus, all three cholangiocarcinoma cell lines under investigation were found to express CD46 to an extent theoretically sufficient to support infection by measles vaccine viruses (Figure 11).

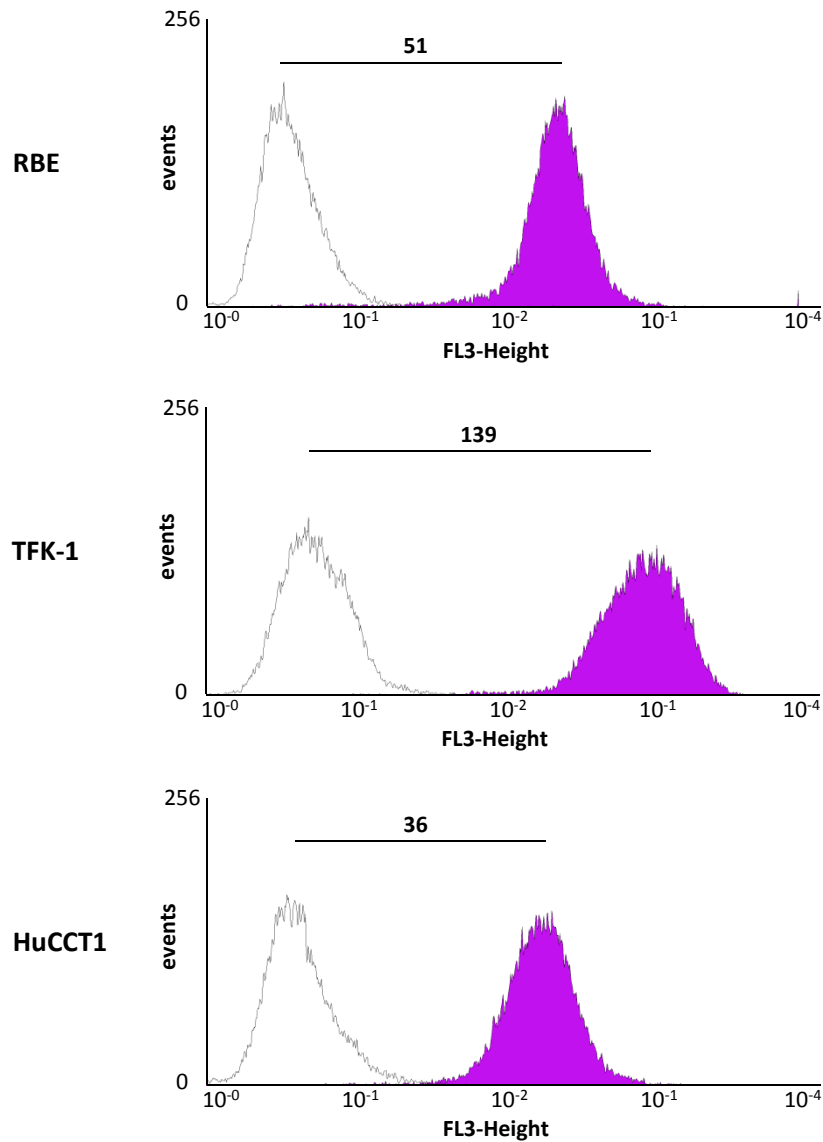


Figure 11. CD46 expression on human cholangiocarcinoma cell lines. Cells were stained with a phycoerythrin-labelled anti-CD46 antibody (purple histogram) or an isotype control (white histogram) and analysed by flow cytometry. Numbers represent the ratios of the mean fluorescence index of the purple histogram:white histogram of three independent experiments. Representative diagrams were chosen for each cell line from these three experiments. Reproduced from [1].

3.2 Cholangiocarcinoma cells are susceptible to MeV infection

To test for the susceptibility to measles vaccine virus, human cholangiocarcinoma cell lines RBE, TFK-1, and HuCCT1 were infected with MeV P-DsRed and analysed by phase contrast and fluorescence microscopy. The backbone of this MeV vector was identical to the Schwarz vaccine strain. Additionally, an open reading frame encoding for the SuperCD suicide gene was inserted into the genome at position 3 (compare Figure 10).

As a result, all human cholangiocarcinoma cell lines were found to be infected with MeV P-DsRed successfully. "Syncytia formation, a fusion of infected cells with neighbouring uninfected cells leading to the typical MeV-mediated cytopathic effect, was observed in all three cell lines, although to different extents." [1] These are marked by the expression of DsRed (e.g. in the lower right corner of Figure 12, in which a syncytium consisting of roughly 8-10 cells can be identified)

Former syncytia can be identified by loss of cell border and an increased number of condensed nuclei (compare the left panel of Figure 12, marked by an arrow). Often, these syncytia are detached from the well bottom and only cell debris remains locally. The corresponding areas in the fluorescence image are dark as an indication that cell integrity of the host cells is lost.

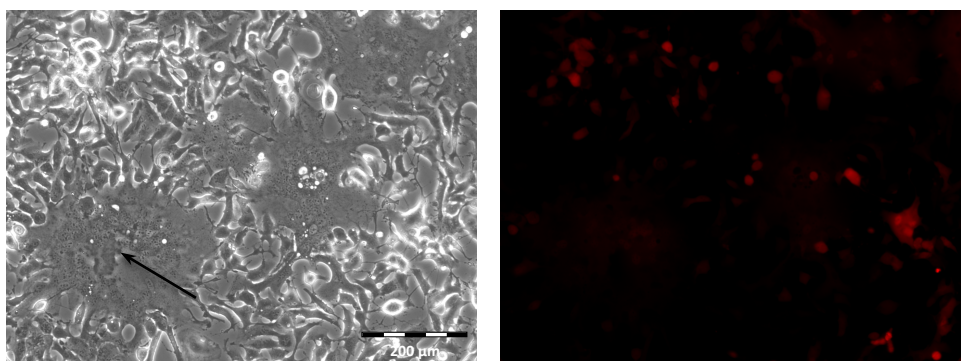


Figure 12. Phase contrast and fluorescence microscopy of syncytia formation in RBE cells 72 hours after infection with MeV P-DsRed. Cells were infected with MeV P-DsRed at an MOI of 0.01, and pictures were taken at three days post-infection. Depicted is a phase contrast (left) and fluorescence (right) image of the same well area. The arrow points to a former syncytia. The scale bar (200 μm) in the left panel applies to both panels.

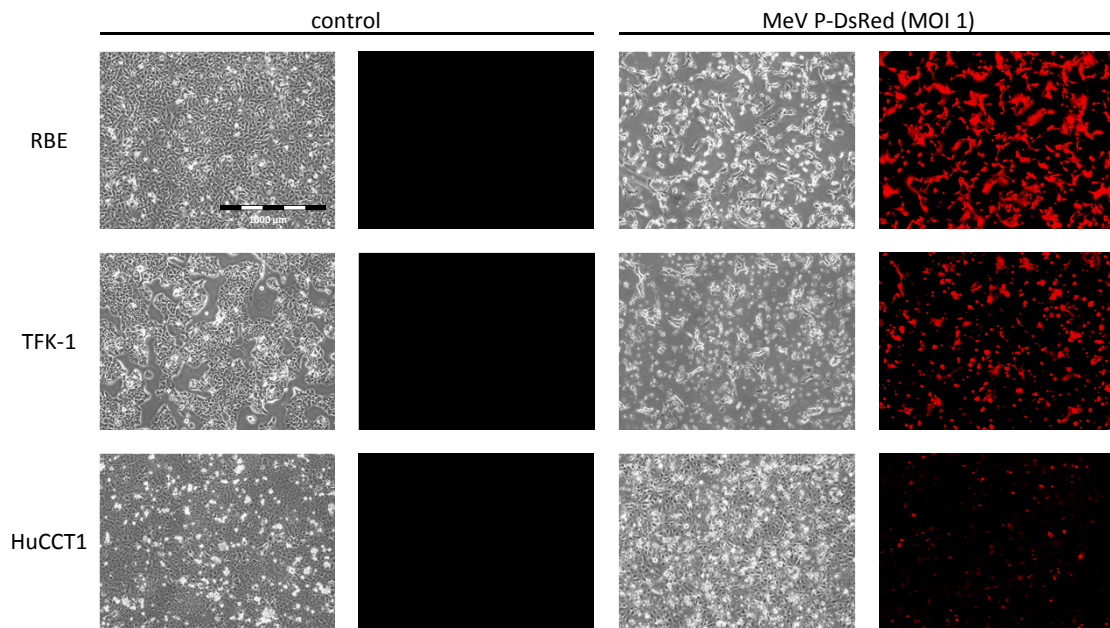


Figure 13. Phase contrast and fluorescence microscopy of human cholangiocarcinoma cells 48 hours after infection with MeV P-DsRed. Cells were infected with MeV P-DsRed at MOI 1, and pictures were taken after two days. Panels show phase contrast (left) and fluorescence (right) pictures. The scale bar (1000 μm) in the top left panel applies to all panels. Reproduced from [1].

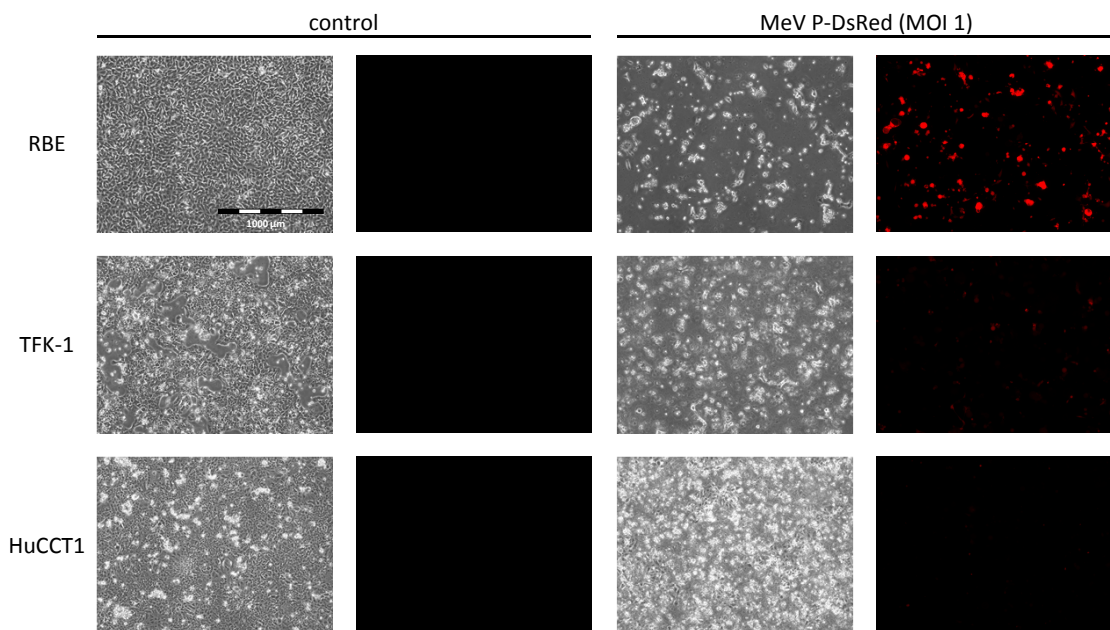


Figure 14. Phase contrast and fluorescence microscopy of human cholangiocarcinoma cells 96 hours after infection with MeV P-DsRed. Cells were infected with MeV P-DsRed at MOI 1, and pictures were taken after four days. Panels show phase contrast (left) and fluorescence (right). The scale bar (1000 μm) in the top left panel applies to all panels.

"After 48 hours, the cytopathic effect of MeV was found to be most profound in TFK-1 cells and was slightly weaker in RBE cells. In contrast, infection of HuCCT1 cells only showed a low-grade infection with limited formation of syncytia (Figure 13)." [1]

96 hours after infection, the cell layers of both RBE and TFK-1 were almost completely eliminated (Figure 14). In contrast, the HuCCT1 cultures shows a large amount of dead cells, that have detached from the well bottom, while the cell layer is still intact and adherend to the well bottom. At 96 hours after infection, all three cell lines show a decreased fluorescence signal compared with Figure 13, which was taken after 48 hours.

3.3 Measles vaccine virus infection leads to transgene expression

Expression of virus-encoded proteins was confirmed by Western blotting in all three human cholangiocarcinoma cell lines (Section 2.8). In this experiment, human vinculin was used as the loading control and detected at 116 kDa. Both measles vaccine virus nucleoprotein and the SuperCD transgene could be detected at their expected molecular weights of 58 kDa and 42 kDa, respectively (Figure 15). "HuCCT1 cells showed a weaker expression of virus-encoded proteins, which was in line with the weaker DsRed expression and the less-pronounced cytopathic effect observed previously." [1]

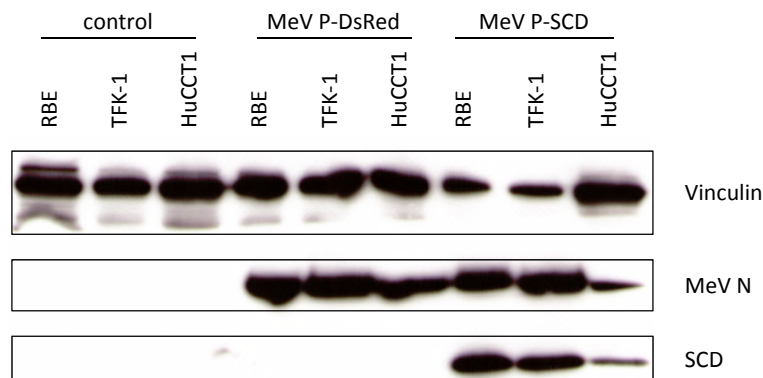


Figure 15. Detection of MeV nucleoprotein and SuperCD in MeV-infected cells. Cells were mock-infected (lanes 1-3) or infected with either MeV P-DsRed (lanes 4-6) or MeV P-SCD (lanes 7-9) at an MOI of 0.1 and harvested 54 hours later. Immunoblotting was performed by employing antibodies against human vinculin (top panel at 116 kDa), measles vaccine virus nucleoprotein (middle panel at 58 kDa), or SuperCD (bottom panel at 42 kDa). Reproduced from [1].

3.4 Differences of MeV replication in cholangiocarcinoma cells

"In order to quantify replication of oncolytic MeV, viral growth curves were performed (Figure 16). MeV P-DsRed replicated efficiently in all three cell lines." [1] Overall, in two out of three cell lines (RBE and TFK-1) and until 96 hours after infection (the last time point in this experiment), more viral particles remained cell-associated than released into the supernatant.

Between 24 and 48 hours, viral titers determined from both supernatant and RBE cells directly rose significantly faster compared with both TFK-1 and HuCCT1 cells and only reached their peak at 96 hours (6.3×10^5 pfu/ml). In TFK-1 cells, the number of cell-associated MeV particles reached a plateau as early as 48 hours after infection (0.45×10^5 pfu/ml), "presumably due to viral oncolysis already causing profound cell death at this time point (as observed in Figure 13). Replication in HuCCT1 cells appeared to be slower compared with RBE and TFK-1 cells, an observation consistent with the weaker transgene expression observed by immunoblotting and microscopy (Figures 13 and 15)." [1]

3.5 Measles vaccine virus spreads rapidly in cell culture

After quantifying the absolute number of infectious particles produced, the rate of infection was assessed by counting the number of DsRed-positive cells by flow cytometry (Section 2.4).

Transgene expression after MeV infection started during the first 24 hours post-infection (see Figure 17). Similar to the preceding experiments, RBE cells were very permissive to infection, and DsRed was expressed in a majority of cells after 24 hours and reached its maximum after 48 hours. Mirroring the results obtained previously (Section 3.4), the maximal amount of TFK-1 cells infected was already reached after 48 hours post-infection. This can be explained by a high susceptibility of TFK-1 to viral oncolysis leading to cell death and thereby to a decrease in virus production and subsequently further spread. In HuCCT1 cells, a multiplicity of infection of 1 was needed for an infection of a meaningful number of tumour cells (> 20%) cells, starting at 48 hours.

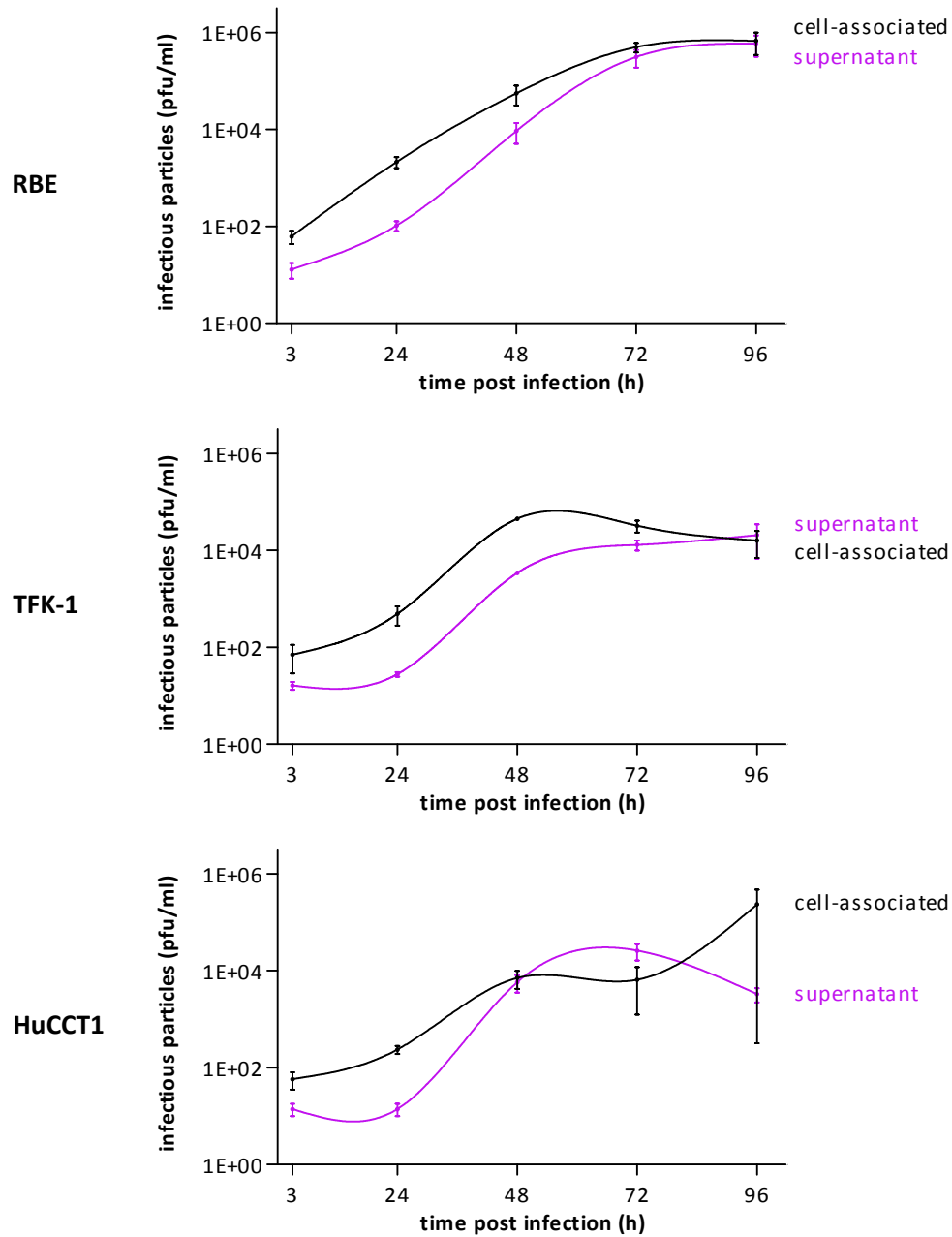


Figure 16. Replication of MeV P-DsRed in human cholangiocarcinoma cell lines. Cells were infected with MeV P-DsRed at MOI 0.1. Cells (black) and supernatant (purple) were harvested daily over four days, and viral titers were determined on Vero cells. Values represent mean \pm SEM from three independent experiments performed in quadruplicate and plotted on a semilogarithmic plot. Reproduced from [1].

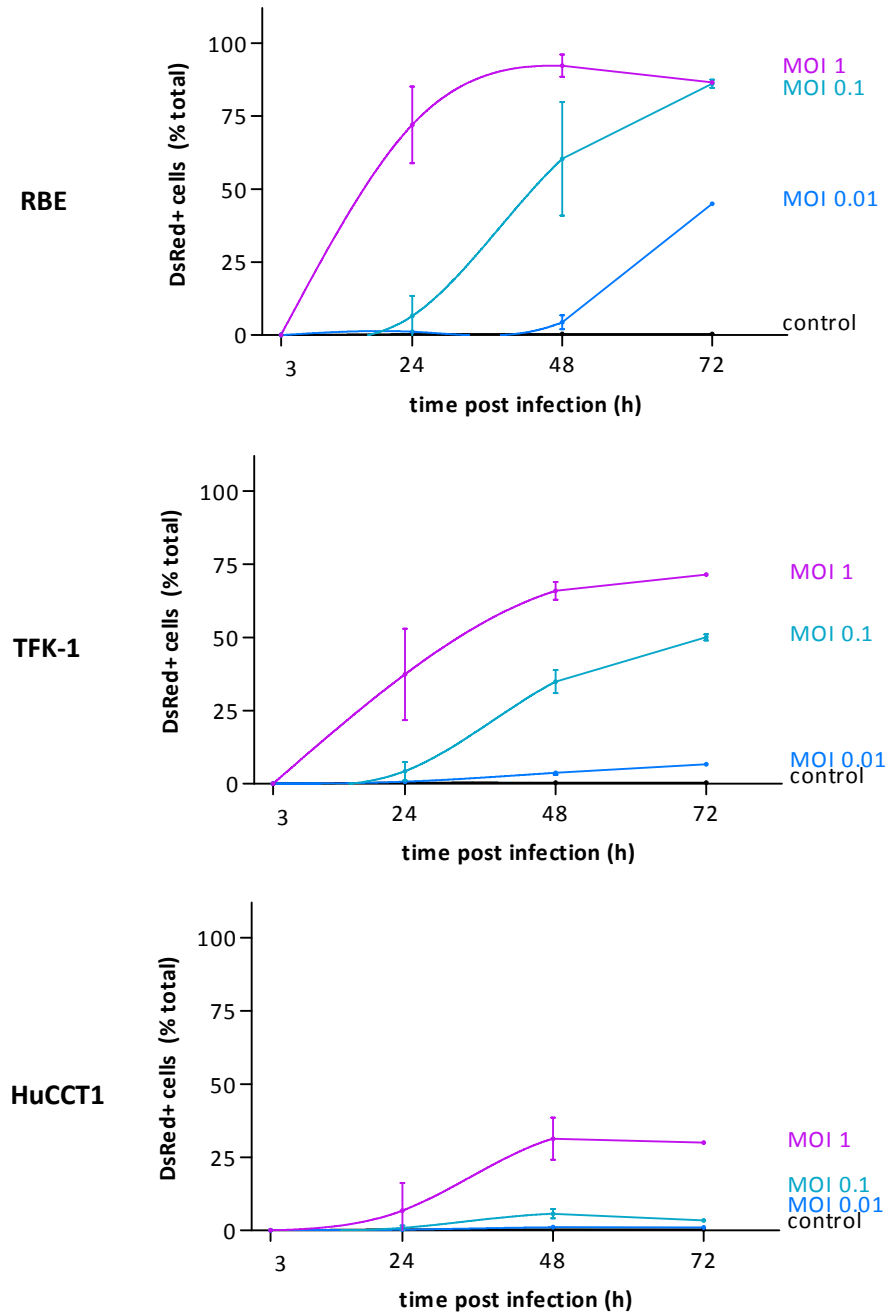


Figure 17. Rate of infection of human cholangiocarcinoma cell lines by MeV P-DsRed. Cells were infected with MeV P-DsRed at various MOIs, ranging from 0.01 to 1. Daily for three days, cells were analysed by flow cytometry to determine the percentage of DsRed-positive cells. Values represent mean \pm SD from three independent experiments.

3.6 Toxicification of the 5-FC prodrug impairs tumour cell growth

"Sensitivity to the activated form of the prodrug is a prerequisite for efficient suicide gene therapy" [1], which in the case of the SuperCD suicide transgene catalyses the intracellular conversion of 5-fluorocytosine to 5-fluorouracil. Therefore, the effects of 5-FU on the selected human cholangiocarcinoma cell lines were investigated by a Sulforhodamine B cell mass assay (Figure 18).

Concentrations of 0.01 – 0.1 mM 5-FU were found to reduce the tumour cell mass in all cell lines to 50% of the control, with an almost complete cell killing at 1 mM. More specifically, the mean remaining tumour cell mass after four days of treatment with 1 mM 5-FU was 17.9% for RBE (IC₅₀ 0.0049 mM), 4.8% for TFK-1 (IC₅₀ 0.0539 mM), and 7.7% for HuCCT1 cells (IC₅₀ 0.0116 mM).

3.7 Therapy with suicide gene-armed MeV vectors and prodrug application efficiently reduces cell survival

"In order to assess both virus-mediated oncolysis alone and cytotoxicity induced by the combination therapy, the effects of a range of MOIs and concentrations of 5-fluorocytosine were tested via the Sulforhodamine B cell mass assay and also a lactate dehydrogenase release assays (Section 2.9)." [1]

"MeV P-SCD proved to be highly cytotoxic in TFK-1 cells (Figure 19, middle panel). At an MOI of 1, even without the addition of 5-FC, 90% of the cells were killed after 96 hours. A similar effect was observed in RBE cells, where approximately 70% of the cells were killed at an MOI of 1. In both cell lines, the addition of the prodrug 5-FC led to a significantly enhanced cytotoxicity: For example, cell death after infection at MOI 0.1 was significantly enhanced by the addition of 1 mM 5-FC in RBE cells from 85.5% to a mean remaining cell mass of only 18.3%, and in TFK-1 cells from 69.8% to 2.7% mean remaining cell mass (Figure 19). These observations were confirmed in lactate dehydrogenase release assays that correlated closely with the rates of cell mass reduction measured in the SRB assay (Figure 20)." [1]

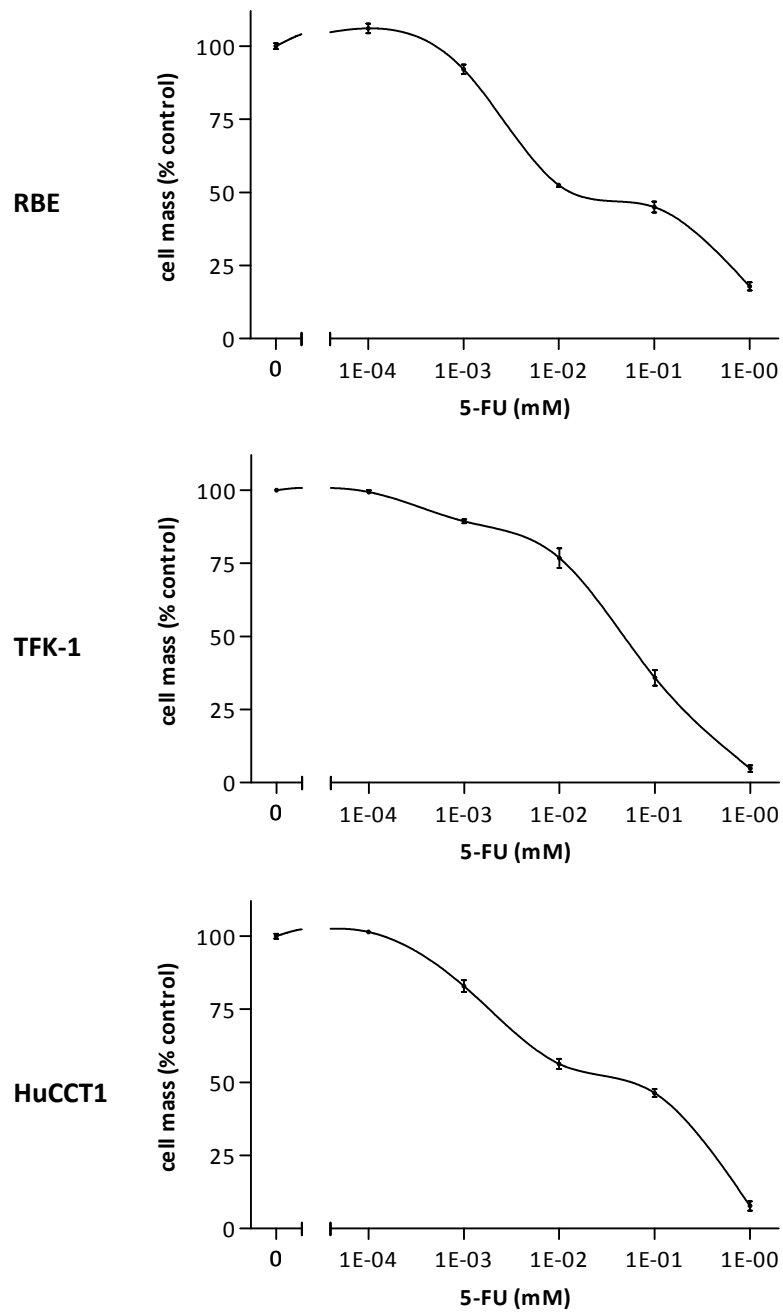


Figure 18. Cytotoxic effect of 5-fluorouracil on RBE, TFK-1, and HuCCT1. Cells were treated with various concentrations of 5-FU for four days. Cell mass was measured in a Sulforhodamine B assay. Values were normalised to the untreated control and represent mean \pm SEM from three independent experiments performed in quadruplicate and plotted on a semilogarithmic plot. Reproduced from [1].

"However, in HuCCT1 cells, where viral replication was less pronounced than in the other two cell lines, even an MOI of 1 was found to be not sufficient to induce a significant tumour cell killing. Importantly, by addition of 5-FC, this low susceptibility to MeV-mediated oncolysis was overcome and cell survival was found to be significantly reduced: from 87.8% (MeV P-SCD at an MOI of 1) to 4.4% remaining cell mass (MeV P-SCD at an MOI of 1 plus 1 mM 5-FC)," [1] indicating the high effectivity of the SuperCD transgene especially in the context of low replication of virotherapeutic vectors in distinct tumour cell types. This large-scale increase in cytotoxicity was confirmed in the LDH release assay.

To test whether the transgene position of SuperCD influenced direct cell death by the measles virus as well as the enhanced oncolytic effect after prodrug application, SRB assays using MeV Id-SCD under the same conditions were performed additionally (Figure 21). The genomic backbone of MeV Id-SCD is identical to MeV P-DsRed, however the SuperCD transgene is positioned at genome position 1 instead of genome position 3 (compare Figure 10).

Examining cell death after MeV infection alone, the remaining cell mass after infection with MeV P-SCD at both MOI 0.1 and 1 was lower in RBE and TFK-1, but not in HuCCT1 cells, compared with MeV Id-SCD. However, when the prodrug 5-fluorocytosine was added, cell mass was markedly decreased in all cells treated with MeV Id-SCD. The most profound difference between the two viruses was found in the HuCCT1 cell line, where remaining cell mass after treatment with MeV Id-SCD (MOI 0.1 plus 1 mM 5-FC) was at only 9.9% compared with 35.3% after treatment with MeV P-SCD. Please refer to Table 4 for a detailed comparison.

These results indicate, that the position of the SuperCD transgene exerts a direct influence on the rate of tumour cell killing. Here, the leader position of the transgene was found to be significantly superior regarding tumour cell death in comparison to positioning the SuperCD transgene between the P and M protein open reading frames.

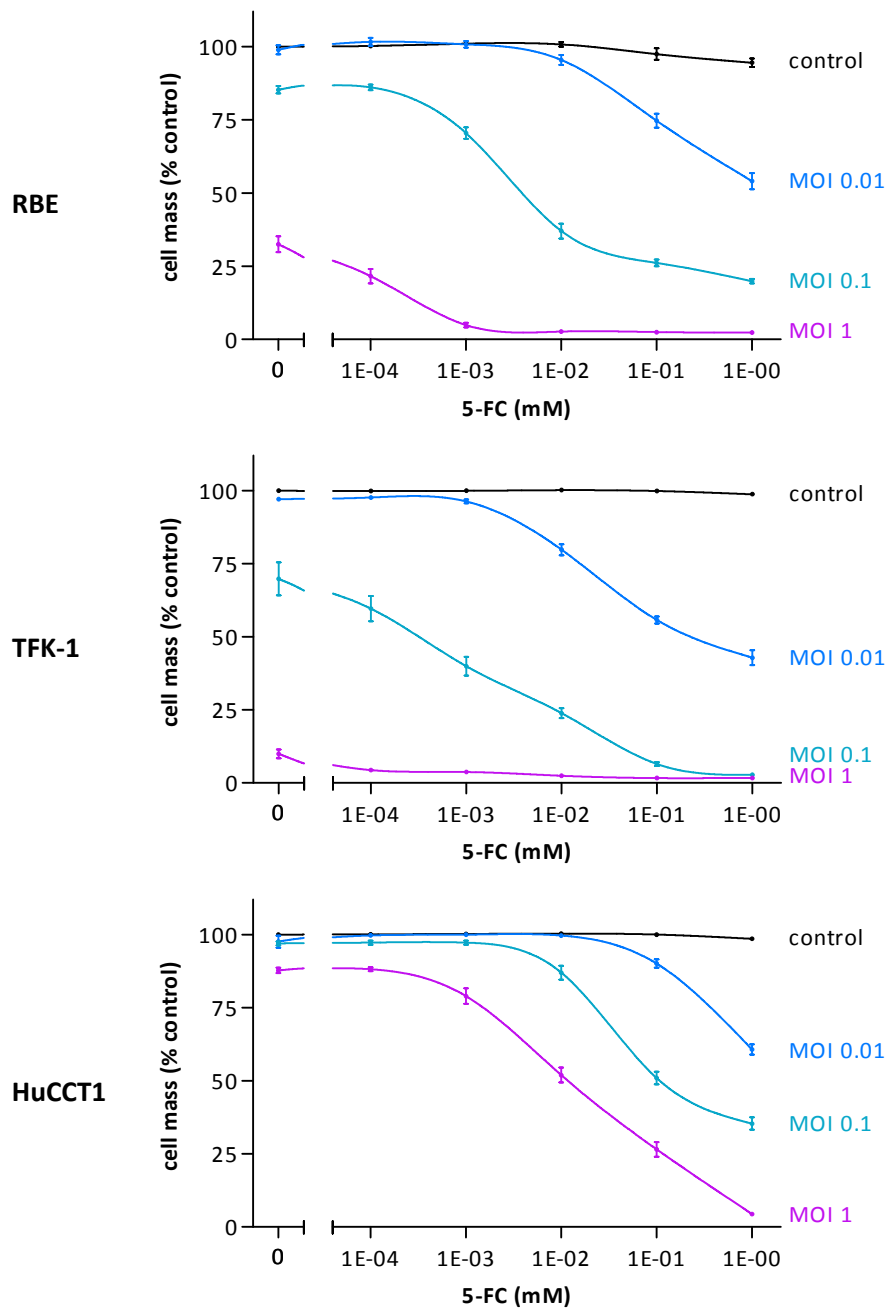


Figure 19. Cytotoxic effects of MeV P-SCD + 5-fluorocytosine. Cells were infected with MeV P-SCD at MOIs 0.01, 0.1 and 1, and incubated with varying concentrations of 5-FC for four days. Remaining cell mass was measured in a Sulforhodamine B assay. Values were normalised to the untreated control and represent mean \pm SEM from three independent experiments performed in quadruplicate and plotted on a semilogarithmic plot. Reproduced from [1].

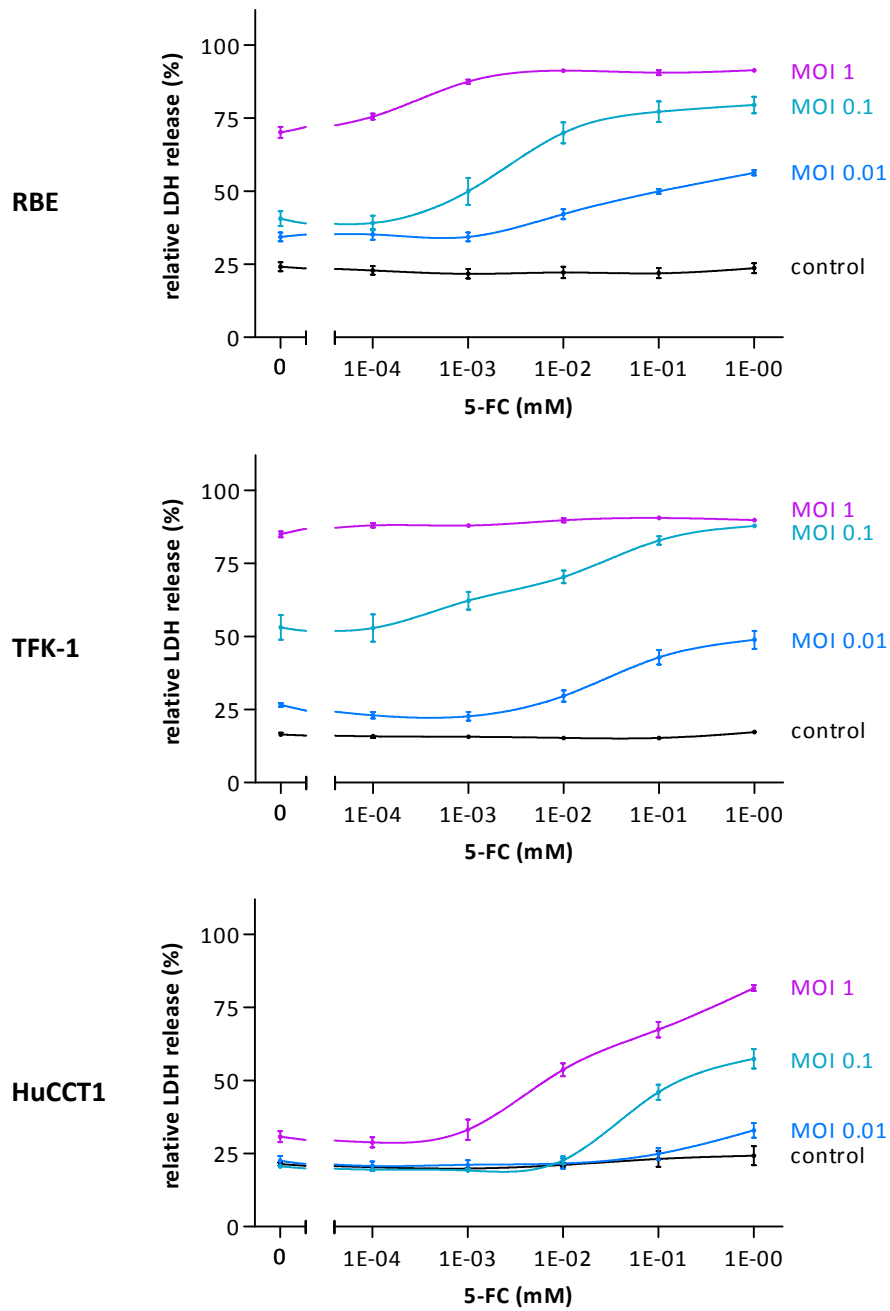


Figure 20. Effects of MeV P-SCD + 5-fluorocytosine. "Cells were infected with MeV P-SCD at MOIs 0.01, 0.1, and 1 and incubated with varying concentrations of 5-FC for four days. Cytotoxicity was measured in a lactate dehydrogenase release assay. Values represent the mean ratio between LDH in the supernatant and the total LDH measured in each well \pm SEM from three independent experiments performed in quadruplicate and plotted on a semilogarithmic plot." [1] Reproduced from [1].

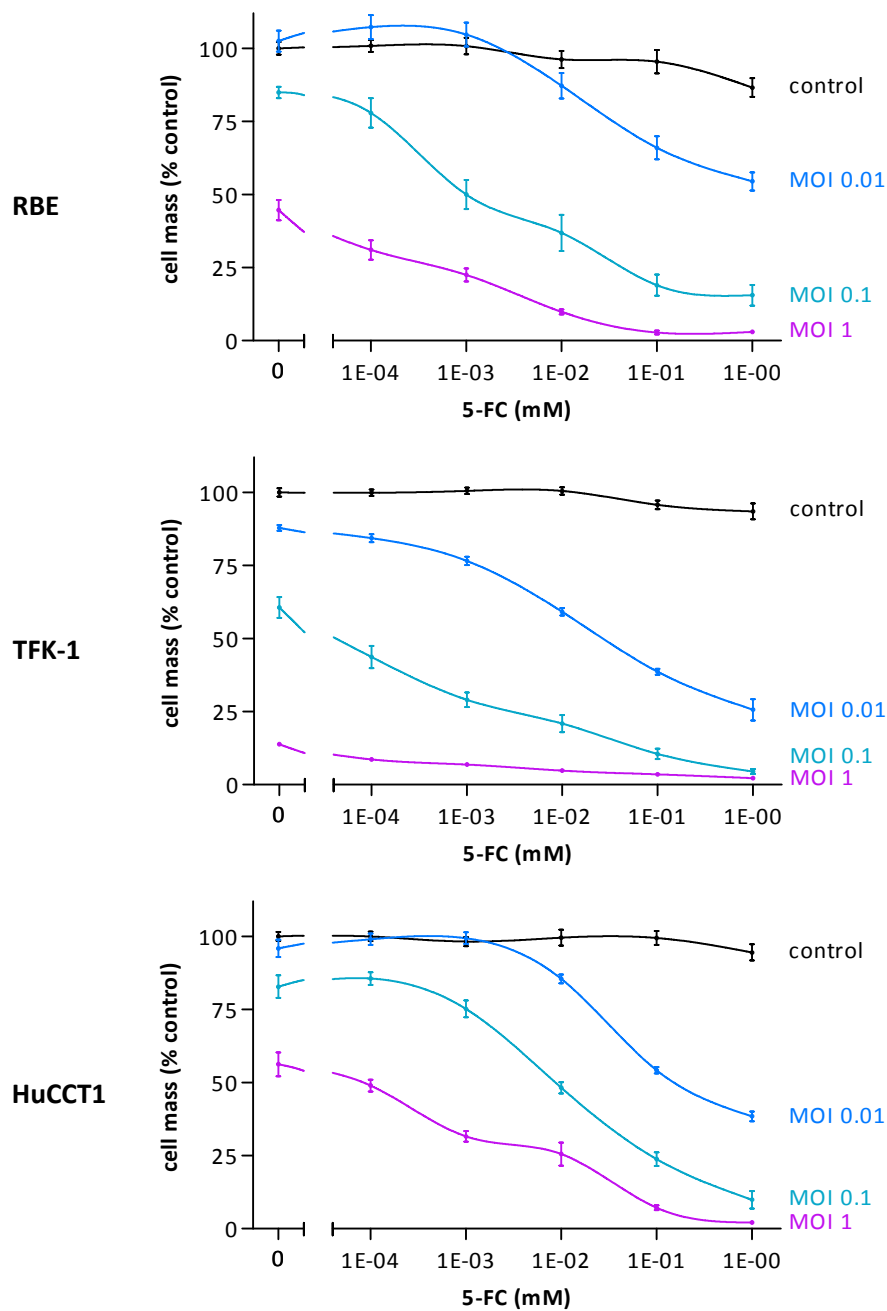


Figure 21. Cytotoxic effects of MeV Id-SCD + 5-fluorocytosine in human cholangiocarcinoma cell lines. Cells were infected with MeV Id-SCD at MOIs 0.01, 0.1, and 1 and incubated with varying concentrations of 5-FC for four days. Cell mass was measured in a Sulforhodamine B cytotoxicity assay. Values were normalised to the untreated control and represent mean \pm SEM from three independent experiments performed in quadruplicate and plotted on a semilogarithmic plot.

Table 4. Oncolytic capacity of MeV P-SCD and MeV Id-SCD in comparison. Cells were infected with MeV P-SCD or MeV Id-SCD (MOI of 0.1 or 1) only or treated additionally with 1 mM 5-fluorocytosine starting three hours post-infection. Values were taken from Figure 19 and Figure 21 and represent remaining cell mass in percent of the control.

| | | MOI 0.1 | MOI 0.1 + 5-FC | MOI 1 | MOI 1 + 5-FC |
|---------------|------------|---------|----------------|-------|--------------|
| RBE | MeV P-SCD | 85.5 | 18.3 | 32.5 | 2.3 |
| | MeV Id-SCD | 84.9 | 15.5 | 43.0 | 3.0 |
| TFK-1 | MeV P-SCD | 69.8 | 2.7 | 9.9 | 1.7 |
| | MeV Id-SCD | 60.6 | 5.4 | 13.8 | 2.2 |
| HuCCT1 | MeV P-SCD | 97.0 | 35.3 | 87.8 | 4.4 |
| | MeV Id-SCD | 82.8 | 9.9 | 56.2 | 2.1 |

3.8 TFK-1 and HuCCT1 cells successfully engraft in nude mice

Before assessing the efficacy of the armed measles vaccine virus vectors *in vivo*, we established different human cholangiocarcinoma xenograft models in nude mice. For this, RBE, TFK-1, or HuCCT1 cells were used to establish subcutaneous human tumours in nude mice (Section 2.10).

TFK-1 and HuCCT1 cells successfully engrafted in 7/10 and 10/10 animals, respectively. No animals injected with RBE cells developed a tumour until the experiment was ended after 61 days of monitoring. An overview of the successful engraftments in all *in vivo* experiments can be found in Table 5.

Tumour volumes for TFK-1 and HuCCT1 were measured three times weekly and are shown in Figure 22.

Table 5. Comparison of successful tumour engraftments of different human cholangiocarcinoma cell lines in nude mice. This table summarises the successfully engrafted tumours (defined as tumour volume larger than 100 mm³) from the experiments in Sections 3.8 to 3.10.

| | Preliminary Tests | MeV Trials | Overall Success |
|---------------|-------------------|------------|-----------------|
| RBE | 0/10 | – | 0% |
| TFK-1 | 7/10 | 31/35 | 84% |
| HuCCT1 | 9/10 | 41/42 | 96% |

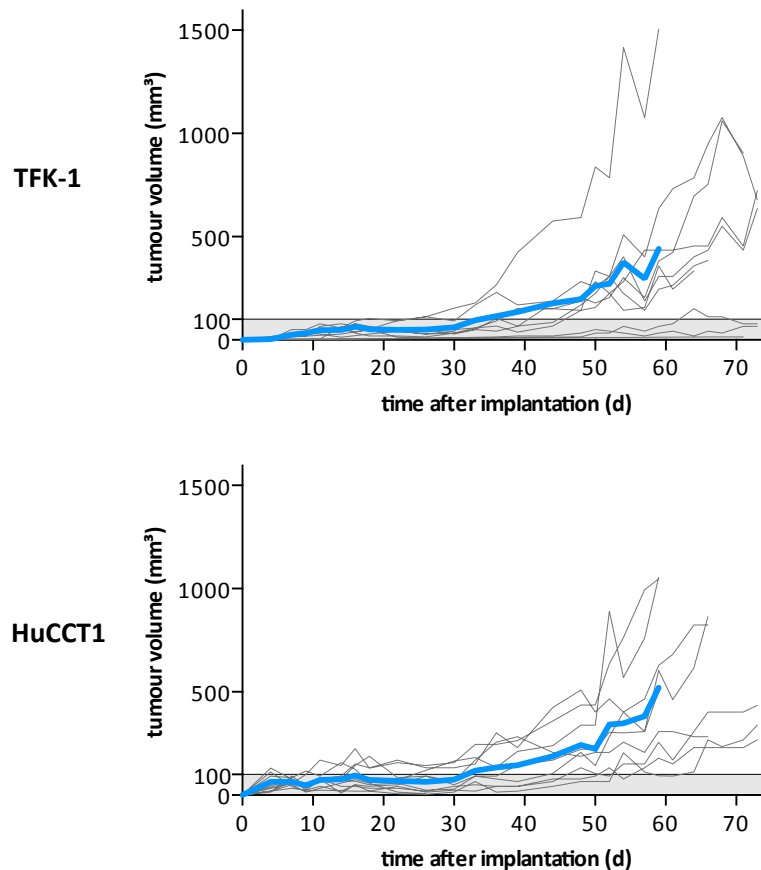


Figure 22. Tumour volumes of nude mice after implantation with TFK-1 or HuCCT1 human cholangiocarcinoma cells. 1×10^7 human cholangiocarcinoma cells were injected into the flank of nude mice in order to establish a xenograft tumour. Tumour volumes were measured until the experiment was ended at a predetermined time point. Each individual tumour is plotted (grey lines) as well as the mean tumour volume on each day (blue line).

3.9 Suicide-gene armed MeV virotherapeutic vectors reduce tumour growth in TFK-1 xenografts

For the first of two *in vivo* experiments, MeV P-SCD was tested in a TFK-1 xenograft mouse model. Tumours were established by the protocol defined earlier (Sections 2.10 and 3.8). "When tumours reached a volume of approximately 100 mm^3 , mice were randomised into four treatment groups: vehicle control (9 mice), vehicle control + 5-fluorocytosine (7 mice), MeV P-SCD only (7 mice), and MeV P-SCD + 5-fluorocytosine (7 mice)." [1] Mice were intratumourally injected for five consecutive days with MeV P-SCD or vehicle control, followed by seven days of intraperitoneal treatment with 5-FC for mice randomised to the prodrug cohorts. Mean tumour volume for each group is plotted in Fig-

ure 23. The experiment was ended 200 days after tumour implantation (173 days and 130 days after start of treatment for the first and last batch respectively).

"Treatment with virus and prodrug significantly inhibited tumour growth compared with the untreated control ($p=0.03$ at day 46), while MeV P-SCD without the addition of 5-FC did not significantly influence tumour growth compared with the control group. 46 days after initiation of treatment (Figure 24), mean tumour volume of mice treated with the combination therapy were found to be smaller (380 mm^3) than the mean tumour volume of mice treated with MeV P-SCD only (637 mm^3); however, this difference was not statistically significant."

[1]

"Tumours from all treatment groups (including the control group) developed central tumour necrosis starting at approximately day 80 after tumour implantation. In most cases, this led to the development of necrotic cysts, which interfered with tumour volume measurements. Therefore, long-term tumour volume measurements were not feasible, and thus survival of mice could not be evaluated."

[1]

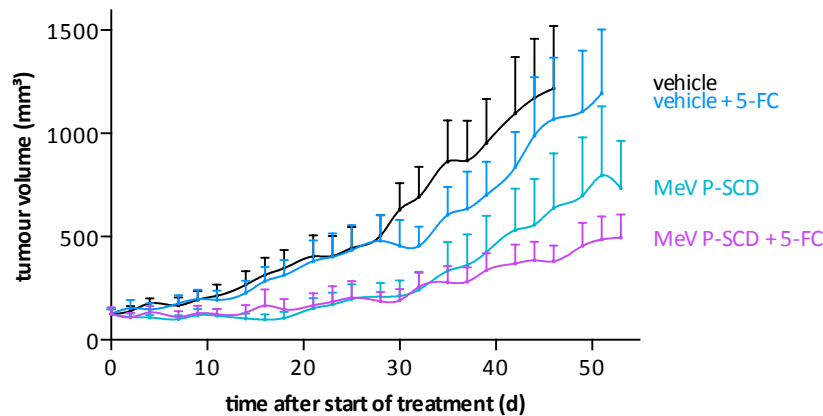


Figure 23. Antitumour effect of MeV P-SCD + 5-fluorocytosine in a TFK-1 human cholangiocarcinoma xenograft mouse model. When tumours reached a volume of approximately 100 mm^3 , mice were randomised into four treatment groups: vehicle control (9 mice), vehicle control + 5-FC (7 mice), MeV P-SCD only (7 mice), and MeV P-SCD + 5-FC (7 mice). Mice were treated daily for five days with intratumoural injections of MeV P-SCD or vehicle control, followed by seven injections of 5-FC intraperitoneally (one per day). Mean tumour volume for each group \pm SEM is plotted until the first animal of each group had to be sacrificed. Reproduced from [1].

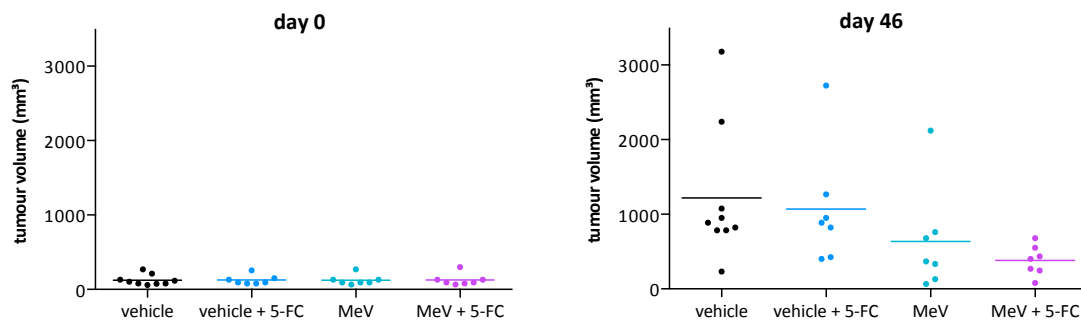


Figure 24. Individual tumour volumes of mice with TFK-1 xenograft tumours treated with MeV P-SCD + 5-fluorocytosine and corresponding controls at start of treatment and on day 46. Experimental setup is detailed in Figure 23. Tumour volumes for day 46 after start of treatment are plotted (this is the last day on which all mice from all treatment groups survived). When comparing groups with the Student's t-test, only the difference of tumour volumes between vehicle control (vehicle) and MeV P-SCD + 5-FC (MeV + 5-FC) can be considered statistically significant ($p=0.03$). Reproduced from [1].

3.10 Treatment with MeV prolongs survival in HuCCT1 xenografts

"We conducted a second *in vivo* experiment, now using the HuCCT1 cell line for which a lower susceptibility to MeV-mediated oncolysis was shown earlier *in vitro* (Section 3.7). HuCCT1 tumour-bearing mice were treated with the same schedule as described above. To further enhance the anti-tumour effect, MeV Id-SCD, in which the SuperCD transgene is expressed from genome position 1 instead of position 3 (Figure 21), was employed. This virus had demonstrated enhanced oncolytic efficacy in comparison with MeV P-SCD *in vitro*, both in the virus-only setting as well as in combination with the prodrug (as described in Section 3.7)." [1]

"Tumours from both virus-treated groups were found to regress in the course of oncolytic treatment, but slightly reinitiated their growth from day 30 onward (Figure 25). Mean tumour volumes after 48 days (Figure 26) were significantly larger in the control group (658 mm^3) than in groups treated with MeV Id-SCD, both with and without the addition of 5-FC (124 mm^3 , $p=0.0008$ and 42 mm^3 , $p<0.0001$ respectively). Tumour volume was slightly larger in the MeV Id-SCD + 5-FC group compared with MeV Id-SCD only; however, this difference was not statistically significant." [1]

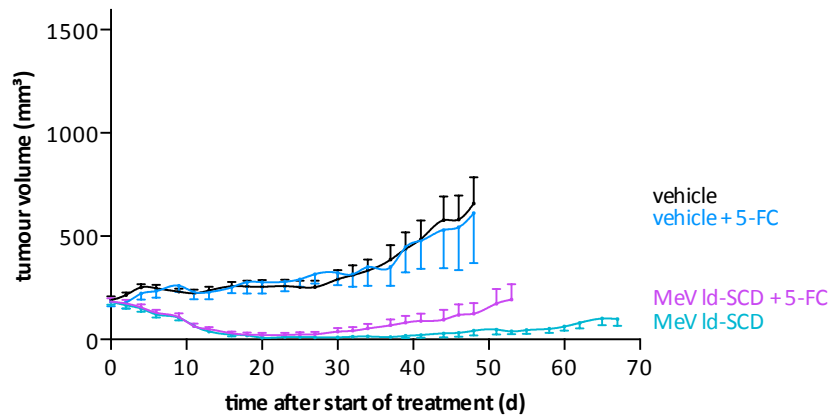


Figure 25. Antitumour effect of MeV Id-SCD + 5-fluorocytosine in a HuCCT1 human cholangiocarcinoma xenograft mouse model. When tumours reached a volume of approximately 100 mm^3 , mice were randomised into four treatment groups: vehicle control (12 mice), vehicle control + 5-FC (5 mice), MeV Id-SCD only (12 mice), and MeV Id-SCD + 5-FC (12 mice). Mice were treated daily for five days with intratumoural injections of MeV Id-SCD or vehicle control, followed by seven injections of 5-FC intraperitoneally (one per day). Mean tumour volume for each group \pm SEM is plotted until the first animal of each group had to be sacrificed. Reproduced from [1].

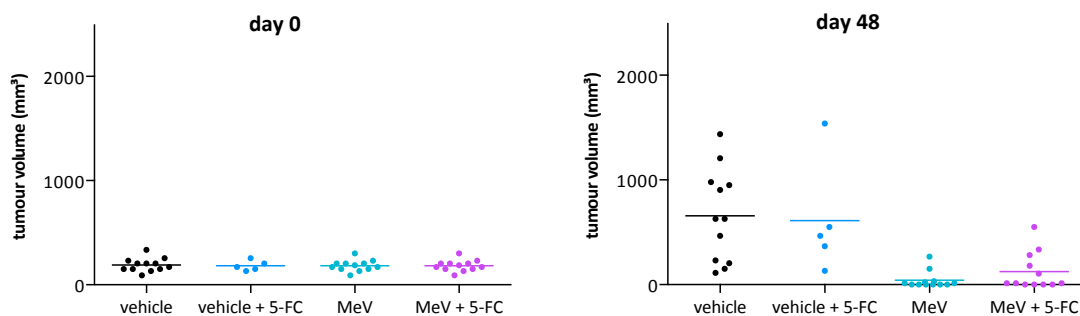


Figure 26. Individual tumour volumes of mice with HuCCT1 xenograft tumours treated with MeV Id-SCD + 5-fluorocytosine and corresponding controls at start of treatment and on day 48. The experimental setup is detailed in Figure 25. Tumour volumes for day 48 after start of treatment are plotted (this is the last day on which all mice from all treatment groups survived). When comparing groups with the Student's t-test, the differences of tumour volumes between vehicle control (vehicle) and MeV Id-SCD + 5-FC (MeV + 5-FC) as well as between vehicle control (vehicle) and MeV Id-SCD only (MeV) can be considered statistically significant ($p=0.0008$ and $p<0.0001$, respectively). Reproduced from [1].

Differences in the survival curves (Figure 27) between the different treatment groups were found: After 242 days, when the experiment was ended (timepoint was determined before starting the experiment), survival was 0/12 animals in the vehicle control group, 1/5 animals for vehicle control + 5-FC, 5/12 for MeV Id-SCD only, and 4/12 for treatment with MeV Id-SCD + 5-FC. There was a statistically significant survival benefit for mice treated with MeV Id-SCD and 5-FC (median survival 93 days) or with MeV Id-SCD only (196 days) compared with the untreated control (55 days; $p=0.0097$ and $p=0.0002$, respectively).

All taken together, our armed MeV vectors showed similar efficacy *in vivo* as in the cell culture experiments described in the beginning of the chapter. In both experiments, tumor mass was significantly smaller in the animals treated with the viruses. While survival could only be evaluated in one experiment, there was a significant survival benefit for the animals treated with MeV Id-SCD.

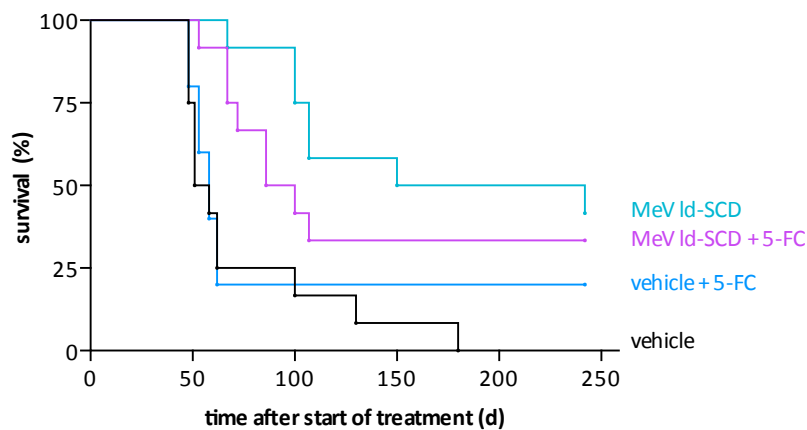


Figure 27. Kaplan-Meier survival curves of mice treated with MeV Id-SCD in combination with 5-fluorocytosine and corresponding controls. The experimental setup is detailed in Figure 25. Survival curves significantly differed between mice treated with MeV Id-SCD and 5-FC (median survival 93 days) or with MeV Id-SCD only (196 days) compared with the untreated control (55 days; $p=0.0097$ and $p=0.0002$, respectively). The difference between survival times of mice treated with MeV Id-SCD with or without the addition of 5-FC was not significant. Reproduced from [1].

CHAPTER 4

DISCUSSION

"Diagnosis of cholangiocarcinoma usually takes place late in the course of the disease, which either makes surgery not feasible or results in an incomplete resection of the tumour. Therefore, novel therapies against advanced stage cholangiocarcinoma are urgently needed. A multitude of new biological compounds are currently under development, involving e.g. targeted small molecules and immunotherapeutics. But so far, no significant, practice-changing improvement in treating this fatal disease has been achieved [16]." [1]

4.1 CD46 expression varies between cholangiocarcinoma cell lines

In our study, we demonstrated that human cholangiocarcinoma cell lines express the CD46 receptor (Section 3.1), which is the entry gateway for the measles vaccine virus and is required for efficient MeV-mediated oncolysis. It had been shown previously that the density of CD46 receptors on the cell membrane is important for virus entry and syncytia formation [92]. In this respective study, the mean fluorescence index was used as a surrogate marker for CD46 receptor density, and a value between 25 and 50 was needed for substantial MeV-mediated oncolysis.

In our study, the CD46 receptor density was lowest on HuCCT1 cells (mean fluorescence index of 36), which in the following experiments proved to be the most resistant to MeV oncolysis alone, i.e. without additional application of 5-FC. This correlation between the cytopathic effect and CD46 expression was previously observed by Berchtold et al. [143], as well. Here, MeV Id-SCD was tested against human

sarcoma cell lines. Three cell lines were defined as 'primary resistant' to oncolysis (remaining cell mass > 50% after 96 hours as determined by SRB assay), and the mean fluorescence index of CD46 was between 20 and 40 for these cells (lower than the susceptible cell lines). In our study, HuCCT1 was the only cell line with a minimum mean fluorescence index < 50, and, under the criteria defined previously, is the only 'primary resistant' cell line exhibiting a 'primary resistance' to infection by MeV.

Nevertheless, low CD46 receptor density very likely does not constitute the only mechanism of resistance to MeV oncolysis. This was demonstrated by Noll et al. [144], where cell lines from solid tumours present in the well-characterised NCI-60 panel (a panel of 60 human tumour cell lines [145]) were screened systematically for resistance to MeV Id-SCD oncolysis. Six cell lines were highly resistant to oncolysis (remaining cell mass > 75% after 96 hours as determined by SRB assay), but no correlation to CD46 expression could be observed.

So far, the mechanisms of resistance to MeV infection and oncolysis have not been unraveled in detail. What seems evident is that innate immunity, especially the induction of an antiviral state of the host cell mediated by the interferon pathway plays a major role in this phenomenon [94, 143].

4.2 Susceptible cell lines exhibit different growth characteristics

Evaluation of the cytopathic effect of MeV infection by light and fluorescence microscopy revealed clear differences between the three cell lines (Section 3.2). These differences in rates of primary infection and spread of MeV P-SCD were reflected by all further *in vitro* experiments, as well (Sections 3.2, 3.4 and 3.5). Overall, RBE and TFK-1 were consistently more susceptible to infection than HuCCT1.

Infection of RBE cells with MeV P-DsRed was found to yield comparable amounts of cell-bound and free virus to TFK-1 cells up until 48 hours post-infection. Then, while the amount of virus produced still increases exponentially in RBE cells, virus production in TFK-1 cells was found to slow down (resulting in a 100-fold

difference in the amount of infectious viral particles being present at 96 hours (Section 3.4)).

We believe that a combination of two factors is responsible for some of the differences observed in the two susceptible cell lines:

First, we found that, two days after infection with MeV P-SCD at an MOI of 1 (Figure 13), a large number of TFK-1 cells had already detached from the well bottom, indicating an early loss of plasma membrane integrity. Additionally, in the cytotoxicity assays, MeV P-SCD caused an increased oncolytic effect in TFK-1 cells compared with RBE cells at all virus concentrations. This pronounced cytopathic effect of the virus on TFK-1 cells leads to a substantial cell death at 48 hpi which decreases virus production.

Second, direct cell-cell contact is a prerequisite for syncytia formation, which is impeded in TFK-1 cells: RBE cells form an adherent monolayer during the exponential growth phase covering the complete well bottom when allowed sufficient time to grow. In contrast, TFK-1 cells, even several days after seeding, form patches of cells without complete floor coverage (please refer to Figure 9 for light microscopy images). An indirect method of evaluating the rate of syncytia formation is comparing the rate of increase in DsRed-positive cells (Figure 17) after infection with a very small amount of DsRed-encoding virus (i.e. MOI 0.01). After 48 hours, the percentage of DsRed-positive cells is negligible in both cell lines; however, after 72 hours, the difference is significant: 45% of RBE cells and 7% of TFK-1 cells express DsRed (compare Figure 17).

4.3 Resistance to MeV oncolysis can be overcome by prodrug-mediated activation of the MeV-encoded SuperCD suicide gene function

As described in the previous section, HuCCT1 cells were more resistant to MeV infection and oncolysis than RBE and TFK-1, which were described in the previous section. After infection with MeV P-SCD at an MOI of 1, HuCCT1 cell mass remained at 88% of the control after four days, which was significantly higher than

for RBE (32%) and TFK-1 (10%) cells. This might be an effect of lower CD46 expression (as explained in [Section 4.1](#)) that leads to lower rates of primary infection ([Section 3.5](#)) and reduced syncytia formation ([Section 3.2](#)). Therefore, this cell line might best reflect the additional benefit of the suicide gene/prodrug combination, as the other two cell lines were very susceptible to MeV oncolysis per se, thereby providing 'not enough additional space' for a significant further improvement of tumour cell killing.

First, we tested the cytotoxic effect of 5-fluorouracil (the intermediate reagent produced by SuperCD) alone ([Section 3.6](#)). The first substantial changes in cell mass occurred at a concentration of 0.001 mM. In further experiments, we found that the cell mass of all cholangiocarcinoma cell lines was reduced to less than 20% of the control after four days at the maximal concentration of 1 mM 5-FU.

It was shown earlier by our group [115] that prodrug conversion by MeV Id-SCD is extremely efficient. In this study, hepatoma cells were infected with MeV Id-SCD at an MOI of 0.01. Conversion of 1 mM 5-FC to 5-FU or a subsequent byproduct was determined by reverse-phase high-performance liquid chromatography. Complete conversion was achieved after 24 hours in Hep3B cells and after 48 hours in HepG2 cells (it was noted by the authors that 'HepG2 cells were found to be less sensitive towards the virus').

Before initiation of the experiments with our human cholangiocarcinoma cell lines, we speculated that the combination of sensitivity to 5-FU alone as well as the rapid conversion of the prodrug into its toxic form should substantially enhance cell killing. Indeed, this hypothesis was found to be supported by the results of two different cytotoxicity assays ([Figures 19 and 20](#), summarised in [Table 4](#)). The addition of 1 mM 5-FC to HuCCT1 cells decreased the remaining cell mass after four days from 88% to 4% of the control when infected with MeV P-SCD at MOI 1. Similarly, treatment of MeV P-SCD-infected RBE and TFK-1 with 5-FC led to increased cytotoxicity.

4.4 Armed MeV reduces tumour growth and prolongs survival in mice

In vivo, we showed that the tumour volume of mice bearing TFK-1 tumours, treated with MeV P-SCD in combination with 5-FC, was significantly reduced compared to mock-treated controls. Unfortunately, survival in this model could not be evaluated due to the development of necrosis in the tumours (Section 3.9).

"Survival of HuCCT1 tumour-bearing mice was significantly prolonged compared with mock controls when treated with MeV Id-SCD alone or in combination with 5-FC (Section 3.10). However, in this tumour model, we did not observe superior effects of the combination therapy compared with treatment with virus alone. This missing enhancement of tumour cell killing when making use of our suicide gene armament might have been due to several reasons:" [1]

(1) "SuperCD-mediated conversion of 5-FC into 5-FU and toxic metabolites might have been insufficient. However, when employing reverse-phase high-performance liquid chromatography for a direct quantification of 5-FC conversion into newly produced 5-FU, an almost complete conversion within 24 hours was measured *in vitro*, even when concentrations up to 1 mM 5-FC were used (as described in Section 4.3). Thus, we conclude that our 5-FC prodrug convertase SuperCD is strong enough to produce sufficient levels of 5-FU in tumour cells, at least under *in vitro* conditions." [1]

"Interestingly, in the context of a vaccinia virus-based expression of FCU1 (which is 100% identical to our SuperCD suicide gene), a maximum concentration of 5.5 ng 5-FU/mg tumour tissue has been observed at 3-8 days post-infection in xenograft human colon carcinoma tumours at one hour after daily single oral dosing of 100 mg/kg 5-FC [146]. This local concentration of 5-FU was calculated as being 20 times higher than the 5-FU concentrations being achieved when applying 5-FU systemically under the conditions of standard chemotherapy protocols. Thus, there is strong evidence that SuperCD/FCU1 constitutes a highly effective system for the

intratumoural conversion of 5-FC into 5-FU under both *in vitro* and *in vivo* conditions." [1]

This confirms earlier studies by Pederson et al. and Stackhouse et. al.: Here, SK-ChA-1 cholangiocarcinoma cells were transduced with an adenovirus vector encoding *E. coli cytosine deaminase* and successfully treated with 5-FC [116, 117]. Additionally, Kojima et al. showed that infection of HuCCT1 cells with an adenovirus expressing *uracil phosphoribosyltransferase* enhances cytotoxicity of 5-FU [118].

(2) "In principle, there might also be a basal inability of 5-FU to kill tumour cells of human cholangiocarcinoma origin. However, when we directly incubated our selected human cholangiocarcinoma cell lines with 5-FU, concentrations as low as 0.1 - 0.01 mM 5-FU were found to reduce the tumour cell mass in all three cell lines to 50% of the control. Furthermore, an almost complete cell killing was achieved at a concentration of 1 mM 5-FU (Section 4.3). These results were found to be quite comparable with the results that were achieved in human hepatoma cell lines by Lampe et al., being also of primary liver origin [115]. Thus, we conclude that 5-FU is functionally active in human cholangiocarcinomas." [1]

(3) "Dosing of 5-FC might have been suboptimal under our current regime applying a 5-FC standard dose of 500 mg/kg body weight, which is quite often used in mouse xenograft tumour models [147, 148]. However, in a recent pre-clinical study, animal groups treated with adenovirus-based vectors (Ad-FCU1) exhibited statistically significant differences in tumour sizes between the group treated with Ad-FCU1 plus 5-FC and the other groups only when 5-FC was given at 1,000 mg/kg body weight per day. Specifically, at 500 and 200 mg/kg body weight per day, no effects of the suicide gene therapy were observed [146]." [1]

"Therefore, one other explanation for our failure to reproduce the effects observed *in vitro* of our prototypic MeV-based virotherapeutic MeV Id-SCD in the HuCCT1 xenograft mouse model could be an underdosing of the 5-FC prod-

rug: 1,000 mg/kg body weight per day could potentially be much more effective than 500 mg/kg body weight per day. However, this should only be true if this high-dose regimen would not be accompanied by a 5-FC-based systemic toxicity which already has been described for this dosing in a prior study [149]."

[1]

(4) "Timing of 5-FC prodrug application might have been suboptimal under our current regime, starting with the 5-FC application after only five days of consecutive vector application. This procedure was inferred from the postulate that early prodrug administration potentially leads to an early abrogation of virus replication [96, 97, 150, 151]. This is supported by the results of a recent systematic dissection of which specific timing of prodrug addition would be optimal in a human xenograft setting when making use of a vector-encoded suicide gene by systemic application of a respective prodrug:" [1] when using a replication-conditional HSV-1-based virotherapeutic vector expressing *yeast cytosine deaminase*, it was observed that 5-FC administration on the day of peak viral replication (three days after intratumoural infection) led to a greater tumour cell killing than any earlier or later 5-FC administration both *in vitro* and *in vivo* [152].

Ungerechts et al. showed that the optimal treatment schedule for the same vector (a CD20-targeted measles vaccine virus armed with *Escherichia coli purine nucleoside phosphorylase*) differs greatly in two similar tumour models (non-Hodgkin's lymphoma and mantle cell lymphoma) [96, 97].

"In general, the optimal time point for prodrug administration might be when virus replication is at its peak. However, it seems very likely that different treatment schedules have to be developed for each combination of tumour entity, virus and encoded suicide gene(s). Pinpointing the exact moment of peak virus replication in each and every tumour patient would require vector-encoded tracking tools (e.g., soluble marker proteins such as carcinoembryonic antigen [153] or membrane channel proteins such as sodium-iodide-symporter [154]) that would enable the repetitive monitoring of virus replication and gene expression in a non-invasive manner." [1]

In our study, we did not measure the viral growth kinetics *in vivo* and based our schedule on older studies employing measles vaccine virus. However, these viruses were not armed with SuperCD. In 2012, after completion of our experiments, Zaoui et al. investigated the treatment of head and neck squamous cell carcinoma with an EGFR-targeted oncolytic measles virus expressing both *E. coli cytosine deaminase* and *uracil phosphoribosyltransferase* [107]. In a xenograft mouse model, the researchers injected the vector intratumourally for five consecutive days and, two days after the last virus injection, started treatment with 5-FC intraperitoneally, following a similar schedule to our study with good efficacy.

"Another aspect is that long-term MeV replication in human xenograft tumours has been observed previously [115, 153]. In these animals, repeated administration of the prodrug alone might be beneficial, whereas in other animals exhibiting continuous tumour growth with no signs of ongoing viral replication, additional cycles of virus plus optimised administration of the respective prodrug might be required to cause late-stage tumour regressions. It is of interest that repeated cycling has already been applied successfully for MeV in the treatment of xenograft lymphomas [97]." [1]

"In our preliminary *in vitro* experiments (data not shown), we found that an early administration of 5-FC (i.e., already at 3 hpi) yields much better results in terms of oncolytic efficiency than any later administration (i.e. at 24 - 72 hpi)." [1] However, other studies from our group showed that delayed addition of the prodrug enhances the overall effect on tumour mass in some cell lines as well: Lampe et al. determined that 48 hours-post infection was the most efficient time point in the Hep3B hepatoma cell line, yet not superior in two other hepatoma cell lines (PLC/PRF/5 and HepG2) [115].

Another work from our group aimed to further optimise prodrug delivery [155]. Importantly, this study showed that the major determinant of cell mass reduction by SuperCD-armed MeV and 5-FC is not the time span between infection and prodrug addition, but the overall time span in which 5-FC (and subsequently 5-FU) is allowed to take effect on the tumour cells.

CHAPTER 5

SUMMARY

"Cholangiocarcinoma is curable only in its early stages by complete surgical resection. Thus, in advanced disease stages in which a complete removal of the tumour mass is no longer possible and palliative chemotherapy only achieves modest success, therapeutics employing new methods of action are needed. Oncolytic viruses employed in clinical studies have been shown to preferentially infect cancer cells. Beyond that, virotherapeutic cell killing can be enhanced by virus-based expression of suicide genes that convert non-toxic prodrugs into toxic reagents." [1]

The aim of this thesis was to evaluate an oncolytic measles vaccine virus expressing SuperCD, a fusion protein of *yeast cytosine deaminase* and *yeast uracil phosphoribosyltransferase* that converts the prodrug 5-fluorocytosine to 5-fluorouracil, an approved chemotherapeutic. This vector was evaluated using three different human cholangiocarcinoma cell lines.

"*In vitro*, all cholangiocarcinoma cell lines were found to be permissive to MeV infection. Partial blocking of MeV-mediated oncolysis could be overcome by utilisation of the SuperCD transgene together with administration of the prodrug 5-fluorocytosine." [1]

In vivo, intratumoural application of SuperCD-armed measles vaccine virus together with a systemic 5-fluorocytosine treatment showed a significant reduction in tumour size in a TFK-1 xenograft mouse model when compared with virus-only treatment. In a second animal experiment employing a HuCCT1

xenograft tumour model, an enhanced SuperCD-armed MeV vector, in which the SuperCD transgene was expressed from a different genomic position, not only led to reduced tumour volumes, but also to a significant survival benefit.

These highly interesting results pave the way to a first phase I trial employing our virotherapeutic vector (MeV Id-SCD) plus oral application of 5-FU in patients with advanced, non-resectable cholangiocarcinoma.

CHAPTER 6

MATERIALS

6.1 Consumables

| | |
|---|----------------------|
| Caliper 150 mm | Brüder Mannesmann |
| Cell scrapers | Corning |
| Centrifuge tubes 15/50 ml | Corning |
| Combitips 1/5/10/50 ml | Eppendorf |
| Cryogenic vials, internal thread | Corning |
| Decosept AF | Dr. Schumacher |
| Filter tips 10/100/200/1000 μ l | Biozym Scientific |
| Forceps | Servoprax |
| Hybond-P | Amersham Biosciences |
| Hyperfilm ECL | Amersham Biosciences |
| Microtiter plates 96 well | Greiner Bio-One |
| Needles 27G/22G | BD Medical |
| Pasteur Pipettes | Wilhelm Ulbrich |
| Photo Film | Fujifilm |
| Pipet tips 10/200/1000 μ l | Carl Roth |
| Round bottom tubes 14 ml | Corning |
| Safe-lock reaction tubes 0.5/1/2 ml | Eppendorf |
| Safe-lock reaction tubes, amber, 1.5/2 ml | Eppendorf |
| Scalpels | B. Braun |
| Sekusept plus | ecolab |
| Serological pipettes 1/2/5/10/25/50 ml | Corning |
| Syringes 1/10 ml | B. Braun |
| Tissue culture dishes 10 cm | Corning |
| Tissue culture dishes 6/15 cm | Corning |
| Tissue culture flasks 25/75/175 cm ² | Corning |
| Tissue culture plates 6/12/24/48/96 well | Corning |

6.2 Reagents

| | |
|-----------------------------------|------------------------------|
| 5-Fluorocytosine | Sigma-Aldrich |
| 5-Fluorouracil | Sigma-Aldrich |
| 0.1% Triton X-100 | Carl Roth |
| Accutase | Innovative Cell Technologies |
| Acrylamid Rotiphorese Gel 30 | Carl Roth |
| Bradford dye reagent | Bio-Rad |
| Dimethyl sulfoxide | Carl Roth |
| DMEM | Sigma-Aldrich |
| Phosphate-buffered saline | PAA Laboratories |
| Fetal bovine serum | PAA Laboratories |
| Formaldehyd | Carl Roth |
| Full Range Rainbow Protein Marker | Amersham Biosciences |
| Isopropanol | Merck |
| LDH P-mono | Analyticon Biotechnologies |
| MycoTOOL PCR Mycoplasma | Roche |
| Nonidet-P40 | Carl Roth |
| Opti-MEM | Gibco |
| Rotiblock | Carl Roth |
| Roti Load Puffer | Carl Roth |
| RPMI-1640 | PAA Laboratories |
| Sulforhodamine B | Sigma-Aldrich |
| Tris | Carl Roth |
| Trypsin-EDTA (0.05%) | PAA Laboratories |
| Tween 20 | Promega |

6.3 Animals

| | |
|--|----------------------------|
| CanN.Cg-Foxn1 ^{nu} /Crl mice | Charles River Laboratories |
| Hsd:Atymic Nude-Foxn1 ^{nu} mice | Harlan Laboratories |

6.4 Manufacturers

| | |
|------------------------------------|-----------------------------|
| Amersham Biosciences/GE Healthcare | München, Germany |
| Analyticon Biotechnologies | Lichtenfels, Germany |
| BD Medical | Heidelberg, Germany |
| Bio-Rad | München, Germany |
| Biozym Scientific | Hessisch Oldendorf, Germany |
| B. Braun | Melsungen, Germany |
| Carl Roth | Karlsruhe, Germany |

| | |
|------------------------------|-----------------------------|
| Charles River Laboratories | Sulzfeld, Germany |
| Corning | Wiesbaden, Germany |
| Dr. Schumacher | Melsungen, Germany |
| ecolab | Monheim am Rhein, Germany |
| Eppendorf | Wesseling-Berzdorf, Germany |
| Fujifilm | Düsseldorf, Germany |
| Gibco/Thermo Fischer | Waltham, MA, USA |
| Greiner Bio-One | Frickenhausen, Germany |
| Harlan Laboratories | Venray, Netherlands |
| Innovative Cell Technologies | San Diego, CA, USA |
| Brüder Mannesmann | Remscheid, Germany |
| Merck | Darmstadt, Germany |
| Millipore | Schwalbach, Germany |
| PAA Laboratories | Pasching, Austria |
| Promega | Mannheim, Germany |
| Roche | Basel, Switzerland |
| Servoprax | Wesel, Germany |
| Sigma-Aldrich | München, Germany |
| Systemc | Wettenberg, Germany |
| Wilhelm Ulbrich | Bamberg, Germany |

CHAPTER 7

REFERENCES

- [1] S. Lange, J. Lampe, S. Bossow, M. Zimmermann, W. Neubert, M. Bitzer, and U. M. Lauer. **A novel armed oncolytic measles vaccine virus for the treatment of cholangiocarcinoma.** *Hum. Gene Ther.*, 24(5):554–64, 2013. [p. 3, 4, 11, 13, 16, 17, 22, 29, 32, 33, 34, 35, 36, 37, 38, 40, 41, 42, 43, 44, 47, 48, 49, 50, 51, 52, 56, 57, 58, 59, 60]
- [2] A. Nakeeb, H. A. Pitt, T. A. Sohn, J. Coleman, R. A. Abrams, S. Piantadosi, R. H. Hruban, K. D. Lillemoe, C. J. Yeo, and J. L. Cameron. **Cholangiocarcinoma. A spectrum of intrahepatic, perihilar, and distal tumors.** *Ann. Surg.*, 224(4):463–73; discussion 473–5, 1996. [p. 4]
- [3] T. Patel. **Worldwide trends in mortality from biliary tract malignancies.** *BMC Cancer*, 2:10, 2002. [p. 4]
- [4] A. Jemal, F. Bray, M. M. Center, J. Ferlay, E. Ward, and D. Forman. **Global cancer statistics.** *CA. Cancer J. Clin.*, 61(2):69–90, 2011. [p. 4]
- [5] I. Endo, M. Gonen, A. C. Yopp, K. M. Dalal, Q. Zhou, D. Klimstra, M. D’Angelica, R. P. DeMatteo, Y. Fong, L. Schwartz, N. Kemeny, E. O’Reilly, G. K. Abou-Alfa, H. Shimada, L. H. Blumgart, and W. R. Jarnagin. **Intrahepatic cholangiocarcinoma: rising frequency, improved survival, and determinants of outcome after resection.** *Ann. Surg.*, 248(1):84–96, 2008. [p. 4]
- [6] T. Patel. **Increasing incidence and mortality of primary intrahepatic cholangiocarcinoma in the United States.** *Hepatology*, 33(6):1353–7, 2001. [p. 4]

- [7] Y. Shaib and H. B. El-Serag. **The epidemiology of cholangiocarcinoma.** *Semin. Liver Dis.*, 24(2):115–25, 2004. [p. 4]
- [8] W. C. Palmer and T. Patel. **Are common factors involved in the pathogenesis of primary liver cancers? A meta-analysis of risk factors for intrahepatic cholangiocarcinoma.** *J. Hepatol.*, 57(1):69–76, 2012. [p. 4]
- [9] S. A. Khan, H. C. Thomas, B. R. Davidson, and S. D. Taylor-Robinson. **Cholangiocarcinoma.** *Lancet*, 366(9493):1303–14, 2005. [p. 4]
- [10] R. Siegel, D. Naishadham, and A. Jemal. **Cancer statistics, 2012.** *CA. Cancer J. Clin.*, 62(1):10–29, 2012. [p. 4]
- [11] S. Mosconi, G. D. Beretta, R. Labianca, M. G. Zampino, G. Gatta, and V. Heinemann. **Cholangiocarcinoma.** *Crit. Rev. Oncol. Hematol.*, 69(3):259–70, 2009. [p. 4, 5]
- [12] M. L. DeOliveira, S. C. Cunningham, J. L. Cameron, F. Kamangar, J. M. Winter, K. D. Lillemoe, M. A. Choti, C. J. Yeo, and R. D. Schulick. **Cholangiocarcinoma.** *Ann. Surg.*, 245(5):755–762, 2007. [p. 4]
- [13] N. Akamatsu, Y. Sugawara, and D. Hashimoto. **Surgical strategy for bile duct cancer: Advances and current limitations.** *World J. Clin. Oncol.*, 2(2):94–107, 2011. [p. 4]
- [14] T. Todoroki, K. Ohara, T. Kawamoto, N. Koike, S. Yoshida, H. Kashiwagi, M. Otsuka, and K. Fukao. **Benefits of adjuvant radiotherapy after radical resection of locally advanced main hepatic duct carcinoma.** *Int. J. Radiat. Oncol. Biol. Phys.*, 46(3):581–7, 2000. [p. 4]
- [15] H. K. Gwak, W. C. Kim, H. J. Kim, and J. H. Park. **Extrahepatic bile duct cancers: surgery alone versus surgery plus postoperative radiation therapy.** *Int. J. Radiat. Oncol. Biol. Phys.*, 78(1):194–8, 2010. [p. 4]
- [16] J. R. A. Skipworth, S. W. M. Olde Damink, C. Imber, J. Bridgewater, S. P. Pereira, and M. Malagó. **Review article: surgical, neo-adjuvant and adjuvant management strategies in biliary tract cancer.** *Aliment. Pharmacol. Ther.*, 34(9):1063–1078, 2011. [p. 5, 52]
- [17] J. Valle, H. Wasan, D. H. Palmer, D. Cunningham, A. Anthony, A. Maraveyas, S. Madhusudan, T. Iveson, S. Hughes, S. P. Pereira, M. Roughton, and

- J. Bridgewater. **Cisplatin plus gemcitabine versus gemcitabine for biliary tract cancer.** *N. Engl. J. Med.*, 362(14):1273–81, 2010. [p. 5]
- [18] M. S. Noel and A. F. Hezel. **New and emerging treatment options for biliary tract cancer.** *Onco. Targets. Ther.*, 6:1545–52, 2013. [p. 5]
- [19] M. Richardson, D. Elliman, H. Maguire, J. Simpson, and A. Nicoll. **Evidence base of incubation periods, periods of infectiousness and exclusion policies for the control of communicable diseases in schools and preschools.** *Pediatr. Infect. Dis. J.*, 20(4):380–91, 2001. [p. 5]
- [20] L. J. Wolfson, R. F. Grais, F. J. Luquero, M. E. Birmingham, and P. M. Strebel. **Estimates of measles case fatality ratios: a comprehensive review of community-based studies.** *Int. J. Epidemiol.*, 38(1):192–205, 2009. [p. 5]
- [21] K. Baczko, U. G. Liebert, M. A. Billeter, R. Cattaneo, H. Budka, and V. ter Meulen. **Expression of defective measles virus genes in brain tissues of patients with subacute sclerosing panencephalitis.** *J. Virol.*, 59(2):472–8, 1986. [p. 5]
- [22] H. Q. McLean, A. P. Fiebelkorn, J. L. Temte, G. S. Wallace, and Centers for Disease Control and Prevention. **Prevention of measles, rubella, congenital rubella syndrome, and mumps, 2013: summary recommendations of the Advisory Committee on Immunization Practices (ACIP).** *MMWR. Recomm. Rep.*, 62(RR-04):1–34, 2013. [p. 5]
- [23] B. Rice. **Image No. 132, Child with characteristic Measles Rash after 4 days.** *Public Heal. Image Libr. Centers Dis. Control.* [p. 6]
- [24] B. W. J. Mahy. **Image No. 12785, Child with characteristic Measles Rash on head, neck and chest.** *Public Heal. Image Libr. Centers Dis. Control.* [p. 6]
- [25] J. F. Enders and T. C. Peebles. **Propagation in tissue cultures of cytopathogenic agents from patients with measles.** *Proc. Soc. Exp. Biol. Med.*, 86(2):277–86, 1954. [p. 6]
- [26] J. F. Enders, S. L. Katz, M. V. Milovanovic, and A. Holloway. **Studies on an attenuated measles-virus vaccine. I. Development and preparations of the vaccine: technics for assay of effects of vaccination.** *N. Engl. J. Med.*, 263:153–9, 1960. [p. 6]

- [27] A. J. Schwarz. **Preliminary tests of a highly attenuated measles vaccine.** *Am. J. Dis. Child.*, 103:386–9, 1962. [p. 6, 17]
- [28] J. S. Rota, Z. D. Wang, P. A. Rota, and W. J. Bellini. **Comparison of sequences of the H, F, and N coding genes of measles virus vaccine strains.** *Virus Res*, 31(3):317–330, 1994. [p. 6]
- [29] D. E. Griffin, C.-H. Pan, and W. J. Moss. **Measles vaccines.** *Front. Biosci.*, 13:1352–70, 2008. [p. 6, 11]
- [30] L. J. Wolfson, P. M. Strebel, M. Gacic-Dobo, E. J. Hoekstra, J. W. McFarland, and B. S. Hersh. **Has the 2005 measles mortality reduction goal been achieved? A natural history modelling study.** *Lancet*, 369(9557):191–200, 2007. [p. 6]
- [31] H. Neuhauser. **Empfehlungen der Ständigen Impfkommision (STIKO) am RKI-Stand:August 2015.** *Epidemiol. Bull.*, (34):105–114, 2015. [p. 6]
- [32] Centers for Disease Control and Prevention (CDC). **Summary of notifiable diseases, United States, 1993.** *MMWR. Morb. Mortal. Wkly. Rep.*, 42(53):i–xvii; 1–73, 1994. [p. 7]
- [33] D. A. Adams, K. M. Gallagher, R. A. Jajosky, J. Kriseman, P. Sharp, W. J. Anderson, A. E. Aranas, M. Mayes, M. S. Wodajo, D. H. Onweh, J. P. Abellera, and C. Division of Notifiable Diseases and Healthcare Information, Office of Surveillance, Epidemiology, and Laboratory Services. **Summary of Notifiable Diseases - United States, 2011.** *MMWR. Morb. Mortal. Wkly. Rep.*, 60(53):1–117, 2013. [p. 7]
- [34] R. A. Lamb and G. D. Parks. **Paramyxoviridae: The Viruses and Their Replication.** *Fields Virol.* 5th Ed., pages 1449–1493. 2007. [p. 7, 8, 9, 10]
- [35] B. W. J. Mahy. **Image No. 12733, Ultrastructural Appearance of the Measles Virus.** *Public Heal. Image Libr. Centers Dis. Control.* [p. 7]
- [36] R. Cattaneo and M. McChesney. **Measles Virus.** *Encycl. Virol.* 2008. [p. 8]
- [37] D. E. Griffin. **Measles Virus.** *Fields Virol.* 5th Ed., pages 1551–1585. 2007. [p. 9]
- [38] D. Nanche, G. Varior-Krishnan, F. Cervoni, T. F. Wild, B. Rossi, C. Roubourdin-Combe, and D. Gerlier. **Human membrane cofactor protein (CD46) acts as a cellular receptor for measles virus.** *J. Virol.*, 67(10):6025–32, 1993. [p. 9]

- [39] R. E. Dorig, A. Marcil, A. Chopra, and C. D. Richardson. **The human CD46 molecule is a receptor for measles virus (Edmonston strain)**. *Cell*, 75(2):295–305, 1993. [p. 9]
- [40] E. C. Hsu, C. Iorio, F. Sarangi, A. A. Khine, and C. D. Richardson. **CDw150(SLAM) is a receptor for a lymphotropic strain of measles virus and may account for the immunosuppressive properties of this virus**. *Virology*, 279(1):9–21, 2001. [p. 9]
- [41] H. Tatsuo, N. Ono, K. Tanaka, and Y. Yanagi. **SLAM (CDw150) is a cellular receptor for measles virus**. *Nature*, 406(6798):893–897, 2000. [p. 9]
- [42] M. D. Mühlebach, M. Mateo, P. L. Sinn, S. Prüfer, K. M. Uhlig, V. H. J. Leonard, C. K. Navaratnarajah, M. Frenzke, X. X. Wong, B. Sawatsky, S. Ramachandran, P. B. McCray, K. Cichutek, V. von Messling, M. Lopez, and R. Cattaneo. **Adherens junction protein nectin-4 is the epithelial receptor for measles virus**. *Nature*, 480(7378):530–3, 2011. [p. 9]
- [43] R. S. Noyce, D. G. Bondre, M. N. Ha, L.-T. Lin, G. Sisson, M.-S. Tsao, and C. D. Richardson. **Tumor cell marker PVRL4 (nectin 4) is an epithelial cell receptor for measles virus**. *PLoS Pathog.*, 7(8):e1002240, 2011. [p. 9]
- [44] R. Cattaneo, G. Reibmann, K. Baczko, V. ter Meulen, and M. A. Billeter. **Altered ratios of measles virus transcripts in diseased human brains**. *Virology*, 160(2):523–6, 1987. [p. 9, 10]
- [45] R. Cattaneo, G. Reibmann, A. Schmid, K. Baczko, V. ter Meulen, and M. A. Billeter. **Altered transcription of a defective measles virus genome derived from a diseased human brain**. *EMBO J.*, 6(3):681–8, 1987. [p. 9]
- [46] B. M. Blumberg, M. Leppert, and D. Kolakofsky. **Interaction of VSV leader RNA and nucleocapsid protein may control VSV genome replication**. *Cell*, 23(3):837–845, 1981. [p. 9]
- [47] S. Vidal and D. Kolakofsky. **Modified model for the switch from Sendai virus transcription to replication**. *J. Virol.*, 63(5):1951–1958, 1989. [p. 9]
- [48] S. N. Manié, S. de Breyne, S. Vincent, and D. Gerlier. **Measles virus structural components are enriched into lipid raft microdomains: a potential cellular location for virus assembly**. *J. Virol.*, 74(1):305–311, 2000. [p. 10]

- [49] G. F. Rall, M. Manchester, L. R. Daniels, E. M. Callahan, a. R. Belman, and M. B. Oldstone. **A transgenic mouse model for measles virus infection of the brain.** *Proc. Natl. Acad. Sci. U. S. A.*, 94(9):4659–4663, 1997. [p. 10]
- [50] B. Mrkic, J. Pavlovic, T. Rulicke, P. Volpe, C. J. Buchholz, D. Hourcade, J. P. Atkinson, A. Aguzzi, and R. Cattaneo. **Measles virus spread and pathogenesis in genetically modified mice.** *J. Virol.*, 72(9):7420–7427, 1998. [p. 10]
- [51] N. Moran. **First gene therapy approved.** *Nat. Biotechnol.*, 30(12):Preface, 2012. [p. 10]
- [52] D. Gaudet, J. Méthot, S. Déry, D. Brisson, C. Essiembre, G. Tremblay, K. Tremblay, J. de Wal, J. Twisk, N. van den Bulk, V. Sier-Ferreira, and S. van Deventer. **Efficacy and long-term safety of alipogene tiparvovec (AAV1-LPL(S447X)) gene therapy for lipoprotein lipase deficiency: an open-label trial.** *Gene Ther.*, (July 2011):1–9, 2012. [p. 10]
- [53] J. Bell and G. McFadden. **Viruses for Tumor Therapy.** *Cell Host Microbe*, 15(3):260–265, 2014. [p. 10, 11]
- [54] K. K. Sanford, W. R. Earle, and G. D. Likely. **The growth in vitro of single isolated tissue cells.** *J. Natl. Cancer Inst.*, 9(3):229–46, 1948. [p. 11]
- [55] A. E. Moore. **The destructive effect of the virus of Russian Far East encephalitis on the transplantable mouse sarcoma 180.** *Cancer*, 2(3):525–34, 1949. [p. 11]
- [56] H. Koprowski and T. W. Norton. **Interference between certain neurotropic viruses and transplantable mouse tumors.** *Cancer*, 3(5):874–85, 1950. [p. 11]
- [57] E. Kelly and S. J. Russell. **History of oncolytic viruses: genesis to genetic engineering.** *Mol. Ther.*, 15(4):651–9, 2007. [p. 11]
- [58] T.-C. C. Liu, E. Galanis, and D. Kirn. **Clinical trial results with oncolytic virotherapy: a century of promise, a decade of progress.** *Nat. Clin. Pract. Oncol.*, 4(2):101–17, 2007. [p. 11]
- [59] H. A. Hoster, R. P. Zanes, and E. von Haam. **Studies in Hodgkin’s syndrome; the association of viral hepatitis and Hodgkin’s disease; a preliminary report.** *Cancer Res.*, 9(8):473–80, 1949. [p. 11]

- [60] G. K. Higgins and G. T. Pack. **Virus therapy in the treatment of tumors.** Bull. Hosp. Joint Dis., 12(2):379–82, 1951. [p. 11]
- [61] C. M. Southam and A. E. Moore. **West Nile, Ilheus, and Bunyamwera virus infections in man.** Am. J. Trop. Med. Hyg., 31(6):724–41, 1951. [p. 11]
- [62] C. M. Southam and A. E. Moore. **Clinical studies of viruses as antineoplastic agents with particular reference to Egypt 101 virus.** Cancer, 5(5):1025–34, 1952. [p. 11]
- [63] J. Georgiades, T. Zielinski, A. Cicholska, and E. Jordan. **Research on the oncolytic effect of APC viruses in cancer of the cervix uteri; preliminary report.** Biul. Inst. Med. Morsk. Gdansk., 10:49–57, 1959. [p. 11]
- [64] T.-C. Liu and D. Kirn. **Gene therapy progress and prospects cancer: oncolytic viruses.** Gene Ther., 15(12):877–84, 2008. [p. 11]
- [65] C. E. Thomas, A. Ehrhardt, and M. a. Kay. **Progress and problems with the use of viral vectors for gene therapy.** Nat. Rev. Genet., 4(5):346–58, 2003. [p. 11]
- [66] National Institutes of Health Recombinant DNA Advisory Committee. **Assessment of adenoviral vector safety and toxicity: report of the National Institutes of Health Recombinant DNA Advisory Committee.** Hum. Gene Ther., 13(1):3–13, 2002. [p. 11]
- [67] Centers for Disease Control and Prevention. **Update: adverse events following civilian smallpox vaccination—United States, 2003.** MMWR. Morb. Mortal. Wkly. Rep., 53(5):106–7, 2004. [p. 11]
- [68] J. M. Lane, F. L. Ruben, J. M. Neff, and J. D. Millar. **Complications of smallpox vaccination, 1968.** N. Engl. J. Med., 281(22):1201–8, 1969. [p. 11]
- [69] K. Rowan. **Oncolytic viruses move forward in clinical trials.** J. Natl. Cancer Inst., 102(9):590–5, 2010. [p. 11]
- [70] T. S. Miest and R. Cattaneo. **New viruses for cancer therapy: meeting clinical needs.** Nat. Rev. Microbiol., 12(December):23–34, 2013. [p. 11]
- [71] E. M. Karapanagiotou, V. Roulstone, K. Twigger, M. Ball, M. Tanay, C. Nutting, K. Newbold, M. E. Gore, J. Larkin, K. N. Syrigos, M. Coffey, B. Thompson, K. Mettinger, R. G. Vile, H. S. Pandha, G. D. Hall, A. A. Melcher, J. Chester, and K. J. Harrington. **Phase I/II Trial of Carboplatin**

- and Paclitaxel Chemotherapy in Combination with Intravenous Oncolytic Reovirus in Patients with Advanced Malignancies.** *Clin. Cancer Res.*, 18(7):2080–9, 2012. [p. 11]
- [72] J. Heo, C. J. Breitbach, A. Moon, C. W. Kim, R. Patt, M. K. Kim, Y. K. Lee, S. Y. Oh, H. Y. Woo, K. Parato, J. Rintoul, T. Falls, T. Hickman, B.-G. Rhee, J. C. Bell, D. H. Kirn, and T.-H. Hwang. **Sequential therapy with JX-594, a targeted oncolytic poxvirus, followed by sorafenib in hepatocellular carcinoma: preclinical and clinical demonstration of combination efficacy.** *Mol. Ther.*, 19(6):1170–9, 2011. [p. 11]
- [73] J. M. Burke, D. L. Lamm, M. V. Meng, J. J. Nemunaitis, J. J. Stephenson, J. C. Arseneau, J. Aimi, S. Lerner, A. W. Yeung, T. Kazarian, D. J. Maslyar, and J. M. McKiernan. **A First in Human Phase 1 Study of CG0070, a GM-CSF Expressing Oncolytic Adenovirus, for the Treatment of Nonmuscle Invasive Bladder Cancer.** *J. Urol.*, 188(6):2391–2397, 2012. [p. 11]
- [74] K. Garber. **China approves world’s first oncolytic virus therapy for cancer treatment.** *J. Natl. Cancer Inst.*, 98(5):298–300, 2006. [p. 11]
- [75] Z.-J. Xia, J.-H. Chang, L. Zhang, W.-Q. Jiang, Z.-Z. Guan, J.-W. Liu, Y. Zhang, X.-H. Hu, G.-H. Wu, H.-Q. Wang, Z.-C. Chen, J.-C. Chen, Q.-H. Zhou, J.-W. Lu, Q.-X. Fan, J.-J. Huang, and X. Zheng. **[Phase III randomized clinical trial of intratumoral injection of E1B gene-deleted adenovirus (H101) combined with cisplatin-based chemotherapy in treating squamous cell cancer of head and neck or esophagus].** *Ai Zheng*, 23(12):1666–70, 2004. [p. 11]
- [76] Y. Fong. **Oncolytic Treatment for Cancer Recommended for Approval.** *Mol. Ther.*, 23(7):1131–1131, 2015. [p. 12]
- [77] R. H. I. Andtbacka, H. L. Kaufman, F. Collichio, T. Amatruda, N. Senzer, J. Chesney, K. A. Delman, L. E. Spitler, I. Puzanov, S. S. Agarwala, M. Milhem, L. Cranmer, B. Curti, K. Lewis, M. Ross, T. Guthrie, G. P. Linette, G. A. Daniels, K. Harrington, M. R. Middleton, W. H. Miller, J. S. Zager, Y. Ye, B. Yao, A. Li, S. Doleman, A. VanderWalde, J. Gansert, and R. S. Coffin. **Talimogene Laherparepvec Improves Durable Response Rate in Patients With Advanced Melanoma.** *J. Clin. Oncol.*, 33(25):2780–2788, 2015. [p. 12]

- [78] S. Hernandez. **Observacion de un caso de enfermedad de Hodgkin, con regresion de los sintomas e infartos ganglionares, postsarampion.** Arch. Cuba. Cancer, 8:26–31, 1949. [p. 12]
- [79] G. Pasquinucci. **Possible effect of measles on leukaemia.** Lancet, 1(7690):136, 1971. [p. 12]
- [80] A. Z. Bluming and J. L. Ziegler. **Regression of Burkitt’s lymphoma in association with measles infection.** Lancet, 2(7715):105–6, 1971. [p. 12]
- [81] Z. Zygiert. **Hodgkin’s disease: remissions after measles.** Lancet, 1(7699):593, 1971. [p. 12]
- [82] S. Gross. **Measles and leukaemia.** Lancet, 1(7695):397–8, 1971. [p. 12]
- [83] H. C. Mota. **Infantile Hodgkin’s disease: remission after measles.** Br. Med. J., 2(5863):421, 1973. [p. 12]
- [84] F. Radecke, P. Spielhofer, H. Schneider, K. Kaelin, M. Huber, C. Dötsch, G. Christiansen, and M. A. Billeter. **Rescue of measles viruses from cloned DNA.** EMBO J., 14(23):5773–5784, 1995. [p. 12, 16]
- [85] H. Schneider, P. Spielhofer, K. Kaelin, C. Dötsch, F. Radecke, G. Sutter, and M. A. Billeter. **Rescue of measles virus using a replication-deficient vaccinia-T7 vector.** J Virol Methods, 64(1):57–64, 1997. [p. 12]
- [86] E. Galanis, L. C. Hartmann, W. A. Cliby, H. J. Long, P. P. Peethambaram, B. A. Barrette, J. S. Kaur, P. J. Haluska Jr., I. Aderca, P. J. Zollman, J. A. Sloan, G. Keeney, P. J. Atherton, K. C. Podratz, S. C. Dowdy, C. R. Stanhope, T. O. Wilson, M. J. Federspiel, K. W. Peng, and S. J. Russell. **Phase I trial of intraperitoneal administration of an oncolytic measles virus strain engineered to express carcinoembryonic antigen for recurrent ovarian cancer.** Cancer Res., 70(3):875–882, 2010. [p. 12, 13]
- [87] P. J. Lech and S. J. Russell. **Use of attenuated paramyxoviruses for cancer therapy.** Expert Rev. Vaccines, 9(11):1275–302, 2010. [p. 12]
- [88] P. Msaouel, A. Dispenzieri, and E. Galanis. **Clinical testing of engineered oncolytic measles virus strains in the treatment of cancer: an overview.** Curr. Opin. Mol. Ther., 11(1):43–53, 2009. [p. 12]
- [89] S. J. Russell, K.-W. Peng, and J. C. Bell. **Oncolytic virotherapy.** Nat. Biotechnol., 30(7):658–670, 2012. [p. 12]

- [90] I. Völker, P. Bach, C. Coulibaly, R. Plesker, T. Abel, J. Seifried, S. Heidmeier, M. D. Mühlebach, U. M. Lauer, and C. J. Buchholz. **Intrahepatic Application of Suicide Gene-Armed Measles Virotherapeutics: A Safety Study in Transgenic Mice and Rhesus Macaques.** *Hum. Gene Ther. Clin. Dev.*, 12(April):130403115452006, 2013. [p. 13]
- [91] Z. Fishelson, N. Donin, S. Zell, S. Schultz, and M. Kirschfink. **Obstacles to cancer immunotherapy: expression of membrane complement regulatory proteins (mCRPs) in tumors.** *Mol Immunol*, 40(2-4):109–123, 2003. [p. 13]
- [92] B. D. Anderson, T. Nakamura, S. J. Russell, and K. W. Peng. **High CD46 receptor density determines preferential killing of tumor cells by oncolytic measles virus.** *Cancer Res.*, 64(14):4919–4926, 2004. [p. 13, 21, 32, 52]
- [93] S. Balachandran and G. N. Barber. **PKR in Innate Immunity, Cancer, and Viral Oncolysis.** *Cancer Genomics and Proteomics*, pages 277–301. Humana Press, Totowa, NJ, 2007. [p. 13]
- [94] C. Achard, N. Boisgerault, T. Delaunay, D. Roulois, S. Nedellec, P.-j. Royer, M. Pain, C. Combredet, M. Mesel-Lemoine, L. Cellerin, A. Magnan, F. Tangy, M. Grégoire, and J.-f. Fonteneau. **Sensitivity of human pleural mesothelioma to oncolytic measles virus depends on defects of the type I interferon response.** *Oncotarget*, 6(42):44892–904, dec 2015. [p. 13, 53]
- [95] R. Cattaneo, T. Miest, E. V. Shashkova, and M. A. Barry. **Reprogrammed viruses as cancer therapeutics: targeted, armed and shielded.** *Nat. Rev. Microbiol.*, 6(7):529–40, 2008. [p. 13]
- [96] G. Ungerechts, C. Springfield, M. E. Frenzke, J. Lampe, P. B. Johnston, W. B. Parker, E. J. Sorscher, and R. Cattaneo. **Lymphoma chemovirotherapy: CD20-targeted and convertase-armed measles virus can synergize with fludarabine.** *Cancer Res.*, 67(22):10939–47, 2007. [p. 13, 58]
- [97] G. Ungerechts, M. E. Frenzke, K.-C. Yaiw, T. Miest, P. B. Johnston, and R. Cattaneo. **Mantle cell lymphoma salvage regimen: synergy between a reprogrammed oncolytic virus and two chemotherapeutics.** *Gene Ther.*, 17(12):1506–16, 2010. [p. 13, 58, 59]
- [98] S. Bossow, C. Grossardt, A. Temme, M. F. Leber, S. Sawall, E. P. Rieber, R. Cattaneo, C. von Kalle, and G. Ungerechts. **Armed and targeted measles virus**

- for chemovirotherapy of pancreatic cancer.** *Cancer Gene Ther.*, 18(8):598–608, 2011. [p. 13]
- [99] G. Ungerechts, C. Springfield, M. E. Frenzke, J. Lampe, W. B. Parker, E. J. Sorscher, and R. Cattaneo. **An immunocompetent murine model for oncolysis with an armed and targeted measles virus.** *Mol. Ther.*, 15(11):1991–7, 2007. [p. 13]
- [100] C. Sioka and A. P. Kyritsis. **Central and peripheral nervous system toxicity of common chemotherapeutic agents.** *Cancer Chemother. Pharmacol.*, 63(5):761–7, 2009. [p. 13]
- [101] P. Erbs, E. Regulier, J. Kintz, P. Leroy, Y. Poitevin, F. Exinger, R. Jund, and M. Mehtali. **In vivo cancer gene therapy by adenovirus-mediated transfer of a bifunctional yeast cytosine deaminase/uracil phosphoribosyltransferase fusion gene.** *Cancer Res.*, 60(14):3813–3822, 2000. [p. 13, 15]
- [102] D. B. Longley, D. P. Harkin, and P. G. Johnston. **5-fluorouracil: Mechanisms of action and clinical strategies.** *Nat. Rev. Cancer*, 3(5):330–8, 2003. [p. 13, 14]
- [103] C. A. Mullen, M. Kilstrup, and R. M. Blaese. **Transfer of the bacterial gene for cytosine deaminase to mammalian cells confers lethal sensitivity to 5-fluorocytosine: a negative selection system.** *Proc. Natl. Acad. Sci. U. S. A.*, 89(1):33–7, 1992. [p. 15]
- [104] F. Kanai, T. Kawakami, H. Hamada, A. Sadata, Y. Yoshida, T. Tanaka, M. Ohashi, K. Tateishi, Y. Shiratori, M. Omata, A. Sudata, Y. Yoshida, and T. Tanaka. **Adenovirus-mediated transduction of Escherichia coli uracil phosphoribosyltransferase gene sensitizes cancer cells to low concentrations of 5-fluorouracil.** *Cancer Res.*, 58(9):1946–1951, 1998. [p. 15]
- [105] R. B. Diasio and B. E. Harris. **Clinical pharmacology of 5-fluorouracil.** *Clin. Pharmacokinet.*, 16(4):215–37, 1989. [p. 15]
- [106] F. Graepler, M.-L. Lemken, W. a. Wybranietz, U. Schmidt, I. Smirnow, C. D. Gross, M. Spiegel, A. Schenk, H. Graf, U. A. Lauer, R. Vonthein, M. Gregor, S. Armeanu, M. Bitzer, and U. M. Lauer. **Bifunctional chimeric SuperCD suicide gene -YCD: YUPRT fusion is highly effective in a rat hepatoma model.** *World J. Gastroenterol.*, 11(44):6910–9, 2005. [p. 15, 17]

- [107] K. Zaoui, S. Bossow, C. Grossardt, M. F. Leber, C. Springfeld, P. K. Plinkert, C. von Kalle, and G. Ungerechts. **Chemovirotherapy for head and neck squamous cell carcinoma with EGFR-targeted and CD/UPRT-armed oncolytic measles virus**. *Cancer Gene Ther.*, 19(3):181–91, 2012. [p. 15, 59]
- [108] M. Moehler, S.-E. Al-Batran, T. Andus, M. Anthuber, J. Arends, D. Arnold, D. Aust, P. Baier, G. Baretton, J. Bernhardt, H. Boeing, E. Böhle, C. Boke-meyer, J. Bornschein, W. Budach, E. Burmester, K. Caca, W. A. Diemer, C. F. Dietrich, M. Ebert, A. Eickhoff, C. Ell, J. Fahlke, H. Feussner, R. Fietkau, W. Fischbach, W. Fleig, M. Flentje, H. E. Gabbert, P. R. Galle, M. Geissler, I. Gockel, U. Graeven, L. Grenacher, S. Gross, J. T. Hartmann, M. Heike, V. Heinemann, B. Herbst, T. Herrmann, S. Höcht, R. D. Hofheinz, H. Höfler, T. Höhler, A. H. Hölscher, M. Horneber, J. Hübner, J. R. Izbicki, R. Jakobs, C. Jenssen, S. Kanzler, M. Keller, R. Kiesslich, G. Klautke, J. Körber, B. J. Krause, C. Kuhn, F. Kullmann, H. Lang, H. Link, F. Lordick, K. Ludwig, M. Lutz, R. Mahlberg, P. Malfertheiner, S. Merkel, H. Messmann, H.-J. Meyer, S. Mönig, P. Piso, S. Pistorius, R. Porschen, T. Rabenstein, P. Reichardt, K. Ridwelski, C. Röcken, I. Roetzer, P. Rohr, W. Schepp, P. M. Schlag, R. M. Schmid, H. Schmidberger, W.-H. Schmiegel, H.-J. Schmoll, G. Schuch, C. Schuhmacher, K. Schütte, W. Schwenk, M. Selgrad, A. Sendler, J. Seraphin, T. Seufferlein, M. Stahl, H. Stein, C. Stoll, M. Stuschke, A. Tannapfel, R. Tholen, P. Thuss-Patience, K. Treml, U. Vanhoefer, M. Vieth, H. Vogelsang, D. Wagner, U. Wedding, A. Weimann, H. Wilke, and C. Wittekind. [**German S3-guideline "Diagnosis and treatment of esophagogastric cancer"**]. *Z. Gastroenterol.*, 49(4):461–531, 2011. [p. 15]
- [109] W. Schmiegel, A. Reinacher-Schick, D. Arnold, U. Graeven, V. Heinemann, R. Porschen, J. Riemann, C. Rödel, R. Sauer, M. Wieser, W. Schmitt, H.-J. Schmoll, T. Seufferlein, I. Kopp, and C. Pox. [**Update S3-guideline "colorectal cancer" 2008**]. *Z. Gastroenterol.*, 46(8):799–840, 2008. [p. 15]
- [110] T. Seufferlein, M. Porzner, T. Becker, V. Budach, G. Ceyhan, I. Esposito, R. Fietkau, M. Follmann, H. Friess, P. Galle, M. Geissler, M. Glanemann, T. Gress, V. Heinemann, W. Hohenberger, U. Hopt, J. Izbicki, E. Klar, J. Kleeff, I. Kopp, F. Kullmann, T. Langer, J. Langrehr, M. Lerch, M. Löhr, J. Lüttges, M. Lutz, J. Mayerle, P. Michl, P. Möller, M. Molls, M. Münter, M. Nothacker, H. Oettle, S. Post, A. Reinacher-Schick, C. Röcken, E. Roeb, H. Saeger, R. Schmid, W. Schmiegel, M. Schoenberg, J. Siveke, M. Stuschke, A. Tannapfel, W. Uhl, S. Unverzagt, B. van Oorschot, Y. Vashist, J. Werner, E. Yekebas,

- Guidelines Programme Oncology AWMF, German Cancer Society eV, and German Cancer Aid. **[S3-guideline exocrine pancreatic cancer]**. *Z. Gastroenterol.*, 51(12):1395–440, 2013. [p. 15]
- [111] A. F. C. Okines, A. R. Norman, P. McCloud, Y.-K. Kang, and D. Cunningham. **Meta-analysis of the REAL-2 and ML17032 trials: Evaluating capecitabine-based combination chemotherapy and infused 5-fluorouracil-based combination chemotherapy for the treatment of advanced oesophago-gastric cancer.** *Ann. Oncol.*, 20(9):1529–34, 2009. [p. 15]
- [112] E. Van Cutsem, P. M. Hoff, P. Harper, R. M. Bukowski, D. Cunningham, P. Dufour, U. Graeven, J. Lokich, S. Madajewicz, J. A. Maroun, J. L. Marshall, E. P. Mitchell, G. Perez-Manga, P. Rougier, W. Schmiegel, J. Schoelmerich, A. Sobrero, and R. L. Schilsky. **Oral capecitabine vs intravenous 5-fluorouracil and leucovorin: integrated efficacy data and novel analyses from two large, randomised, phase III trials.** *Br. J. Cancer*, 90(6):1190–7, 2004. [p. 15]
- [113] U. J. Buchholz, S. Finke, and K. K. Conzelmann. **Generation of bovine respiratory syncytial virus (BRSV) from cDNA: BRSV NS2 is not essential for virus replication in tissue culture, and the human RSV leader region acts as a functional BRSV genome promoter.** *J. Virol.*, 73(1):251–9, 1999. [p. 15]
- [114] J. Lampe. **Armed Oncolytic Measles Vaccine Virus for the Treatment of Hepatocellular Carcinoma.** PhD thesis, 2012. [p. 16]
- [115] J. Lampe, S. Bossow, T. Weiland, I. Smirnow, R. Lehmann, W. Neubert, M. Bitzer, and U. M. Lauer. **An armed oncolytic measles vaccine virus eliminates human hepatoma cells independently of apoptosis.** *Gene Ther.*, 20(11):1033–41, 2013. [p. 16, 55, 57, 59]
- [116] L. C. Pederson, D. J. Buchsbaum, S. M. Vickers, S. R. Kancharla, M. S. Mayo, D. T. Curiel, and M. A. Stackhouse. **Molecular chemotherapy combined with radiation therapy enhances killing of cholangiocarcinoma cells in vitro and in vivo.** *Cancer Res.*, 57(19):4325–32, 1997. [p. 17, 57]
- [117] M. A. Stackhouse, L. C. Pederson, W. E. Grizzle, D. T. Curiel, J. Gebert, K. Haack, S. M. Vickers, M. S. Mayo, and D. J. Buchsbaum. **Fractionated radiation therapy in combination with adenoviral delivery of the cytosine deaminase gene and 5-fluorocytosine enhances cytotoxic and antitumor**

- effects in human colorectal and cholangiocarcinoma models.** *Gene Ther.*, 7(12):1019–26, 2000. [p. 17, 57]
- [118] Y. Kojima, K. Honda, H. Hamada, and N. Kobayashi. **Oncolytic gene therapy combined with double suicide genes for human bile duct cancer in nude mouse models.** *J. Surg. Res.*, 157(1):e63–70, 2009. [p. 17, 57]
- [119] Z. B. Zhu, Y. Chen, S. K. Makhija, B. Lu, M. Wang, A. a. Rivera, M. Yamamoto, S. Wang, G. P. Siegal, D. T. Curiel, and J. M. McDonald. **Survivin promoter-based conditionally replicative adenoviruses target cholangiocarcinoma.** *Int. J. Oncol.*, 29(5):1319–29, 2006. [p. 17]
- [120] W. R. Jarnagin, J. S. Zager, M. Hezel, S. F. Stanziale, P. S. Adusumilli, M. Gonen, M. I. Ebricht, A. Culliford, N. J. Gusani, and Y. Fong. **Treatment of cholangiocarcinoma with oncolytic herpes simplex virus combined with external beam radiation therapy.** *Cancer Gene Ther.*, 13(3):326–34, 2006. [p. 17]
- [121] A. Pugalenti, K. Mojica, J. W. Ady, C. Johnsen, D. Love, N. G. Chen, R. J. Aguilar, A. A. Szalay, and Y. Fong. **Recombinant vaccinia virus GLV-1h68 is a promising oncolytic vector in the treatment of cholangiocarcinoma.** *Cancer Gene Ther.*, 22(12):591–596, dec 2015. [p. 17]
- [122] G. E. Moore, R. E. Gerner, and H. A. Franklin. **Culture of normal human leukocytes.** *JAMA*, 199(8):519–24, 1967. [p. 18]
- [123] H. Eagle. **Nutrition needs of mammalian cells in tissue culture.** *Science*, 122(3168):501–14, 1955. [p. 18]
- [124] W. Strober. **Monitoring Cell Growth.** *Curr. Protoc. Immunol.* John Wiley & Sons, Inc., Hoboken, NJ, USA, 2001. [p. 19]
- [125] R. I. Freshney. **Culture of Animal Cells.** John Wiley & Sons, Inc., Hoboken, NJ, USA, 2010. [p. 19]
- [126] M. Enjoji, H. Sakai, H. Nawata, K. Kajiyama, and M. Tsuneyoshi. **Sarcomatous and adenocarcinoma cell lines from the same nodule of cholangiocarcinoma.** *In Vitro Cell. Dev. Biol. Anim.*, 33(9):681–3, 1997. [p. 19]

- [127] M. Miyagiwa, T. Ichida, T. Tokiwa, J. Sato, and H. Sasaki. **A new human cholangiocellular carcinoma cell line (HuCC-T1) producing carbohydrate antigen 19/9 in serum-free medium.** *In Vitro Cell Dev Biol.*, 25(6):503–510, 1989. [p. 19]
- [128] S. Saijyo, T. Kudo, M. Suzuki, Y. Katayose, M. Shinoda, T. Muto, K. Fukuhara, T. Suzuki, and S. Matsuno. **Establishment of a new extrahepatic bile duct carcinoma cell line, TFK-1.** *Tohoku J. Exp. Med.*, 177(1):61–71, 1995. [p. 19]
- [129] Y. Yasumura and M. Kawakita. **The research for the SV40 by means of tissue culture technique.** *Nippon Rinsho*, 21:1201–1219, 1963. [p. 20]
- [130] J. Desmyter, J. L. Melnick, and W. E. Rawls. **Defectiveness of interferon production and of rubella virus interference in a line of African green monkey kidney cells (Vero).** *J. Virol.*, 2(10):955–61, 1968. [p. 20]
- [131] V. Grachev, D. Magrath, and E. Griffiths. **WHO requirements for the use of animal cells as in vitro substrates for the production of biologicals (Requirements for biological substances no. 50).** *Biologicals*, 26(3):175–93, 1998. [p. 20]
- [132] C. Spearman. **The method of ‘right and wrong cases’ (‘constant stimuli’) without Gauss’s formula.** *Br J Psychol*, (2):227–242, 1908. [p. 23]
- [133] G. Kärber. **Beitrag zur kollektiven Behandlung pharmakologischer Reihenversuche.** *Arch Exp Pathol Pharmacol*, 162(4):480–483, 1931. [p. 23]
- [134] W. Bryan. **Interpretation of host response in quantitative studies on animal viruses.** *Ann. N. Y. Acad. Sci.*, 69(4):698–728, 1957. [p. 24]
- [135] Z. Govindarajulu. **Statistical Techniques in Bioassay.** Karger, 2 edition, 2001. [p. 24]
- [136] N. H. Wulff, M. Tzatzaris, and P. J. Young. **Monte Carlo simulation of the Spearman-Kaerber.** *J. Clin. Bioinforma.*, 2(1):5, 2012. [p. 24]
- [137] M. M. Bradford. **A rapid and sensitive method for the quantitation of microgram quantities of protein utilizing the principle of protein-dye binding.** *Anal. Biochem.*, 72:248–54, 1976. [p. 25]
- [138] U. K. Laemmli. **Cleavage of structural proteins during the assembly of the head of bacteriophage T4.** *Nature*, 227(5259):680–5, 1970. [p. 25]

- [139] P. Skehan, R. Storeng, D. Scudiero, A. Monks, J. McMahon, D. Vistica, J. T. Warren, H. Bokesch, S. Kenney, and M. R. Boyd. **New colorimetric cytotoxicity assay for anticancer-drug screening.** *J Natl Cancer Inst*, 82(13):1107–1112, 1990. [p. 28]
- [140] W. E. Wacker, D. D. Ulmer, and B. L. Vallee. **Metalloenzymes and Myocardial Infarction.** *N. Engl. J. Med.*, 255(10):449–456, 1956. [p. 28]
- [141] L. Galluzzi, S. A. Aaronson, J. Abrams, E. S. Alnemri, D. W. Andrews, E. H. Baehrecke, N. G. Bazan, M. V. Blagosklonny, K. Blomgren, C. Borner, D. E. Bredesen, C. Brenner, M. Castedo, J. A. Cidlowski, A. Ciechanover, G. M. Cohen, V. De Laurenzi, R. De Maria, M. Deshmukh, B. D. Dynlacht, W. S. El-Deiry, R. A. Flavell, S. Fulda, C. Garrido, P. Golstein, M.-L. Gougeon, D. R. Green, H. Gronemeyer, G. Hajnóczky, J. M. Hardwick, M. O. Hengartner, H. Ichijo, M. Jäättelä, O. Kepp, A. Kimchi, D. J. Klionsky, R. A. Knight, S. Kornbluth, S. Kumar, B. Levine, S. A. Lipton, E. Lugli, F. Madeo, W. Malorni, J.-C. Marine, S. J. Martin, J. P. Medema, P. Mehlen, G. Melino, U. M. Moll, E. Morselli, S. Nagata, D. W. Nicholson, P. Nicotera, G. Nuñez, M. Oren, J. Penninger, S. Pervaiz, M. E. Peter, M. Piacentini, J. H. M. Prehn, H. Puthalakath, G. A. Rabinovich, R. Rizzuto, C. M. P. Rodrigues, D. C. Rubinsztein, T. Rudel, L. Scorrano, H.-U. Simon, H. Steller, J. Tschopp, Y. Tsujimoto, P. Vandenabeele, I. Vitale, K. H. Vousden, R. J. Youle, J. Yuan, B. Zhivotovsky, and G. Kroemer. **Guidelines for the use and interpretation of assays for monitoring cell death in higher eukaryotes.** *Cell Death Differ.*, 16(8):1093–1107, 2009. [p. 28]
- [142] M. M. Tomayko and C. P. Reynolds. **Determination of subcutaneous tumor size in athymic (nude) mice.** *Cancer Chemother Pharmacol*, 24(3):148–154, 1989. [p. 29]
- [143] S. Berchtold, J. Lampe, T. Weiland, I. Smirnow, S. Schleicher, R. Handgretinger, H.-G. Kopp, J. Reiser, F. Stubenrauch, N. P. Malek, M. Bitzer, and U. M. Lauer. **Innate immune defense defines susceptibility of sarcoma cells to measles vaccine virus based oncolysis.** *J. Virol.*, 34(4):1055–66, 2013. [p. 52, 53]
- [144] M. Noll, S. Berchtold, J. Lampe, N. P. Malek, M. Bitzer, and U. M. Lauer. **Primary resistance phenomena to oncolytic measles vaccine viruses.** *Int. J. Oncol.*, 43(1):103–12, 2013. [p. 53]

- [145] R. H. Shoemaker. **The NCI60 human tumour cell line anticancer drug screen.** *Nat. Rev. Cancer*, 6(10):813–823, 2006. [p. 53]
- [146] P. Erbs, A. Findeli, J. Kintz, P. Cordier, C. Hoffmann, M. Geist, and J.-M. M. Balloul. **Modified vaccinia virus Ankara as a vector for suicide gene therapy.** *Cancer Gene Ther.*, 15(1):18–28, 2008. [p. 56, 57]
- [147] M.-H. You, W.-J. Kim, W. Shim, S.-R. Lee, G. Lee, S. Choi, D.-Y. Kim, Y. M. Kim, H. Kim, and S.-U. Han. **Cytosine deaminase-producing human mesenchymal stem cells mediate an antitumor effect in a mouse xenograft model.** *J. Gastroenterol. Hepatol.*, 24(8):1393–400, 2009. [p. 57]
- [148] L.-Y. Deng, J.-P. Wang, Z.-F. Gui, and L.-Z. Shen. **Antitumor activity of mutant bacterial cytosine deaminase gene for colon cancer.** *World J. Gastroenterol.*, 17(24):2958–64, 2011. [p. 57]
- [149] K. C. Sia, H. Huynh, N. Chinnasamy, K. M. Hui, and P. Y. P. Lam. **Suicidal gene therapy in the effective control of primary human hepatocellular carcinoma as monitored by noninvasive bioimaging.** *Gene Ther.*, 19(5):532–42, 2012. [p. 58]
- [150] O. Wildner, J. C. Morris, N. N. Vahanian, H. Ford, W. J. Ramsey, and R. M. Blaese. **Adenoviral vectors capable of replication improve the efficacy of HSVtk/GCV suicide gene therapy of cancer.** *Gene Ther.*, 6(1):57–62, 1999. [p. 58]
- [151] E. Seo, M. Abei, M. Wakayama, K. Fukuda, H. Ugai, T. Murata, T. Todoroki, Y. Matsuzaki, N. Tanaka, H. Hamada, and K. K. Yokoyama. **Effective gene therapy of biliary tract cancers by a conditionally replicative adenovirus expressing uracil phosphoribosyltransferase: significance of timing of 5-fluorouracil administration.** *Cancer Res.*, 65(2):546–52, 2005. [p. 58]
- [152] S. Yamada, T. Kuroda, B. C. Fuchs, X. He, J. G. Supko, A. Schmitt, C. M. McGinn, M. Lanuti, and K. K. Tanabe. **Oncolytic herpes simplex virus expressing yeast cytosine deaminase: relationship between viral replication, transgene expression, prodrug bioactivation.** *Cancer Gene Ther.*, 19(3):160–70, 2012. [p. 58]
- [153] K.-W. Peng, S. Fecteau, T. Wegman, D. O’Kane, and S. J. Russell. **Non-invasive in vivo monitoring of trackable viruses expressing soluble marker peptides.** *Nat. Med.*, 8(5):527–31, 2002. [p. 58, 59]

- [154] D. Dingli, K. W. Peng, M. E. Harvey, P. R. Greipp, M. K. O'Connor, R. Cattaneo, J. C. Morris, and S. J. Russell. **Image-guided radiovirotherapy for multiple myeloma using a recombinant measles virus expressing the thyroidal sodium iodide symporter.** *Blood*, 103(5):1641–1646, 2004. [p. 58]
- [155] C. Yurttas, S. Berchtold, N. P. Malek, M. Bitzer, and U. M. Lauer. **Pulsed versus continuous application of the prodrug 5-fluorocytosine to enhance the oncolytic effectiveness of a measles vaccine virus armed with a suicide gene.** *Hum. Gene Ther. Clin. Dev.*, 25(2):85–96, 2014. [p. 59]

ZUSAMMENFASSUNG

Die einzige kurative Therapie des Cholangiokarzinoms besteht in einer chirurgischen Resektion in einem frühen Stadium. In fortgeschrittenen Stadien, in welchen eine chirurgische Resektion des Tumors nicht mehr möglich ist und etablierte palliative Chemotherapie-Regime wenig Linderung und nur eine geringe Lebensverlängerung erzielen, werden dringlich neuartige Therapieansätze benötigt. In klinischen Studien wurde gezeigt, dass sich onkolytische Viren vorzugsweise in Krebszellen ausbreiten. Darüber hinaus kann dieser virotherapeutische Effekt durch eine Suizidtherapie verstärkt werden. Hierbei werden durch Enzyme, welche im Virusgenom kodiert sind, inaktive Medikamentenvorstufen in aktive Metabolite mit starker antitumorale Wirkung überführt.

Ziel dieser Doktorarbeit war die Evaluierung zweier neuartiger Masern-Impfviren, welche für eine Super-Cytosin-Deaminase (SuperCD; ein Fusionsgen der Hefe-Cytosin-Deaminase und der Hefe-Uracil-Phosphoribosyltransferase) kodieren. Das SuperCD Suizid-Protein wandelt die klinisch zugelassene, ungiftige Medikamentenvorstufe 5-Fluorcytosin in 5-Fluoruracil um, das bei einer Vielzahl von Tumoren erfolgreich als Chemotherapeutikum verwendet wird. Die Wirksamkeit dieses Masern-Impfvirus-Vektors wurde in drei humanen Cholangiokarzinomzelllinien (RBE, TFK-1 und HuCCT1) untersucht.

Alle Zelllinien konnten erfolgreich mit den Masern-Impfviren infiziert werden. In einer Zelllinie war die Infektions- und Absterberate, welche durch das Virus verursacht wurden, im Vergleich zu den beiden anderen Zelllinien deutlich reduziert. Diese Resistenz gegenüber der alleinigen Masern-Impfvirus-Onkolyse konnte durch die Zugabe von 5-Fluorcytosin durchbrochen werden.

In mehreren Tierexperimenten wurde die Wirkung dieses armierten Masern-Impfvirus weiter untersucht: In einem xenogenen subkutanen TFK-1-Mausmodell führte die intratumorale Gabe des Virus zusammen mit einer systemischen Applikation von 5-FC zu einer signifikanten Verringerung der Tumorgroße im Vergleich zu der alleinigen Gabe des Virus. In einem zweiten Experiment mit der Zelllinie HuCCT1 konnte über eine Verringerung der Tumorgroße hinaus auch eine Verlängerung der mittleren Überlebenszeit im Vergleich zu den Kontrolltieren nachgewiesen werden.

Diese Ergebnisse haben den Weg zu einer präklinischen Phase-I-Studie geebnet: Hier wird dieser neuartige Masern-Impfvirus-Vektor (MeV Id-SCD) in Kombination mit einer oralen Gabe von 5-FC bei Patienten mit fortgeschrittenen, nicht-resektablen Cholangiokarzinomen eingesetzt.

VERÖFFENTLICHUNGEN

Diese Dissertation ist Bestandteil einer Publikation desselben Autors:

S. Lange, J. Lampe, S. Bossow, M. Zimmermann, W. Neubert and U. M. Lauer. **A novel armed oncolytic measles vaccine virus for the treatment of cholangiocarcinoma.** *Human Gene Therapy*, 24(5):554-64, 2013.

Weitere Publikationen, an welcher der Autor während der Entstehung der Dissertation beteiligt war:

M. Zimmermann, J. Lampe, S. Lange, I. Smirnow, A. Königsrainer, C. Hann-von-Weyhern, F. Fend, M. Gregor, M. Bitzer and U. M. Lauer. **Improved reproducibility in preparing precision-cut liver tissue slices.** *Cytotechnology*, 61(3):145-152, 2009.

M. Zimmermann, S. Armeanu, S. Bossow, J. Lampe, I. Smirnow, A. Schenk, S. Lange, T. S. Weiss, W. Neubert, U. M. Lauer and M. Bitzer. **Attenuated and protease-profile modified sendai virus vectors as a new tool for virotherapy of solid tumors.** *PLoS One*, 5;9(3):e90508, 2014.

ERKLÄRUNG ZUM EIGENANTEIL

Ich erkläre hiermit, dass ich meine der Medizinischen Fakultät der Universität Tübingen zur Promotion eingereichte Arbeit mit dem Titel: "Evaluation of a novel, suicide gene-armed measles vaccine virus for the treatment of cholangiocarcinoma" selbständig ohne unzulässige Hilfe Dritter und ohne Benutzung anderer als der angegebenen Hilfsmittel angefertigt habe. Die aus fremden Quellen direkt oder indirekt übernommenen Gedanken sind als solche kenntlich gemacht. Ich versichere an Eides statt, dass diese Angaben wahr sind und dass ich nichts verschwiegen habe. Mir ist bekannt, dass die falsche Abgabe einer Versicherung an Eides statt mit einer Freiheitsstrafe bis zu drei Jahren oder mit einer Geldstrafe bestraft wird.

Diese Arbeit wurde in der Abteilung Innere Medizin I der Medizinischen Universitätsklinik Tübingen unter der Betreuung von Herrn Professor Dr. med. Ulrich M. Lauer durchgeführt.

Sämtliche Versuche wurden von mir durchgeführt. Bei der Konzeption der Studie, der Auswahl und Auswertung des Materials sowie bei der Erstellung des Manuskriptes habe ich Unterstützungsleistungen von folgenden Personen erhalten:

Professor Dr. med. Ulrich M. Lauer (Oberarzt und Arbeitsgruppenleiter)

Dr. rer. nat. Johanna Lampe (Naturwissenschaftliche Doktorandin)

Dr. rer. nat. Martina Zimmermann (Naturwissenschaftliche Doktorandin)

Die statistische Auswertung erfolgte eigenständig nach Beratung durch das Institut für Klinische Epidemiologie und angewandte Biometrie der Universität Tübingen.

Teile dieser Dissertation wurden mit gleichem Wortlaut bereits in einer früheren Publikation veröffentlicht:

S. Lange, J. Lampe, S. Bossow, M. Zimmermann, W. Neubert and U. M. Lauer. **A novel armed oncolytic measles vaccine virus for the treatment of cholangiocarcinoma.** *Human Gene Therapy*, 24(5):554-64, 2013.

Diese sind im Text durch Anführungszeichen kenntlich gemacht.

Ich habe die Versuche, welche in den Figures 1, 2, 3, 4 und 5 der oben genannten Veröffentlichung dargestellt sind, sowie deren Auswertung durchgeführt und die dazugehörigen Abbildungen erstellt. Ich war an der Konzeption der Studie beteiligt, habe die Literaturrecherche durchgeführt und habe den ersten Entwurf des Manuskriptes selbständig verfasst. Ich habe in der Folge die Korrekturen des Manuskriptes bearbeitet und das Manuskript in die finale Fassung gebracht sowie abschließend das Manuskript zur Veröffentlichung eingereicht.

Frau Dr. Johanna Lampe war an der Konzeption dieser Studie beteiligt, hat die Arbeit betreut und das Manuskript korrigiert. Frau Dr. Johanna Lampe hat die in dieser Studie eingesetzten Masern-Impfvirus-Vektoren (Figure 1 A) zur Verfügung gestellt, Hilfestellung bei den Zellkulturexperimenten (Figures 1 B, 1 C, 2 und 3) gegeben und bei den durchgeführten Tierversuchen (Figures 4 und 5) mitgearbeitet, eigenständig Kontrollmessungen durchgeführt sowie Teile der Tiere selbständig obduziert.

Herr Dr. Sascha Bossow hat in Zusammenarbeit mit Herrn Professor Dr. Wolfgang Neubert die Klonierung der hier eingesetzten Masern-Impfvirus-Vektoren (Figure 1 A) durchgeführt.

Frau Dr. Zimmermann hat Hilfestellung bei der Durchführung der SDS-Page und des Western Blots (Figure 1 C) sowie der Zellkulturexperimente (Figures 1 B, 2 B und 3) gegeben.

Frau Smirnow hat die SDS-Page sowie den Western Blot in Zusammenarbeit mit mir durchgeführt (Figure 1 C).

Frau Schenk und Frau Smirnow haben die Zellen für die Tierversuchexperimente vorbereitet (Figures 4 und 5).

Herr Professor Dr. Michael Bitzer war an der Konzeption der Studie beteiligt und hat das Manuskript korrigiert.

Herr Professor Dr. Ulrich M. Lauer war an der Konzeption der Studie beteiligt, hat die Arbeit betreut, war in der Planung der Versuche beteiligt und hat das Manuskript korrigiert.

Alle wörtlich übernommenen Abschnitte dieser Originalpublikation wurden ursprünglich alleine von mir verfasst.

Die vorgelegte Dissertation wurde bisher weder im Inland noch im Ausland in gleicher oder ähnlicher Form einer anderen Prüfungsbehörde vorgelegt. Mit der Arbeit wurde weder ein akademischer Grad erworben noch eine staatliche Prüfung absolviert. Den Grad eines Dr. med. habe ich noch nicht erworben.

Mir ist bekannt, dass falsche oder unvollständige Angaben zur Folge haben können, dass die Fakultät ein Verfahren zur Entziehung eines eventuell verliehenen akademischen Titels einleitet.

DANKSAGUNG

CURRICULUM VITAE